Optimal Tuning of H Infinity Speed Controller for Sensorless BLDC Motor using PSO and its Simulation Study in Underwater Applications

A Thesis

Submitted By

K. VINIDA

For the award of the degree

of

DOCTOR OF PHILOSOPHY

(Faculty of Technology)

DEPARTMENT OF SHIP TECHNOLOGY

COCHIN UNIVERSITY OF SCIENCE AND TECHNOLOGY

KOCHI -682022

SEPTEMBER 2018

DEDICATION

To my family

DECLARATION

This is to certify that the thesis entitled **"Optimal Tuning of H Infinity Speed Controller for Sensorless BLDC Motor using PSO and its Simulation Study in Underwater Applications"** submitted to the Cochin University of Science and Technology in partial fulfillment of the requirements for the award of the degree of Doctor of Philosophy is a bonafide record of research work carried out by me. The contents of this thesis have not been submitted and will not be submitted to any other University or Institute for the award of any degree.

Thrikkakara
15-09-2018

K. Vinida
Research Scholar
(Regn No. 4690)
Department of Ship Technology
Cochin University of
Science and Technology,
Kochi-22

DEPARTMENT OF SHIP TECHNOLOGY
COCHIN UNIVERSITY OF SCIENCE AND TECHNOLOGY
KOCHI – 682022, KERALA, INDIA

Telephone: Off: 2575714 E-mail: ship@cusat.ac.in

CERTIFICATE

This is to certify that the thesis entitled **"Optimal Tuning of H Infinity Speed Controller for Sensorless BLDC Motor using PSO and its Simulation Study in Underwater Applications"** submitted by K. Vinida to the Cochin University of Science and Technology in partial fulfillment of the requirements for the award of the degree of Doctor of Philosophy is a bonafide record of research work carried out by her under my supervision. The contents of this thesis have not been submitted and will not be submitted to any other University or Institute for the award of any degree.

Thrikkakara
15-09-2018

Research Guide
Dr. Mariamma Chacko
Associate Professor & HOD,
Department of Ship Technology
Cochin University of
Science and Technology,
Kochi-22

DEPARTMENT OF SHIP TECHNOLOGY
COCHIN UNIVERSITY OF SCIENCE AND TECHNOLOGY
KOCHI – 682022, KERALA, INDIA

Telephone: Off: 2575714 E-mail: ship@cusat.ac.in

CERTIFICATE

This is to certify that all relevant corrections and modifications suggested by the audience during the pre-synopsis seminar and recommended by the Doctoral Committee of K.Vinida have been incorporated in the thesis.

Thrikkakara
15-09-2018

Research Guide
Dr. Mariamma Chacko
Associate Professor & HOD,
Department of Ship Technology
Cochin University of
Science and Technology,
Kochi-22

ACKNOWLEDGEMENT

As I complete my research work, I realize and recognize numerous hands that have helped me in many ways, and I thank them all with my whole heart.

I express my sincere gratitude to my supervising guide Dr. Mariamma Chacko, for the zeal with which she guided me in carrying out my Ph. D study and research work. It has been a great learning experience working with her. I am deeply indebted to her for her valuable guidance, patience, constant encouragement and suggestions throughout the course of my work. I would like to thank Dr. Sumam Mary Idicula, Computer Science Department who is a member of Doctoral Committee, for her valuable guidance and insightful comments for the improvement of my work. I am also indebted to Dr. James Kurian & Dr. Nandakumar, for supporting me all throughout the process. I would like to thank all the department research committee members for their comments, encouragement and also for their questions which widened my research from various perspectives.

I remember my father with deep love for his blessings bestowed upon me. I am also thankful to my mother, my husband Ranjan, son Vaishnav and daughter Reshma for their support and prayers in my hard times without which I would not be able to complete this thesis. I also extend my gratitude to my fellow research scholars and my friends who always stood by my side during my difficult times.

I thank God Almighty for the uncountable blessings bestowed upon me all through my life and especially during the period of my thesis work. With a heart full of gratitude, I submit this thesis. Once again I thank all who walked with me to make this venture a grand success.

K. VINIDA

ABSTRACT

Brushless DC motor (BLDC) exhibits tremendous advantages such as elimination of sparking, better speed versus torque characteristics, noiseless operation, higher speed ranges, better service life and rugged construction. Sensorless techniques for the rotor position detection to achieve the cost-effective control of BLDC motors exhibit a widely appreciated field of research. The robust control of BLDC motors is a vast developing area as it finds its applications in military, aerospace, marine electric propulsion, industrial automation, etc. Insensitivity to disturbances, uncertainties and modeling errors is expected from the motors used in these applications. The aim of controller design is to minimize the effects of disturbance and at the same time track the speed and current commands with specified damping and response time. H infinity control, which is one of the robust control methods, has been widely used to guarantee performance and stability requirements. For shaping the frequency response of the system, weight functions have to be introduced for an H infinity controller. For problems concerning requirements on both closed loop sensitivity and complementary sensitivity functions, it is not possible to arbitrarily choose weights since the two are coupled.

A novel control technique with the implementation of H infinity controller with its coefficients of weights optimized by PSO for the speed control of BLDC motor is proposed in this research work. Particle swarm optimization technique has been chosen for the optimization of coefficients of weights as this provides a faster convergence. Simulation studies in MATLAB / SIMULINK environment as well as experimental studies are conducted. The results are compared with a PI speed controller with its gains optimized by PSO. Adaptation of one of the sensorless techniques in this research work makes the motor independent of a mechanical sensor and reduced maintenance.

The increasing concern of environmental issues such as CO_2 emission and fuel consumption in marine applications pilots the scientific community to come up with new inventions in electric propulsion. The abrupt variation in load due to waves and weather is a continuous disturbance in the electrical system of marine vehicles. This necessitates the need for robust control in marine applications. Two case studies have been conducted by incorporating the proposed controller strategy in BLDC motors used as electric propulsion motor in submarines and as thruster motors coupled with propellers in AUVs. In the case of AUVs four quadrant operation of the motor drive has been studied with both controllers.

An improvement in peak time, percentage overshoot, settling time and steady-state error has been observed during the sudden application and removal of the load. The current ripples during braking modes with the proposed controller strategy are found to be less which implies the reduction of torque ripples.

CONTENTS

LIST OF TABLES

LIST OF FIGURES

ABBREVIATIONS

ADC	Analog to Digital Converter
AES	All Electric Ships
AMB	Active Magnetic Bearing
ASIC	Application Specific Integrated Circuit
AUV	Autonomous Underwater Vehicle
BLDC	Brushless Direct Current
CCS	Code Composer Studio
CSM	Continuous Sliding Mode
DC	Direct Current
DSO	Digital Storage Oscilloscope
EMF	Electromotive Force
EKF	Extended Kalman Filter
EEDI	Energy efficiency Design Index
FOSM	Fractional Order Sliding Mode
GA	Genetic Algorithm
HIL	Hardware In Loop
IFEP	Integrated full electric propulsion
IMO	International maritime Organisation
KYP	Kalman – Yakubovich - Popov
LTI	Linear Time Invariant
LMI	Linear Matrix Inequality
LQR	Linear quadratic Regulator
MCU	Microcontroller Unit
MEMS	Micro Electro-Mechanical System
MRAS	Model Reference Adaptive System
PISMC	Proportional Integral Sliding Mode Control

PMSM	Permanent Magnet Synchronous Motor
PSO	Particle Swarm Optimization
PID	Proportional Integral Derivative
PLL	Phase Locked Loop
PWM	Pulse Width Modulation
QFT	Quantitative feedback theory
SCI	Serial Communication Interface
SEEMP	Ship Energy Efficiency Management Plan
SMC	Sliding mode control
SMO	sliding mode observer
SOC	Start Of Conversion
UART	Universal Asynchronous Receiver/Transmitter
USB	Universal Serial Bus
ZCP	Zero Cross Point

LIST OF SYMBOLS

R	Stator resistance per phase in Ω,
L	Stator self-inductance per phase in Henry
M	Mutual inductance in Henry
V_a, V_b, V_c	Phase voltages in Volts in three phases A, B and C
i_a, i_b, i_c	Phase currents in Amperes in three phases A, B and C
e_a, e_b, e_c	Back EMFs in Volts in three phases A, B and C
Ep	Peak value of induced EMF
B	Flux density of the field in webers per meter squared
l	Rotor length
N	Number of turns per phase
ω	Electrical angular speed in rad/sec
Φ	Flux in webers
λ	Total flux linkage
T_e	Electromagnetic Torque
P	Number of poles
Kt	Torque constant
T_l	Load torque in Nm
K_e	Back EMF constant
V_d	DC bus voltage
J	Moment of inertia in Kg. m^2
B	Friction coefficient in Nms
M_s	Maximum value of sensitivity function
A	Maximum allowed steady state offset and
ω_b	System bandwidth

Chapter 1
INTRODUCTION

Contents

Brushless Direct Current (BLDC) motors are Permanent Magnet Synchronous machines having a trapezoidal induced electromotive force (EMF). These motors are preferred extensively because of their tremendous advantages such as the elimination of sparking, better speed versus torque characteristics, noiseless operation, better service life and rugged construction. They find a vast range of applications in industrial automation, computers, aerospace, marine electric propulsion, military etc. They also find some of the open loop applications such as fans and blowers as well as closed loop speed control applications such as fuel pumps, washing machines, dryers and electronic steering in automotive which demand high accuracy and better dynamic response. The terms sensorless BLDC motor imply the replacement of physical sensors such as hall sensors, optical encoders, and resolvers for rotor position sensing with the sensorless techniques which attract increasing research interest because of saving of cost, space and maintenance.

1.1 Scope of research

A high-performance BLDC motor should have the following features. It should be able to

- Deliver better start-up operation
- Sustain continuous operation
- Provide highest possible efficiency as well as fast speed response system
- Recover speed from disturbances

In order to achieve these features in most effective manner, the controllers are used in a BLDC motor drive. But while designing a control system, the mathematical model of the plant does not represent the completely accurate real physical system how detailed it may be. The analytical and computational models do not exactly represent the real system since there can be uncertainties due to modeling errors that can arise because of inadequate plant data, unknown dynamics of plants, complexity, non-linearity, and lack of skills for modeling. There can be other uncertainties due to sudden disturbances and sensor noise. Robust control deals with control of plants with unknown dynamics due to unknown disturbances [1]. For a control system to be stable, the position of poles is very important which should be on the left half of s plane. A small variation in the coefficients of s polynomial may move the poles to the right half of s plane which may lead to instability.

The performance specification for the control system from a system's perspective starts with stability followed by sensitivity, disturbance rejection, and noise rejection. For a system to be robust, the controller should convene stability and performance requirements when the system gains and parameters are not exactly known. In order to handle model uncertainty, the objectives such as performance and robustness have to be balanced. From the existing literature, it has been found that H infinity control, which is one of the robust control methods, has been widely used in

the speed control of various motors such as Switched Reluctance motor, Permanent Magnet synchronous motor, Brushed DC motor which acts effectively with uncertainties and modeling inaccuracies. H infinity control is a design technique with state space computational technique which utilizes frequency dependent weighting functions to tune the controller's performance and robustness characteristic [2]. It is a robust controller which is based on H infinity norm which represents the maximal gain of the frequency response of the system.

Usually, reference signals and disturbances occur at low-frequency region whereas noises and modeling errors appear at the high-frequency region. For good reference tracking, the error should be equal to zero and for good disturbance rejection, the disturbance should have a negligible effect on output. To accomplish this, sensitivity *'S'* should be made small. Similarly to be insensitive to sensor noise, modeling errors as well as to reduce control sensitivity, complementary sensitivity *'T'* should be made small. But due to the existing constraint $S+T = I$ where I is the identity matrix, both S and T cannot be made small. The trade-off is to make S small in low-frequency region and T small at high-frequency region. Since both S and T cannot be minimized over all frequencies due to design constraints, weights are introduced to shape the closed loop response characteristics [3].

The uncertainty factors due to parameter changes of motor resistance, inductance, and load of the system must be translated into weights. These weight functions are the lead-lag compensators which shape the frequency response of the system in order to obtain a minimum H infinity norm. As per state of art, no definite criterions exist for the selection of weights and also they are specific to the system. Usually, suitable weights of H infinity control are obtained by trial and error method primarily based on engineering judgement and intuition [4]. For control problems involving requirements on

both closed loop sensitivity and complementary sensitivity functions, it is not possible to arbitrarily choose weights since the two are coupled.

Optimized weight selection can be achieved using well-known algorithms. Various random search methods have been employed for improving controller's performance by obtaining the optimal values of the gains/weights. Particle swarm optimization (PSO), ant colony optimization and Genetic Algorithm (GA) are some of the optimization approaches used for obtaining optimal values of PID controller and weights of H infinity controller. [5-11]. From the literature, it has been found that PSO has a stable convergence feature in a minimum time thereby creating the best quality solution [12]. It is one of the search methods inspired by the behaviour of the swarm of particles. With the cooperation between the particles of swarm through communication and learning, the ultimate intelligence could be achieved.

The increasing concern of the environmental issues pilots the scientific community to come up with new inventions including electric propulsion in marine propulsion systems. The average loading of engines to maintain the safety margins of power generation system increases fuel consumption and environmental emissions. With the introduction of mandatory measures such as Energy efficiency Design Index (EEDI) for new ships and the Ship Energy Efficiency Management Plan (SEEMP) for all ships by the 62nd session of the International maritime Organization (IMO) Marine Environment Protection Committee (MEPC) [13], it is compulsory for the vessel owners to implement various energy efficient methods including electric propulsion in their vessels. BLDC motor is preferred in electric propulsion due to its low noise, reduced vibration, and good manoeuvrability. In these applications, the operating environment is harsh due to severe humidity, vibration or high temperature. In the case of

underwater vehicles, the use of sensors for rotor position detection increases not only the number of external wiring/connections between the motor and driver but also the maintenance requirement caused by vibration. Moreover, the sensors cannot be used in applications with the rotor in a closed housing or in applications where the motor is immersed in liquids.

Thus the scope of this research work is in following areas.

- Implementation of H infinity control theory based speed controller for achieving robust speed control in terms of better reference tracking and disturbance rejection in the presence of external load disturbances in sensorless BLDC motor drive.
- For H infinity synthesis the uncertainty factors of the system must be translated into weights. The more truthful are the weights, the better will be the H infinity control. Hence the weight selection can be treated as an optimization problem in order to obtain an optimal controller.
- The abrupt variation in load due to waves and weather is a continuous disturbance in the electrical system of marine vehicles such as submarines and AUVs. This necessitates the need for robust control in these applications.

1.2 Motivation

As the BLDC motor exhibits tremendous advantages as well as applications in every segment of market, this motor has been chosen. But the stability issues arise when disturbances and uncertainties occur in the system. The optimization of stability issues lead to the incorporation of robust control in BLDC motors. Among various existing robust control techniques, H infinity control synthesizes a robust controller which achieves stability with guaranteed performance under the influence of uncertainties in

the model of the system to be controlled or when there are external disturbances influencing the behaviour of the system. It has been found to be used in some applications such as to compensate the current disturbance, the disturbance effect due to load change, to control the speed in Permanent Magnet Synchronous Motor Servo System, to control current in active magnetic bearing system and to control speed in Switched Reluctance Motor. This control is found to be robust against load disturbances and uncertainties in measurements due to sensor noises. Though the H infinity control theory has been adopted in the form of a de-convolution filter which is being characterized by computational complexity, and a hybrid control with a combination of PI control, the implementation of H infinity controller in the speed control of BLDC motor is not found in the Literature. This led to the scope of adopting this controller for the speed control of BLDC motor in the presence of disturbances. For shaping the frequency response of the system, weight functions have to be introduced for an H infinity controller. The weight selection depends on engineering intuition and experience and there are no definite criteria for selection of these weights. The choice of these weights can be viewed as an optimization problem since the nature of the relationship between weights and H infinity performance is complex. PSO has been adopted for weight selection, as this optimization technique provides an even convergence at a faster rate.

Compared to induction machines, high- speed BLDC motors are preferred for off-shore and shipboard applications such as submarines, Autonomous Underwater Vehicles (AUV) etc., due to the better power to weight ratio, smaller size, higher efficiency, and low electromagnetic interference. Moreover, the use of sensorless technique for rotor position sensing in the BLDC motor reduces maintenance, expenses, external wiring, and space occupied. The necessity of robust control in these applications arise due to the requirement of less noise signature and vibration for

escaping from enemy detection as well as for achieving quick maneuverability and high reliability. This motivates the study of performance characteristics by simulating the proposed control strategy in BLDC motors used in submarines and AUVs.

This research work focuses on design and implementation of a robust controller based on H infinity norm as speed controller for sensorless BLDC motor drive. PSO optimization has been adopted for optimizing coefficients of weights of H infinity controller. Performance comparison of proposed controller strategy with PI speed controller with its gains optimized by PSO has been done. Validation of the controller has been done through hardware implementation. Case studies in submarines and Autonomous underwater vehicles (AUV) have been conducted through simulation, for the performance comparison of both controllers.

1.3 Problem statement

The main problem is the implementation of robust control of sensorless BLDC motor drive and its performance study in the presence of load disturbances as well as change in reference speed.

The sub problems include

- Implementation of H infinity controller as its speed controller
- Implementation of PSO for optimization of coefficients of weights of this controller in order to obtain an optimal controller.
- Experimental validation
- Simulation of case studies in underwater vehicles with electric propulsion.

1.4 Objectives

- To model a BLDC motor with the adaptation of existing sensorless algorithm for rotor position detection.
- To propose an H infinity control strategy for the robust speed control of sensorless BLDC motor drive.
- To apply PSO for weights selection of H infinity controller for the shaping of closed-loop transfer function as well as the gain selection of PI controller.
- To conduct a simulation study in order to compare the performance parameters of BLDC motor with both PI and proposed controllers.
- To implement the above control in hardware in order to validate the simulation results.
- To incorporate proposed controller in BLDC motors used for marine applications such as submarines with a standard operational profile as well as AUVs as case studies and to conduct a performance analysis through simulation.

1.5 Thesis structure

The thesis has been organized as follows.

Chapter 1: Introduction

This chapter introduces the BLDC motor with its advantages and applications. It also deals with the necessity of H infinity theory in its robust control and requirement of optimal tuning of coefficients of its weights. The scope and motivation of this research work are discussed.

Chapter 2: Theoretical Background

This chapter discusses the theory of BLDC motor speed control, H infinity control and PSO.

Chapter 3: Literature review

This chapter explores the related works done in the fields of sensorless techniques for rotor position detection in BLDC motor, application of H infinity norm in the control loop and its possible implementation in the speed control, weights optimization using search methods, existing methods of implementation in hardware and application of BLDC motors in marine applications.

Chapter 4: Design and tuning of H infinity speed controller

This chapter deals with the transfer function modeling of BLDC motor, adaptation of existing sensorless technology, implementation of H infinity speed controller and optimization of coefficients of weights using PSO.

Chapter 5: Simulation study of PSO optimized PI and H infinity speed controllers

This chapter compares the simulation results of the model by incorporating both PI and H infinity controllers as speed controllers with their gains and weights being optimized by PSO respectively.

Chapter 6: Hardware Realization of the proposed controller strategy

This chapter explains in detail about the implementation of proposed controller in hardware using a microcontroller, driver board, and BLDC motor by importing the simulation code through USB interface which provides a UART serial connection between PC and microcontroller. It also

discusses about the experimental results during a change in reference speed and under load variations thereby validating the simulation studies.

Chapter 7: Case studies

This chapter explores through simulation, the implementation of the proposed speed controller strategy in the propulsion motors of submarines with a standard operational profile and analyses the four quadrant operation of AUVs.

Chapter 8: Conclusion

This chapter summarizes the research work carried out and concludes the significant research findings.

*****

Chapter 2

Theoretical Background

Contents

In order to comprehend the speed control of BLDC motor the theoretical understanding of its working, uniform torque generation, the necessity of speed controller, need for its robust control and optimization is essential and it has been discussed briefly in the following sections.

2.1 Permanent magnet BLDC motor drive

In a BLDC motor, only two phases conduct current at a time, and the third phase is non-conducting. Since the two phases are in series with the full wave inverter, the current through these two phases is equal in magnitude but opposite in direction. The stator currents in the three phases are electronically commutated according to the rotor orientation in order to obtain a unidirectional torque. The rotor aligns with the stator flux which is being generated by the stator currents. Maximum torque is produced when the angle between stator flux and rotor flux produced by permanent magnets is 90°. Therefore it is important to know the position of the rotor in order to ensure alignment of stator flux close to 90 degrees [14].

The main attraction of this motor over other motors is its simplicity of control, as the sequence of commutation of currents in the three phases can be determined from the rotor magnet position which can be obtained from start and end of the constant portion of trapezoidal back-EMF [15]. This requires the tracking of only six discrete points in each electrical cycle

that is at every 60 degrees in a three-phase machine which is clear from the waveforms of back-EMFs and phase currents shown in Fig. 2.1. Generally, three hall sensors which are displaced from each other by 120 degrees, mounted on the shaft provide the information about rotor position. But the use of hall sensors leads to external wiring, increase in initial cost, increase in maintenance and chance of disruption in case of failure of sensors. Moreover, their use is not adaptable for submersible motors.

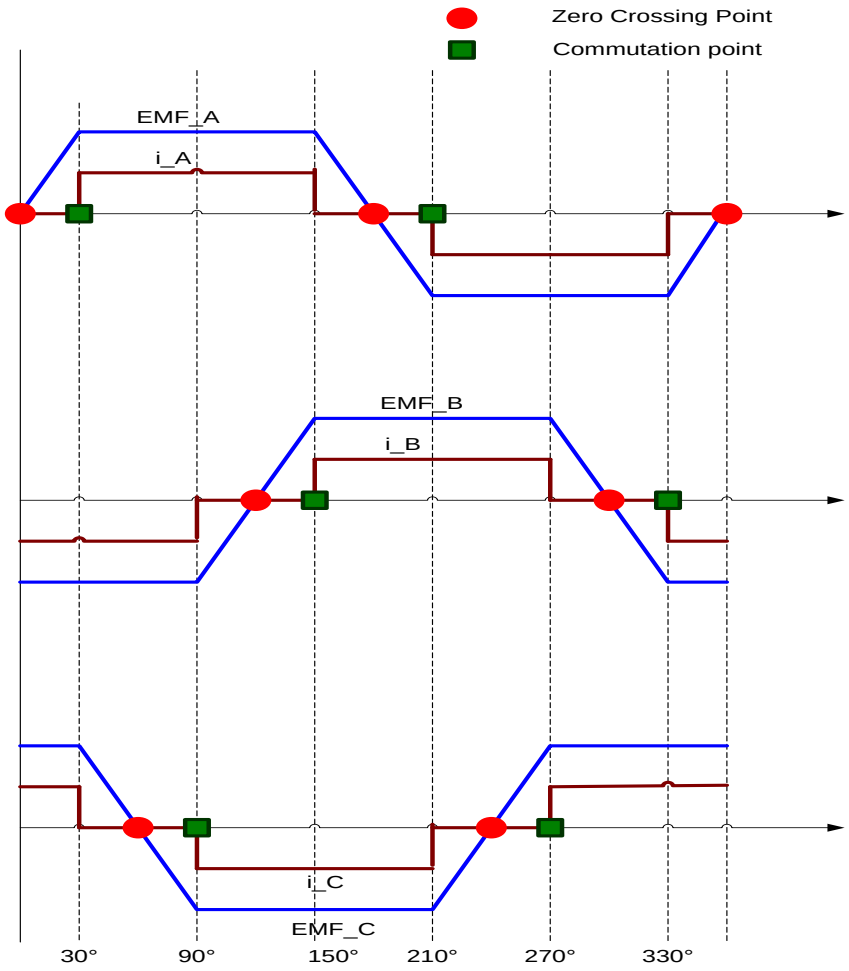

Fig. 2.1 Waveforms showing zero crossing points of back EMFs and commutation points of phase currents

Obtaining rotor position information from electrical measurements without any position sensor is the technique used in a sensorless permanent magnet BLDC motor drive. The zero crossing of trapezoidal back-EMF induced in stator winding by the movement of a permanent magnet rotor is used to detect the rotor position. When one of the back-EMF signals crosses zero, the controller should change the supply to the phases by appropriate switching whereby the process of commutation is achieved.

2.2 Speed controller for BLDC motor

There are three control loops which are to be considered in a BLDC motor control, out of which the innermost loop is to obtain rotor position. Once the rotor position is known, the magnitude of stator flux has to be controlled by controlling input current in the current loop and the outermost is the speed regulation loop. Since the rotor follows the magnetic flux vector, the speed at which the rotor is forced to the next position is determined by the strength of magnetic field which is in turn controlled by applied voltage [16]. The control of applied voltage can be achieved by switching on and off of inverter switches through high-frequency Pulse Width Modulated (PWM) pulses. The schematic diagram of the control circuit for sensorless BLDC motor drive [17] is shown in Fig. 2.2. The reference speed is compared with the speed that is being estimated using phase voltage feedback and the error is passed onto the speed controller.

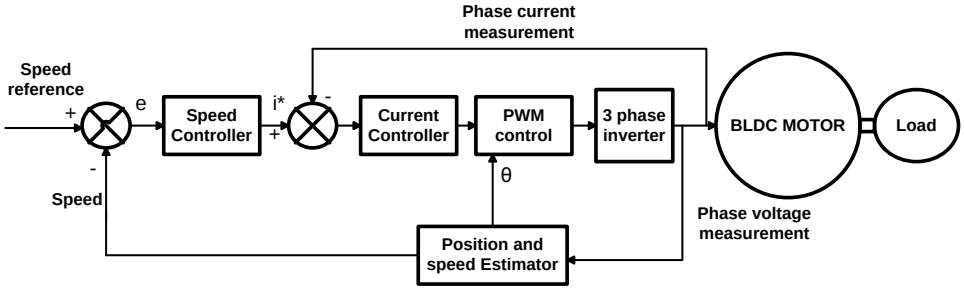

Fig. 2.2 Schematic diagram of the control for sensorless BLDC motor drive

The aim of speed controller design is to minimize the effects of disturbance and at the same time, track the speed commands with specified damping and response time. Robust control is concerned with the problem of designing control systems when there is uncertainty about the model of the system to be controlled or when there are external disturbances influencing the behaviour of the system. Models describing dynamics of systems typically contain some inaccuracies when compared with the real device. This is mostly caused by simplifications of the model, neglecting some factors influencing the dynamics or general modeling inaccuracy [18]. The modern approach to design controllers which are robust against model uncertainties is provided by adaptive control, fuzzy control, Lyapanov method, parameter estimation techniques as well as H_2 and H infinity control theory [19]. The details have been discussed in chapter 3.

2.3 H infinity controller

H infinity controller provides maximum amplification of sinusoidal signal of frequency ω as it passes through the plant. H infinity is the Hardy space with the infinite norm. The infinity norm of the system G(s) exists if and only if G(s) is proper with no poles on the imaginary axis. Let *P* be a Linear Time Invariant (LTI) system which comprises subsystems that are involved in the interconnection. Let *K*, *u* and *y* represent controller, control input and measured output respectively. *w* can be exogenous inputs like reference commands, load disturbances, and sensor noise whereas the robust output variable *z* can be tracking errors, performance variables, and actuator signals [20]. From the H infinity control problem which is the closed loop interconnection as shown in Fig. 2.3, the primary aim of the controller design is to achieve a robust output *z*, that is independent of *w*.

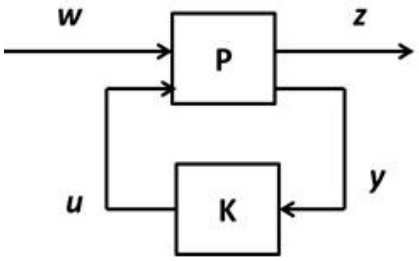

Fig. 2.3 Block diagram showing H infinity control problem

If P is partitioned as

$$P = \begin{bmatrix} P_{11} & P_{12} \\ P_{21} & P_{22} \end{bmatrix} \tag{2.1}$$

From Fig. 2.3, it can be written as

$$\begin{bmatrix} z \\ y \end{bmatrix} = \begin{bmatrix} P_{11} & P_{12} \\ P_{21} & P_{22} \end{bmatrix} \begin{bmatrix} w \\ u \end{bmatrix} \tag{2.2}$$

and

$$u = Ky \tag{2.3}$$

Then,

$$z = P_{11}w + P_{12}u \tag{2.4}$$

$$y = P_{21}w + P_{22}u \tag{2.5}$$

Substituting for u in equation (2.5), we get

$$y = P_{21}w(1 - P_{22}K)^{-1} \tag{2.6}$$

From equations (2.3), (2.4) and (2.6), we get

$$z = w[P_{11} + P_{12}K(1 - P_{22}K)^{-1}P_{21}] \tag{2.7}$$

$$z = wF_l(P, K) \tag{2.8}$$

Where F_l represent lower linear fractional transformation. From equation (2.8) it is clear that to minimize error *z* due to *w*, the function $F_l(P,K)$ has to be minimized.

Therefore the objective of H infinity control design is to obtain a controller *K* such that H infinity norm of $F_l(P,K)$ is minimized over the space of all realizable controllers *K(s)* that stabilize the closed-loop system. This norm is minimized when the input signal is normalized to unity, which implies the maximum energy gain between disturbances and performance outputs are minimized [21] which can be mathematically expressed as

$$min\ \|F_l(P,K)\|_\infty = min(sup\ \ \bar{\sigma}\big(F_l(P,K)(j\omega)\big) \tag{2.9}$$

This can be achieved by solving Ricatti equations which is being done by tools supplied by MATLAB robust control toolbox [22]. MATLAB script '*hinfsyn'* provides exact frequency domain loop shaping with appropriate weighting functions. The limitations of using '*hinfsyn'* are that the plant must be

(a) stabilizable from the control inputs u and

(b) detectable from the measurement output y.

This MATLAB function '*hinfsyn'* employs γ iteration technique which is a bisection algorithm starting from high and low values of H infinity cost γ in order to achieve an optimal H infinity controller. At each iteration, the algorithm checks there exists a solution for a given γ. The following conditions are checked while finding a solution with Riccatti equation 'ric' method [23], [24].

- H and J Hamiltonian matrices (which are formed from the state-space data of P and the γ level) must have no imaginary-axis eigenvalues.

- The stabilizing Riccati solutions X_∞ and Y_∞ associated with the Hamiltonian matrices must exist and be positive, semi-definite.
- Spectral radius of (X_∞, Y_∞) must be less than or equal to γ.

This algorithm stops when the relative error tolerance for γ is less than TOLGAM (default=0.01). But the function '*hinfsyn'* does not claim a fully well-posed optimization setup. This is because H infinity norm has a uniform bound over all the frequencies on the transfer function. Due to bandwidth limitations of actuators and sensors, it is required to track signal of frequencies to a certain bandwidth [2]. Under these situations, the straightaway implementation of H infinity control may lead to a non-optimal solution. This necessitates the inclusion of weighting functions which are typically first order filters. As per state of art, no definite criterions exist for the selection of weights and also they are specific to the system.

2.4 Particle Swarm Optimization

For the tuning of coefficients of weights, PSO has been employed in this work in order to obtain an optimal controller. A group known as the swarm of random individuals referred to as particles is initialized in PSO. Each particle is a possible candidate solution for the optimization problem. The mathematical model is based on the following information.

- Current Position $\overrightarrow{x_i}(t)$
- Current velocity $\overrightarrow{v_i}(t)$.
- Personal Best $\overrightarrow{p_i}(t)$
- Global Best $g(t)$

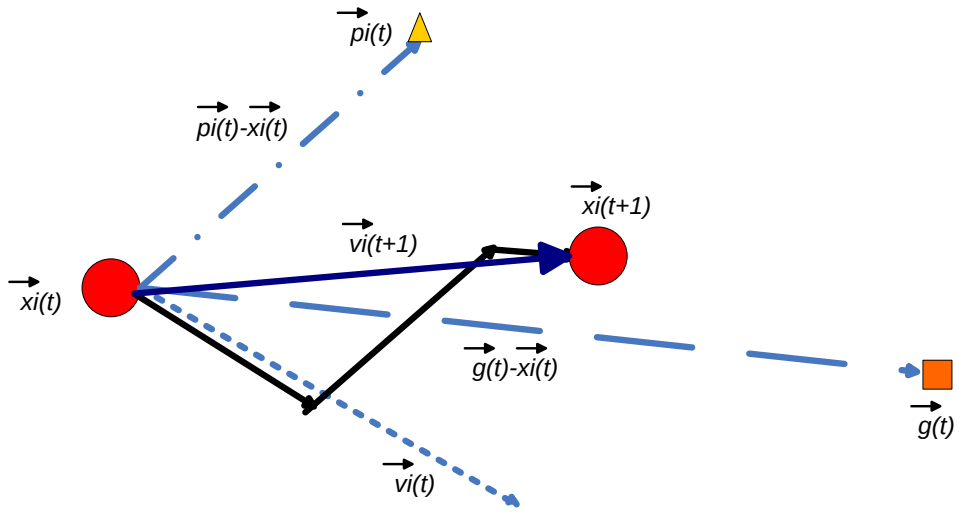

Fig. 2.4 Mathematical model depicting PSO

The mathematical model of PSO is shown in Fig. 2.4. A particle *i* has a current position $\overrightarrow{x_i}(t)$ and it is moving with a current velocity $\overrightarrow{v_i}(t)$. In addition to position and velocity, each particle has a memory about its personal best which is denoted by $\overrightarrow{p_i}(t)$. This is the best experience that the particle had undergone. Apart from this, there is another memory about the best experience undergone by the members of the whole swarm which is represented by $g(t)$. On every iteration of PSO, the position and velocity of each particle have been updated based on this information. From Figure 2.4, the following vectors can be obtained.

- The vector from the current position to personal best = $\overrightarrow{p_i}(t) - \overrightarrow{x_i}(t)$
- The vector from the current position to global best = $g(t) - \overrightarrow{x_i}(t)$
- The current velocity $\overrightarrow{v_i}(t)$

Each particle moves towards a new position parallel to these three components. The new velocity $\overrightarrow{v_i}(t+1)$ can be obtained by adding these three vectors from initial position $\overrightarrow{x_i}(t)$ to newly updated position $\overrightarrow{x_i}(t+1)$.

The new velocity can thus be obtained as

$$\overrightarrow{v_{ij}}(t+1) = \underbrace{\omega\overrightarrow{v_{ij}}(t)}_{(a)} + \underbrace{r_1 C_1(\overrightarrow{p_{ij}}(t) - \overrightarrow{x_{ij}}(t))}_{(b)} + \underbrace{r_2 C_2(\overrightarrow{g_j}(t) - \overrightarrow{x_{ij}}(t))}_{(c)} \quad (2.10)$$

Hence the equation for updating the position of the particle is given by (2.11)

$$\overrightarrow{x_{ij}}(t+1) = \overrightarrow{x_{ij}}(t) + \overrightarrow{v_{ij}}(t+1) \quad (2.11)$$

The subscript *ij* represents i^{th} particle with j^{th} component, ω represents inertia coefficient, r_1 and r_2 are uniformly distributed random numbers in the range 0 to 1, C_1 and C_2 are acceleration coefficients. The term (a) in equation (2.10) represents inertia term, (b) represent the cognitive component and (c) represent the social component [25] - [27]. The result is that each particle fly towards a minimum thereby searches for the best solution. The closeness of a particle to the global optimum is measured using a predefined fitness function.

Chapter Summary

The theoretical background of BLDC motor, its commutation points, role of speed controller, H infinity controller, necessity of weight selection, and the mathematical model of PSO for optimization of weights have been discussed in detail.

*****

Chapter 3

Literature Review

Contents

In this study, the state of art of research in the field was investigated topic wise starting from rotor position sensing of BLDC motors using sensors and sensorless techniques, robust control of BLDC motor, applications of H infinity control theory, selection of weights and optimizations of gains of PID controller. Various techniques adopted in the implementation of controller in hardware, and adaptations of BLDC motors in electric propulsion that have been found in literature are also studied in order to understand the chronological development in the field.

BLDC motors are constructed just like AC synchronous motors having permanent magnets on the rotor and 3 phase coils wound on a cylindrical shaped magnetic core forming armature windings on the stator. They have a typical trapezoidal back-EMF. Commutators and brushes are responsible for mechanical commutation in a Brushed DC motor whereas a three phase inverter and a rotor position sensor are responsible for the electronic commutation of BLDC motors. In order to produce constant unidirectional torque, stator excitation of BLDC motor has to be

synchronized with rotor speed and position. There are two ways of rotor position sensing in a Brushless DC Motor, which are by use of sensors and by sensorless methods.

Normally a BLDC motor drive uses one or more sensors giving positional information for proper commutation. Such implementation of sensors in a motor is expensive and also results in increase in size of the motor. Moreover the sensors cannot be used in applications with rotor in a closed housing or in submersible motors. Therefore position sensorless control technology currently becomes one of the most promising trends of BLDC motor control system.

3.1Rotor position detection using sensors

The position information obtained from rotor position sensors is used to generate precise firing commands for the power converter, ensuring drive stability and fast dynamic response and maximum torque.

Pragasen Pillay *et al* [28] presented the modeling, simulation and analysis of BLDC motor using hall sensors for detecting the rotor position. A novel three branches vertical Hall sensor for brushless motor control which gives three position signals phase shifted by 120 degrees, corresponding to the motor driving signals has been presented [29]. Devendra. P *et al* [30] introduced an algorithm which used the hall sensor signals to control BLDC motors with additional features like auto restart and auto power down while maintaining constant speed. A Fuzzy logic PID (Proportional Integral Derivative) controlled Brushless DC Motor drive has been developed based on state space model where the rotor position is determined by three hall sensors [31], [32]. Mohd Tariq *et al* [33] presented the complete analysis of six modes of operation of six switch inverter with position of rotor signals obtained from hall sensors. Some of the rotor position detection techniques

other than hall sensors include a hybrid sliding mode observer with hall sensor, and a wireless sensing node integrated with a MEMS (Micro Electro-Mechanical System) sensor which uses induction power generated by the motor's shaft rotation have also been reported [34], [35].

The merits of the rotor position detection using sensors are fast response time, reduction of sensitivity to packaging stresses and less noise. The demerits of using sensors are they are expensive, occupy space and their sensitivity depends on the distance at which they are mounted and cannot operate at high temperature.

3.2 Rotor position detection using sensorless techniques

Obtaining rotor position information from electrical measurements without any position sensor is the technique used in a permanent magnet brushless sensorless drive.

Various aspects of BLDC motor control which include types of PWM techniques used, methods for rotor position detection, initial rotor position detection methods, recent advances in the position sensorless control of BLDC motors, the expected future research works to provide insight in sensorless drive techniques and their benefits have been discussed in the literature [36] – [40].

The research efforts carried out on the three basic types of sensorless control schemes that are found in the literature are described below.

3.2.1 Position estimation using inductance measurements and flux measurements

The inductance of a phase which includes both self and mutual inductances and hence the flux linkage, varies with the rotor position. The flux linkage is calculated using measured voltages and currents. From the initial position, machine parameters, and the flux linkages' relationship to

rotor position, the rotor position can be estimated. Since flux linkage is independent of speed, it is used to detect the rotor position at low speeds.

Tae-Hyung Kim *et al* defined a flux linkage function which is speed independent to control BLDC motors at low speed operations [41]. Extraction of commutation signals directly from the specific average line to line voltages with simple RC circuits and comparators has been proposed. This method is insensitive to common mode noise since the neutral voltage is not required [42]. Wang H. B *et al* proposed detection of zero-cross point of back-EMF from the rotor position where the rotor reaches the equal self-inductance position. This method does not depend on the back-EMF and it can be operated at very low speeds but torque ripple is bigger than that in the conventional method [43]. The position-sensorless direct torque and indirect flux control of BLDC motor by estimating the electrical rotor position using winding inductance and stationary reference frame stator flux linkages and currents has been investigated [44]. Though this method is speed independent it has a drawback of significant estimation error at low speed.

3.2.2 Research efforts on back EMF detection

The zero crossing of trapezoidal back-EMF induced in stator winding by the movement of a permanent magnet rotor is used to detect the rotor position. When one of the back-EMF signals crosses zero, the controller should change the supply to the phases by appropriate switching whereby the process of commutation is achieved. The back-EMF detection methods can be classified into direct and indirect back-EMF detection.

Direct back-EMF detection usually uses hardware low pass filter or software detecting method to filter out the noise signal. Jianwen Shao *et al* proposed a method to detect the motor back-EMF during PWM "off" time at start-up and low speed, and during PWM "on" time at high speed [45], [46]. Zicheng Li *et al* proposed line-to-line back-EMF calculation for BLDC

motor drives and demonstrated that the zero-crossing of line-to-line back-EMF is actual commutation instant [47].

Ming Lu *et al* [48] proposed two methods for extracting the true back-EMF Zero Cross Point (ZCP) by detecting voltage difference between the terminal voltage of the floating phase and the control voltage modulated by buck modulator as well as by detecting ZCP of line voltage between two floating phases. A new sensorless control based on coordinate transformation where the rotor-position signals are constructed by the two-phase terminal voltages which can be used for commutation and a modified six-step square wave pattern with pulse-width modulation to simplify the conventional coordinate transformations technique have been developed [49], [50]. Obtaining a differential signal by manipulating the three phase voltages, the line voltage difference, back-EMF difference and by calculating the sum of the terminal voltages of the motor are some of the techniques used for detection of back-EMF ZCP [51] - [55].

Merits of direct back-EMF detection methods are that it is easy to detect the ZCP of the phase back-EMF indirectly by utilizing the terminal voltage since the neutral point is required in order to extract back-EMF directly which is not offered in the manufacturing process of a motor. Demerits of this method are that it tends to have a narrow speed range and poor start-up characteristics. Moreover, the estimated commutation points that are shifted by 30 ° from zero crossing of indirect back-EMF have position error in the transient state.

Indirect back-EMF detection method utilises the signals such as third harmonic signal of back-EMF which keeps a constant phase relationship with the rotor flux for any speed and load condition or current flowing through a freewheeling diode in silent phase when the active phase switches are turned off to obtain the ZCP of back-EMF.

Detection of position information on the basis of the conducting state of the freewheeling diodes connected in antiparallel with power transistors has been proposed [56]. Shen J. X. *et al* [57] proposed the ASIC (Application-specific integrated circuit) integrated with a phase locked loop (PLL). This setup detects the terminal voltage of the un-energized winding which contains the information about the back-EMF to ensure the exact commutation sequence of BLDC motor. This method reduces commutation retarding and improves the motor performance. A novel sensorless scheme using back-EMF mapping with six-step control has been presented where all commutation instances, corresponding to 30 electrical degrees, at various speeds can precisely be calculated using a single known reference slope and a back EMF point considered at the same speed [58]. Ashish P. R *et al* proposed the sensorless operation using the third harmonic back-EMF as the zero crossings of the third harmonic component occur at 60 electrical degrees, exactly at every desired current commutation instant [59].

Advantages of indirect back-EMF detection methods are that they are free of noises and hence require a small amount of filtering. Third harmonic signal can be detected and processed at low speeds and hence starting of motor is superior. There is no need to access stator neutral. Disadvantages are that when the speed is very low or when load varies; the back-EMF voltage is found to be distorted. In both cases the commutation signal are not precise to locate. The most serious drawback of freewheeling diode conduction method is the requirement of six additional isolated power supplies for the comparator circuitry to detect current flowing in each freewheeling diode.

In general, back-EMF sensing method is a sensorless method hence cost is reduced and space is saved. But it has some disadvantages such as since back-EMF is zero at standstill and proportional to speed, zero crossing

of back-EMF is difficult to detect at very low speeds. Moreover there exists the rotor position detecting error when low-pass or band-pass filters are employed to get zero crossings.

3.2.3 Research efforts on Estimation and model based observers

Various strategies of rotor position sensing based on estimators and model based observers are discussed below.

Sliding mode control (SMC), is a nonlinear control method that changes the dynamics of a nonlinear system by application of a discontinuous control signal thereby forcing the system to "slide" along a cross-section of the system's normal behaviour. This control can be used in the design of state observers. These non-linear high-gain observers have the ability to bring coordinates of the estimator error dynamics to zero in finite time.

A hybrid rotor position self-sensing approach for full speed range by combining stator core saturation method and sliding mode observer (SMO) method has been developed [60]. The application of proportional integral sliding mode control (PISMC) techniques for controlling the rotor position of Permanent Magnet DC motor drive system has been studied [61]. Deenadayalan A. *et al* [62] introduced speed component in the back-EMF observer gain thereby modifying the sliding mode observer, which eliminates multiple zero at low speeds and phase shift at higher speeds.

Sliding mode control is characterized with order reduction, disturbance depression, insensitivity to parameter alterations, and it requires lesser amount of information. Disadvantages of this method are chattering problem and exhibition of multiple zero crossing in back-EMF which leads to commutation problem at low speed.

Extended Kalman Filter (EKF) is an optimal recursive estimation algorithm for nonlinear systems that are disturbed by random noise.

Dhaouadi R *et al* [63] designed the extended Kalman filter for the on-line estimation of the speed and rotor position by using measurements of the motor voltages and currents of a permanent magnet synchronous motor (PMSM) without a position sensor. The online estimation of speed and rotor position of the BLDC motor based on the application of the EKF has been reported in the literature [64] – [66].

Its advantages are easy usage, proper working in practical estimation problems and computational efficiency. It has demerits such as less responsive to systems with considerable non-linearities, measurement model and dynamic model functions need to be differentiable, estimation accuracy decreased at lower speeds, computationally intensive, has a high degree of dependence on the motor's parameter and requires proper initialization.

Model Reference Adaptive System (MRAS) estimator creates a closed loop controller with parameters, that can be updated based on the error between output of the system and reference model to change the response of the system. The idea is to converge the parameters to ideal values so that the plant response matches the response of the reference model.

Mohamed Rasheed *et al* [67] proposed an indirect-rotor-field-oriented-control scheme for sensorless speed control of a PMSM by estimating the rotor-flux position by direct integration of the estimated rotor speed. The rotor-flux speed and magnitude are estimated adaptively using stable model reference adaptive system estimators. Kojabadi H.M [68] presented an active power equation and model reference adaptive system approach to estimate the rotor resistance of an induction motor. G. Sunil *et al* [69] proposed a speed estimation algorithm based on MRAC (Model Reference Adaptive Control) to correct the speed error estimated using back- EMF which has an advantage of being responsive to both low speeds and high speeds.

The attracting feature of MRAS method is its desired closed loop performance. The structural limitation of Model Reference approach is the "tuned system" to which MRAS converge under a model matching design rule may not have an acceptable level of stability robustness or an acceptable sensitivity function.

Back-EMF observer methods can be used for real-time estimation of the rotor position and speed. The trapezoidal back-EMF is modelled as an unknown input and the proposed unknown input observer estimates line-to-line back-EMF as well as phase back-EMFs in real time to detect the rotor position [70], [71]. Cassio Luciano Baratieri *et al* [72] used a new BLDC motor dynamic model expressed in a synchronous reference frame with back-EMF vectors. Samuel Wang *et al* [73] proposed a new back-EMF difference detection method based on disturbance observer structure which can detect the back-EMF as well as back-EMF difference signal.

Rotor position detection based on estimators and observers has high performance at low speed range as the information of rotor position is calculated independently of the rotor speed.

3.3 Initial rotor position detection

Initial rotor position information is essential for BLDC motor in order to ensure its stable operation. An estimator based on the variation of the current response caused by the magnetic saturation of the stator core of the BLDC motor, a method based on simple detection and comparison of phase voltages and dc link current responses thus relating it with stator inductances, a start-up method based on improved inductance method and EMF integration [74] – [76] are some of the methods proposed in the literature for initial rotor position detection.

3.4 Robust control of BLDC motor

Due to the non- linearity that exists in the design of speed and position control of BLDC motor, various robust control techniques have been proposed and validated in the literature.

Designing of a robust Fuzzy speed controller of BLDC motor described by Takagi-Sugeno (TS) Fuzzy model has been carried out by Wudhichai Assawinchaichote *et al* Sufficient conditions for BLDC motor to achieve H infinity performance have been derived using Linear Matrix Inequality (LMI) approach in order to overcome the effects of non- linearity and disturbance [77].

A robust sliding mode controller in which the linear control component optimized by LMI has been developed by H M Soliman *et al* in order to challenge system uncertainty due to changes in load inertia [78]. An experimental validation of continuous sliding mode (CSM) and fractional order sliding mode (FOSM) controller in the speed control of BLDC motor has been carried out in order to prove the better trajectory tracking performance of FOSM compared with CSM [79].

For achieving robust position tracking system of BLDC motor, in the presence of disturbances such as friction and backlash, a robust linear quadratic sliding mode controller has been proposed [80]. This control algorithm combines a linear quadratic control and non-linear sliding mode control. An LQ controller along with a load observer in order to detect load disturbance has been presented for robust position control of BLDC motor [81].

An expression for speed dependent sampling rate system has been derived which focuses on the importance of presence of uncertainties resulted from variable sampling rate. The micro controller synthesis has

been employed in order to attain a robust controller for BLDC motor [82]. The effect of system nonlinearities due to reluctance variations and magnetic saturation have been accounted for developing a feedback control law based on transformational theory of non-linear systems [83]. This law has been appended to overall control structure in order to obtain a better tracking system in the presence of modelling errors and pay-load uncertainties.

P. Bharat Kumar *et al* proposed a Quantitative feedback theory (QFT) based controller for the robust control of BLDC motor and compared it with various control techniques such as Fuzzy controller and Genetic Algorithm based controller. The step response characteristics of QFT were found to be better than other control techniques [84]. A control law has been formulated by Vishnu C S *et al* [85] in order to minimize the performance index thereby, achieving robust and optimal control. The speed of BLDC motor has been controlled using a linear Quadratic Regulator (LQR) and a Linear Quadratic Gaussian (LQG) controllers. In order to overcome state error caused by parameter variations and forced disturbances, a dual passive adaptive control loop has been proposed by Kiyoshi Ohishi *et al*. [86]

Thirusakthimurugan P. in his thesis [87] proposed robust control scheme of Permanent magnet BLDC motor which included a cascade control structure with generalized predictive control (GPC). MozaffariNiapour S. A. KH. *et al* [88] proposed a novel robust stochastic H infinity deconvolution filter for sensorless BLDC motor drives with the aim of improving the robustness and dynamic performance in a vast speed range. In order to optimally tune the PID speed controller parameters, Genetic algorithm with H infinity norm as the optimization objective has been proposed [89].

3.5 Application of H infinity control theory to motors and other systems

H∞ control theory which is one of the robust control techniques has been widely used in the speed control of various motors including Permanent magnet DC motor, Permanent magnet Synchronous motor, Switched Reluctance motor, Brushless DC motor. This theory has also found its applications in active magnetic bearing position control, vertical aircraft control Electric vehicles etc.

H infinity control theory has been applied to DC motor speed control system to get controller which acts effectively with control object including uncertainties and modelling inaccuracy [90] - [92]. Ashu Ahuja *et al* proposed an approach that poses the design problem as a controller for DC Motor Speed Control with mixed sensitivity H∞ method. Particle Swarm Optimization (PSO) and Genetic Algorithm (GA) are adopted to solve the optimization problem for finding the optimal controller [93].

Liu Bingyou proposed a robust control strategy for Permanent Magnet Synchronous Motor Servo System in which the current disturbance was compensated by the H infinity tracking controller [94]. A robust H infinity controller that can be adopted to control the speed of Permanent Magnet Linear Synchronous motor has been designed [95], [96]. Huaiquan ZANG *et al* designed a robust H-infinity controller based on genetic algorithm optimization for space vector control model of permanent magnet synchronous motor to improve the speed of tracking performance [97].

Rajendran A. *et al* proposed control technique to identify the position of the rotor whose variation is identified from the speed performance of the motor and obtained the optimal transfer function matrix weight by genetic algorithm (GA) [98], [99].

Safanah M. Raafat *et al* developed a design procedure that considers intelligently estimated uncertainty bounds and optimized performance weighting function in H infinity robust controllers for single axis servo positioning system [100]. Guangzhong Cao *et al* developed the robust control of current-controlled active magnetic bearing system using H infinity controller [101].

3.5.1 Selection of weights

In H infinity control design, the weights are tuned in order to obtain satisfactory performance margins such as rise time, percentage overshoot, settling time and steady state error. But the adjustment of these weights is based on experience and engineering intuition. There is no hard and fast rule for weight selection. This leads to control engineer to rely upon his engineering judgement. Many researchers addressed this problem by various methods, which have been detailed below.

Jiankun Hu *et al* proposed a novel method for the selection of weighting functions in H infinity mixed sensitivity design to control the percentage overshoot directly by the roll-angle control design of a vertical take-off aircraft. It has been observed that a definite relationship between weighting function and percentage overshoot holds good only if a pair of dominant poles is present in the plant [102].

Guang-Ren Duan *et al* [103] addressed the robust stabilization of active magnetic bearings (AMB) by appropriate selection of the free parameters in the robust controller. Sarath S Nair *et al* proposed an algorithm for the synthesis of Robust H infinity controller along with a novel automatic weight selection algorithm [104], [105].

A first order approximation of the controller is a function of small weight adjustment done in the initial control design problem itself. This

avoids the next step of synthesis involving the adjusted weights [4]. Various parameters involved in H infinity controller design such as relative weights between input and outputs, frequency dependent weightings, magnitudes and structures for the plant uncertainties etc., have been discussed in detail [3], [106]. Selection criteria for weight selection depending upon the frequency ranges has been elaborated thoroughly. PSO based weight selection has been implemented for pneumatic servo system in order to track the reference signal, reject disturbances and to provide robust performance in the presence of model uncertainties [107]. A design procedure that considers intelligently estimated uncertainty bounds and optimized performance weighting function in H infinity robust controllers for single axis servo positioning system has been reported [108]. GA based weight selection for H infinity control technique has been proposed by Anna-Karin Christiansson et al. It has been found that reasonable control energy can be used with H infinity control with its weights being optimised by GA [109].

3.6 Optimization of gains of PID speed controller

Though PID controller is one of the widely used controllers because of its simplicity, the tuning of gains of this controller poses a problem. Usually it has been tuned by trial and error method based on the experience of the control engineer. Various tuning strategies have been found in the literature including Ziegler- Nichols method, PSO, GA optimization techniques and generalized KYP (Kalman-Yakubovich–Popov) synthesis [12], [110] - [116]. PSO technique to tune the parameters of PID controller is one of the commonly implemented technique because of its ability to avoid premature convergence of GA and to provide high quality solution with better computation efficiency [117] - [120].

3.7 Hardware implementation

The hardware realization of the motor with these control techniques is inevitable for proper validation of its performance on load. For hardware implementation of speed controller, various microcontrollers have been found in the literature. An ARM 2148 microcontroller along with HPCL 3120 MOSFET driver circuit has been used in a BLDC motor with hall sensors for position sensing and with a dynamometer as brake, to study its speed torque characteristics with the motor running in either direction [121]. Sensorless BLDC motor control has been achieved using TMS320F240 in which the zero crossing of back EMF in non-fed phase has been computed by subtracting neutral voltage from voltage in non-fed phase. An imbalance corrector module has to be incorporated [122], [123]. PIC16F877A microcontroller has been used in the hardware implementation of speed controller of BLDC motor using PI controller [17]. A spartan-3 FPGA is used to generate the firing pulses for the MOSFETs of three phase fully controlled bridge which in turn control the speed of BLDC motor [124]. TMS320C242 DSP Controller has been used for providing Hall Effect sensor output equivalent position information. The six commutation instants can be obtained by an algorithm which involves the calculation of neutral point voltage and thereby attaining back EMF of the non-fed phase [125].

Various current sensing techniques for torque / current control in order to implement efficient closed loop control have been discussed in the literature. In order to achieve linear torque control, it is essential to obtain the average phase current feedback to the current regulator.

A maximum value of current has been generated based on a mean DC component from quasi square wave currents which directly controls maximum torque [126] - [128]. This has been found to be improving efficiency as well as reducing acoustic noise. The three phase current values have been generated

from a single sensor placed on the DC link. This avoids the imbalances in the phase currents thereby reduces the pulsating torque [129] - [131]. Since the DC link current does not reveal the phase current values during PWM "off time", this has been sampled at the midpoint of PWM "on time". This method of sampling provides average load current since the load current flows through DC link only during PWM "on time" [132].

Implementing the current sensing amplifiers in low-side of the inverter in series with the switches, one in each leg, high-side of the inverter in-line immediately after the supply voltage and in-line with the motor terminals have been discussed in detail by Jason Bridgmon *et al* [133], [134]. Various current control regulators have been used in the literature for current control in the inner loop such as hysteresis current controller [135], [136], constant inverter switching frequency predictive current controller [137] - [140], fuzzy logic based current controller [141] - [145], and Neural network based current controller [146] - [150]. The parameters of PI controller have been tuned using SNR (Signal to Noise Ratio) optimization technique in order to obtain optimal performance characteristics [151].

3.8 Studies on BLDC motor under loaded conditions

The variation in speed torque characteristics, current drawn by the motor and back EMF have been analysed under no load as well as loaded conditions with both aiding and opposing loads by conducting a simulation study in SIMULINK/MATLAB. [152]. A self- tuning fuzzy PID controller has been compared with model reference adaptive control with PID compensator for good reference tracking under load disturbances and parameter variations [153]. A PISMC current control scheme has been experimentally validated for efficient speed tracking using National Instruments Data Acquisition Card 6229 as the interface with MATLAB environment [154]. An experimental study of BLDC motor using ARM

controller and HPCL 3120 driver with the motor being rotated in both forward and in reverse directions under various load torque conditions and the corresponding speed torque characteristics have been studied [155]. Since the BLDC motor has the disadvantage of jerky behaviour during sudden application and removal of load, a comparative study has been conducted with conventional PID controller and a Fuzzy PID controller under these conditions. It has been found that gradual removal of load minimizes jerks with Fuzzy PID controller when compared with sudden application of loads [156].

3.9 Marine electric propulsion

The importance of environmental concerns such as reduced emission, spill and damage to coral reef while anchoring and the requirement of less vibration as well as noise signatures to provide on board comfort in cruise vessels, yachts, leisure boats, warships and submarines lead to the necessity of electric propulsion. The evolution of electricity in marine vessels in the form of light bulbs to the era of purely battery driven all electric ships (AES) and the evolution of electric warships including submarines has been detailed [157], [158]. In the present scenario, electric propulsion is used in cruise vessels, ferries, dynamic positioning drilling vessels, shuttle tankers, pipe layers; icebreakers supply vessels and warships [159]. Integrated full electric propulsion (IFEP) system uses advanced electric motors such as induction motors and permanent magnet propulsion motors [160], [161]. A detailed study of all electric ships and hybrid electric ships has been carried out in order to analyse the type of energy used to charge batteries and total space occupied by the system [162].

3.9.1 Submarines

The impacts of electric propulsion in submarines such as efficiency, volume and weight using electric motors with different pole pairs have been examined [163]. The potential of energy saving in submarines with the use of BLDC motors have been elaborately discussed in literature. In a submarine, a drive that works efficiently with very low noise signatures is essential for long dives and for achieving challenging boat detection by enemies [164], [165]. A configuration of a set of two mechanically coupled BLDC motors with ratings equal to one third and two third of a single motor rating with a proper design of control algorithm in order to increase efficiency of submarine propulsion system has been proposed [166]-[170].

In order to study energy and data hybrid transmission technology in submarines, a submarine motor control system has been developed combining hybrid transmission technology and BLDC motor control technology. The high voltage DC power transmission and high speed data have been coupled on the same single coaxial cable by capacitance [171].

3.9.2 Autonomous Underwater Vehicle (AUV)

In recent years, a lot of research work is going on in trajectory tracking control laws and path following techniques of Autonomous Underwater Vehicle (AUV) for precise maneuvering. A mission control system controls various units such as navigation, vehicle guidance and control, actuator control, data logging, communication, environmental inspection and vehicle support systems [172], [173]. Of these, vehicle guidance and control block provides the reference speed to be achieved based on the reference trajectory inputs from mission control system and navigation system to the actuator control system. This is necessary for the proper trajectory tracking in the presence of uncertainties such as variation in vehicle parameters and external disturbances like varying sea currents and

weather disturbances. An optimal disturbance rejection control has been derived from Riccatti and Sylvester equations for achieving optimal control in the presence of external wave disturbances [174]. To maintain the position of AUV at a perticular depth, the scaling factors of Fuzzy logic controller have been tuned with a radial basis function metamodel and a comparative study has conducted with offline optimization approach using genetic algorithm [175].

Thruster motors with dedicated controller play an important role in the propulsion of AUV for maintaining the speed. Brushless Direct Current motors with hall sensors used as thruster motors have been found in the literature for propelling AUV [176]. The electrical and mechanical systems of a hydro quad rotor has been designed and implemented using BLDC motors as thruster motors in order to study its static stability at various depths [177]. A seven phase BLDC motor for the propulsion of AUV has been functionally modelled and simulated in MATLAB/SIMULINK for studying its dynamic characteristics [178]. The analysis of electrical characteristics using Finite Element Analysis along with a comparative analysis of PI and Fuzzy controller has been done for a seven phase BLDC motor [179]. The simulation model of a BLDC motor which is mechanically designed as a low cost thruster in AUV has been studied for its compatibility in a depth of more than 1 meter [180]. A prototype of electrical thrusters using permanent magnet BLDC motor has been designed and implemented with 2D Finite Element Method in order to optimize the speed and torque ranges, to minimize cogging torque and to maximize efficiency [181].

Chapter Summary

A detailed study of the research work in the field of robust control of BLDC motor with sensorless drive has been carried out in order to have a

deep understanding. The merits and demerits of using hall sensors for rotor position detection have been discussed. Various sensorless techniques available in rotor position detection have been studied and found that the back EMF detection using line voltage difference has been favorable since it provides the exact commutation points avoiding phase correction circuitry. For addressing stability issues during change in reference speed and external load disturbances, various robust control techniques have been analyzed. It has been found that H infinity controller addresses these issues with good performance and stability. Since the selection of weights of H infinity controller is based on engineering intuition, the optimization technique PSO has been adapted. Marine electric propulsion is one of the major developments in the shipping industry due to environmental concerns. The use of BLDC motor in underwater applications for example submarines and AUVs is solicited because of its advantages such as low EMI, less vibration, low noise, high efficiency and low maintenance.

*****

Chapter 4

Design and Tuning of H Infinity Speed Controller

Contents

The mathematical model of BLDC motor speed control system with the incorporation of H infinity speed controller is discussed in detail. The corresponding SIMULINK models developed are also presented. Optimization of coefficients of weights of H infinity controller and gains of PI controller using PSO is elaborated with corresponding flowcharts.

4.1BLDC motor speed control system

Generally the main components in a BLDC motor control system include power converter, rotor position sensing, controller and motor as shown in Fig. 4.1. Here the power converter is the inverter which converts power from DC source to AC source for applying three phase power to three phase windings of Permanent Magnet BLDC motor. Only two of the three phase windings are energized at a time based on the rotor position and corresponding six step commutation has been achieved at every sixty degrees as shown in Table 4.1. The inverter MOSFET switches are switched on and off according to the commutation signals and thereby the stator windings are given the supply sequentially in order to produce uniform rotational torque.

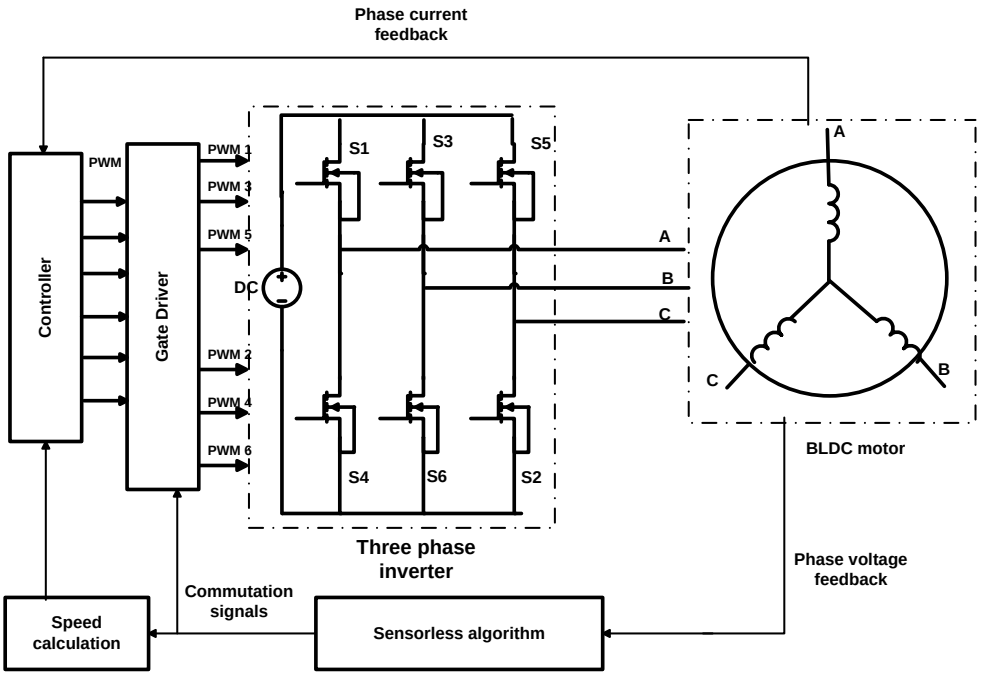

Fig. 4.1 Functional Block diagram of BLDC motor control

Table 4.1 Six step commutation table

Angle in degrees	Mode	Conducting switches	I_a	I_b	I_c
0-30	Mode 6	S5 & S6	0	-VE	+VE
30-90	Mode 1	S1 & S6	+VE	-VE	0
90-150	Mode 2	S1 & S2	+VE	0	-VE
150-210	Mode 3	S3 & S2	0	+VE	-VE
210-270	Mode 4	S3 & S4	-VE	+VE	0
270-330	Mode 5	S5 & S4	-VE	0	+VE
330-360	Mode 6	S5 & S6	0	-VE	+VE

Here the applied voltage has been varied by varying the duty cycle of PWM signal as the speed of motor is directly proportional to applied voltage. The speed controller based on H-infinity norm with its weights being optimized by PSO has been implemented for robust control in the presence of uncertainties such as modeling errors and unexpected external disturbances. The output of speed controller has been passed on to the current controller, which is a PI controller in this work and the PWM has been generated.

The steps involved in the model design and tuning of speed controller are

- Simulation of BLDC motor model with sensorless drive using SIMULINK
- Development of H infinity controller code in MATLAB editor using *' hinfsyn'*
- Development of PSO optimization program for achieving optimal tuning of weights.

4.2 Development of simulation model

The SIMULINK model of this work has been developed by the following steps.

- Modeling of BLDC motor
- Generation of switching signals through sensorless algorithm
- Implementation of control circuit using H infinity speed controller with the coefficients of weights being optimized by PSO and PI as current controller.

4.2.1Modelling of BLDC motor

The equivalent circuit of BLDC motor is shown in Fig. 4.2 in which R represents stator resistance per phase in Ω, L represents stator self-inductance per phase in Henry, whereas V_a, V_b, V_c represent the voltages in Volts, i_a, i_b, i_c represent phase currents in Amperes, and e_a, e_b, e_c represent corresponding back EMFs in Volts in three phases A, B and C respectively. The mutual inductance M between the phases for surface mounted BLDC motor can be neglected due to the independency of the flux path in the machine. Phase voltages are difficult to detect as there are only two phases conducting at a time and the third phase is not conducting. Therefore

mathematical model based on line voltages is more valid [182]. Based on Kirchhoff's voltage equation the following equations can be derived.

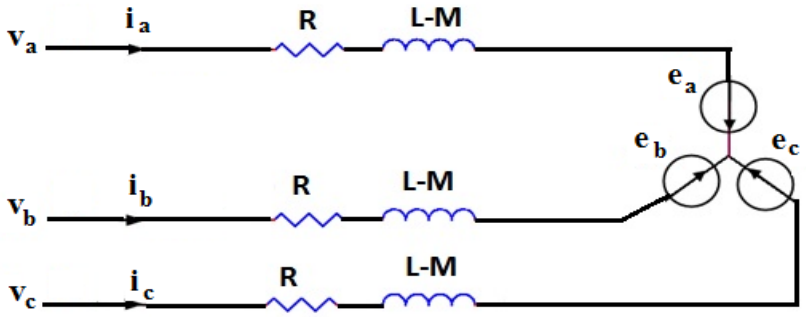

Fig. 4.2 Equivalent circuit of BLDC motor

$$V_{ab} = R(i_a - i_b) + L\frac{d}{dt}(i_a - i_b) + e_a - e_b \quad (4.1)$$

$$V_{bc} = R(i_b - i_c) + L\frac{d}{dt}(i_b - i_c) + e_b - e_c \quad (4.2)$$

$$V_{ca} = R(i_c - i_a) + L\frac{d}{dt}(i_c - i_a) + e_c - e_a \quad (4.3)$$

For a balanced three phase circuit, at any instant

$$V_{ab} + V_{bc} + V_{ca} = 0 \quad (4.4)$$

$$i_a + i_b + i_c = 0 \quad (4.5)$$

From these equations the model can be further simplified as

$$2V_{ab} + V_{bc} = 3Ri_a + 3L\frac{d}{dt}i_a + 2e_a - e_b - e_c \quad (4.6)$$

$$-V_{ab} + V_{bc} = 3Ri_b + 3L\frac{d}{dt}i_b + 2e_b - e_a - e_c \quad (4.7)$$

The phase currents can be generated from equations (4.5), (4.6) and (4.7). The induced EMFs are all assumed to be trapezoidal, whose peak value is given by

$$Ep = (Blv)N = N(Blr\omega) = NBA\omega = N\Phi\,\omega = \lambda\omega \quad (4.8)$$

where B is the flux density of the field in webers per meter squared, l is the rotor length, N is the number of turns per phase, ω is the electrical angular speed in rad/sec, Φ represents flux in webers which is equal to Blr, λ represents the total flux linkage given as the product of number of conductors and flux linkage/conductor. The induced EMFs can be written as a function of rotor angle $f_a(\theta)$, $f_b(\theta)$, and $f_c(\theta)$.

$$e_a = f_a(\theta)\lambda\omega \tag{4.9}$$

$$e_b = f_b(\theta)\lambda\omega \tag{4.10}$$

$$e_c = f_c(\theta)\lambda\omega \tag{4.11}$$

Suppose at an instant when phase a and phase b are conducting, phase c is floating, then i_a = - i_b = i where i is the phase current at that instant. Since only two phases are switched on, electromagnetic torque T_e can also be written as

$$T_e = 2P\lambda_m i = K_t i \tag{4.12}$$

Where P represents number of poles, λ_m represents flux linkages in two phases, K_t is the torque constant. In terms of mechanical parameters the torque equation is given by

$$T_e - T_l = J\frac{d}{dt}\omega_m + B\omega_m \tag{4.13}$$

Where T_l is the load torque in Nm, J is the moment of inertia in Kg. m^2 and B is the friction coefficient in Nms.

Rotor speed and position are related as

$$\frac{d\theta}{dt} = \frac{P}{2}\omega_m \tag{4.14}$$

When only two phases a and b are turned on, e_a is exactly equal and opposite to e_b. From equation (4.1), it can be derived that

$$V_{ab} = V_d = R_a i + L_a \frac{d}{dt} i + K_e \omega_m \quad (4.15)$$

Where R_a = 2 R, L_a = 2L, K_e is back emf constant and V_d is dc bus voltage. Thus, the transfer function of BLDC motor can be obtained as

$$G(s) = \frac{\omega_m}{V_d} = \frac{K_t}{(L_a J s^2 + (R_a J + L_a B)s + R_a B + K_e K_t)} \quad (4.16)$$

4.2.2 Switching signals through sensorless algorithm

In a BLDC motor, the rotor is positioned forcibly by determining the active phases and commutation of proper phase. Thus the knowledge of present position of rotor is important in the determination of correct commutation sequence. Usually hall sensors are used for detecting rotor position for proper commutation of phases. For saving of cost and space which is an important constraint, sensorless techniques pose a significant research development. By calculating the difference in terminal voltage difference which contains the information about exact commutation point that is 30 degrees lagging from zero crossing instant of back EMF has been adopted in this work [52], [53].

The corresponding phase voltages can be represented by equations (4.17) - (4.19).

$$V_a = R i_a + L \frac{d}{dt} i_a + e_a \quad (4.17)$$

$$V_b = R i_b + L \frac{d}{dt} i_b + e_b \quad (4.18)$$

$$V_c = R i_c + L \frac{d}{dt} i_c + e_c \quad (4.19)$$

The line voltages can be derived as (4.20) - (4.22).

$$V_a - V_c = V_{ac} = R(i_a - i_c) + L \frac{d(i_a - i_c)}{dt} + e_a - e_c \quad (4.20)$$

$$V_b - V_a = V_{ba} = R(i_b - i_a) + L \frac{d(i_b - i_a)}{dt} + e_b - e_a \quad (4.21)$$

$$V_c - V_b = V_{cb} = R(i_c - i_b) + L\,\frac{d(i_c - i_b)}{dt} + e_c - e_b \quad (4.22)$$

$$V_{ba} - V_{ac} = V_{baac} = R(i_b - 2i_a + i_c) + L\frac{d}{dt}(i_b - 2i_a + i_c) + e_b - 2e_a + e_c \quad (4.23)$$

$$V_{cb} - V_{ba} = V_{cbba} = R(i_c - 2i_b + i_a) + L\frac{d}{dt}(i_c - 2i_b + i_a) + e_c - 2e_b + e_a \quad (4.24)$$

$$V_{ac} - V_{cb} = V_{accb} = R(i_a - 2i_c + i_b) + L\frac{d}{dt}(i_a - 2i_c + i_b) + e_a - 2e_c + e_b \quad (4.25)$$

In a BLDC motor only two phases are connected to the supply at an instant and the third one is open, the phase which is connected to positive terminal of the supply has a positive current and the phase which is connected to the negative terminal of the supply has negative current and the open phase has zero current through it. Hence it can be found that when phase B is connected to positive and phase C is connected to negative terminal phase A is open. This implies not only that $i_b = -i_c$ and i_a is zero but also$e_b = -e_c$. Substituting these conditions in (4.23), we get (4.26)

$$V_{baac} = -2e_a \quad (4.26)$$

Similarly from (4.24) and (4.25), it can be written that

$$V_{cbba} = -2e_b \quad (4.27)$$

$$V_{accb} = -2e_c \quad (4.28)$$

From equations (4.26) - (4.28), it can be observed that the magnitude of difference of terminal voltages equals twice the back EMF with an opposite direction. Thus by detecting zero crossing of difference in line voltages, the exact commutation points can be detected. The estimated hall sensor signals which are the switching signals have been used for attaining the commutation of phases.

4.2.3 Control circuit

The design of a speed controller circuit is very important for imparting desired transient and steady state performance of the motor. The H infinity control strategy with its weights being optimized by PSO has been incorporated as speed controller along with simplified PI control as current controller. The reference speed is being compared with the estimated speed and the error is passed onto the speed controller whose output is the torque reference. This is converted into current reference and is compared with actual current values. The output of current controller is compared with carrier waveform and corresponding PWM signals are generated. Usually the inverter switches are controlled using PWM which converts a DC voltage into a modulated voltage that easily and efficiently limits the start-up current as well as controls speed and torque.

4.3 Proposed H infinity controller strategy for speed control of BLDC motor

The block diagram for the incorporation of proposed H infinity controller as speed controller is depicted in Fig. 4.3 where the plant *G* is the sensorless BLDC motor whose speed is to be controlled. The plant has two inputs such as *w*, the inputs due to external causes and *u*, the control signal and two outputs such as estimated speed *y* and the robust output *z*. The estimated speed *y* is compared with the reference speed *r* and the error *e* is passed on to the H infinity controller *K* to produce a controlled output *u*, the reference torque.

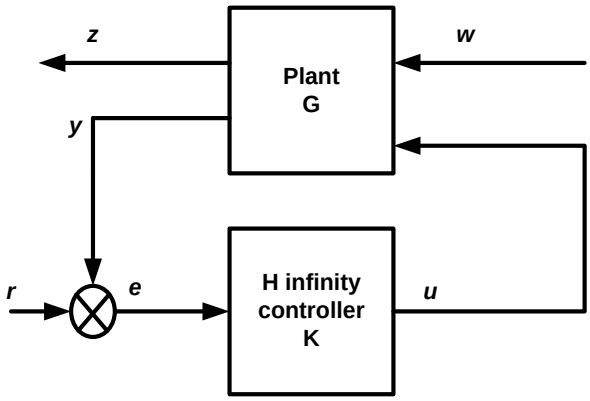

Fig. 4.3 Block diagram incorporating H infinity control in a BLDC motor

The objective is to find *K* which makes the closed loop system stable satisfying the expression (4.29).

$$\|T_{zw}\|_\infty \triangleq \begin{bmatrix} W_1 S \\ W_2 R \\ W_3 T \end{bmatrix} \leq \gamma \tag{4.29}$$

In this $\|T_{zw}\|$ is the weighted mixed sensitivity where *S* is the sensitivity function that represents the transfer matrix from *w* to *z*, *R* is the input sensitivity function which represents the transfer matrix from *w* to *u* and *T* is the complementary sensitivity function. In order to achieve disturbance rejection from external signals in the low frequency region, the sensitivity given by expression (4.30) has to be made small as ω→0

$$S = \frac{I}{(I+GK)} \tag{4.30}$$

Similarly in order to reduce effect of errors due to modelling which occur in the high frequency region, the complementary sensitivity function $T = I - S$ should be small in high frequency region as ω→∞. [183].

Once the H infinity loop has been closed, the unstable poles in the specified bandwidth have been replaced with its mirror image. Thus this strategy exhibits precise frequency domain loop shaping using suitable weight strategies [184]. If the plant is augmented with frequency dependent

weights as shown in Fig. 4.12, the MATLAB script '*hinfsyn'* synthesizes a controller which shapes the signals in order to achieve the required performance and robustness [22]. Thus by suitable selection of weights, frequency domain loop shaping can be achieved. This implies that the solution of *H* infinity control problem is based on the augmented state space representation of *G* with suitable weighting functions W_1, W_2 and W_3 for the error signal *e*, control signal *u* and output signal *y* respectively.

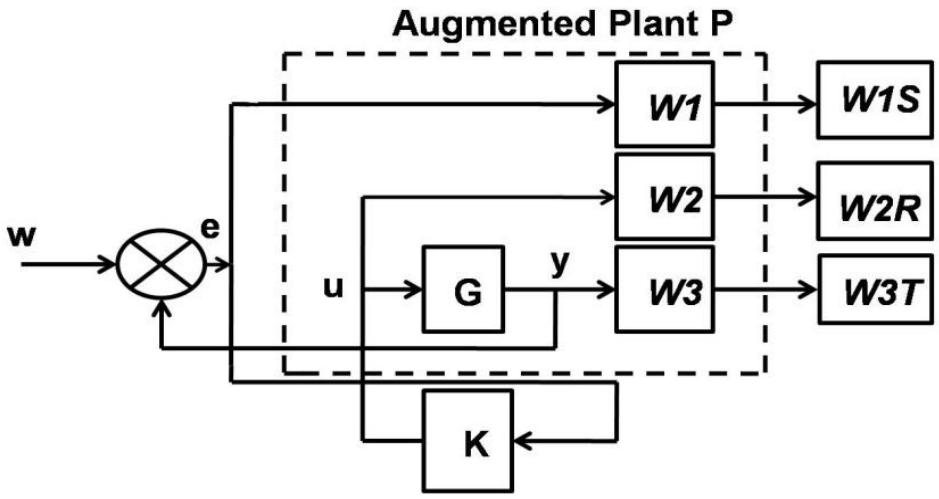

Fig. 4.4 Functional block diagram of H infinity controller with augmented plant

From Fig. 4.4, equation (4.31) can be derived as

$$\begin{bmatrix} W1S \\ W2R \\ W3T \\ e \end{bmatrix} = \begin{bmatrix} W1 & -W1G \\ 0 & W2 \\ 0 & W3G \\ I & -G \end{bmatrix} \begin{bmatrix} w \\ u \end{bmatrix} \tag{4.31}$$

The mathematical model of augmented plant *P* is obtained as (4.32)

$$P = \begin{bmatrix} W1 & -W1G \\ 0 & W2 \\ 0 & W3G \\ I & -G \end{bmatrix} \tag{4.32}$$

The MATLAB function *augw* is used to generate the augmented plant *P* as in equation (4.33)

$$P = augw\ (G, W1, W2, W3) \tag{4.33}$$

The MATLAB function '*hinfsyn'* synthesizes an H infinity controller *K* for the augmented plant matrix *P* as given by equation (4.34) and the corresponding transfer function *KT* is obtained from equation (4.35)

$$K = hinfsyn(P) \tag{4.34}$$

$$KT = tf\ (K) \tag{4.35}$$

The selection of suitable weight filters is an important criteria for proper controller design. The selection should satisfy the specification for various frequency ranges as mentioned below.

- In the low frequency range, the main objective is to make the closed loop gain from disturbance to tracking error small.
- In the medium frequency range, acceptable stability margins have to be ensured.
- In the high frequency range, the control signal has to be kept limited.

The weighting function $W_1$of sensitivity function should be so chosen such that it reflects the desired time response characteristics [3]. A low pass filter is used with the low frequency gain approximately equal to the inverse of the desired steady state error and high frequency gain to limit overshoot.

Hence a simple low pass filter represented by equation (4.36) has been selected for W_1.

$$W_1 = \frac{1}{M_s}\frac{\tau_p s+1}{\tau_p s+{}^{A}/_{M_s}} \tag{4.36}$$

Where $\tau_p = {}^{1}/_{M_s \omega_b}$

M_s represents the maximum value of sensitivity function, A represents the maximum allowed steady state offset and ω_b represents the system bandwidth [100]. For the choice of other weights, the recommendation put forth by Anna-Karin Christiansson et al [109] has been taken into consideration, which says that in order to keep the controller order low, the choice of as many weights as possible to be made constant. Moreover in order to keep the control signal to a limited value, a constant has been assigned for W_2 and W_3.

There are a total of six coefficients of parameters *a, b, c* and *d* of W_1, g of W_2 and h of W_3 which are to be chosen properly in order to attain suitable weights. Some thumb rules have been presented in the literature for the tuning of weights [106]. In this work, these coefficients of weights are optimized using PSO in order to achieve robust control.

$$W_1 = \frac{a(s+b)}{cs+d} \tag{4.37}$$

$$W_2 = g \tag{4.38}$$

$$W_3 = h \tag{4.39}$$

4.4 Particle Swarm Optimization for weights selection

For H infinity synthesis the uncertainty factors of the system must be translated into the weights. The more truthful are the coefficients of weights; the better will be the H infinity control. In this proposed approach, this is viewed as an optimization problem since the nature of relation between weights and H infinity performance is complex. For solving this problem, PSO has been used so that an optimal controller can be synthesized.

In PSO, the momentum effect on particle movement allows faster convergence thereby creating a best quality solution. A group known as swarm of random individuals referred to as particles is initialized in PSO. A set of all candidate solution for the optimization problem has been defined as the search space. The range of search area is specified with minimum and maximum values of coefficients of W_1, W_2 and W_3. The population members are initialized and each particle's random position and velocity are generated. The objective function value is memorized using personal best. It is compared with the neighbour's personal best and the best value is stored in global best. The particle moves towards the new position with a new velocity along with the information regarding its current velocity, its own personal best and global best [25] – [27]. The optimization problem is the minimization of global best cost which is equal to sum of absolute values of error which is achieved by finding out the best coefficients for the weighting functions using PSO. With this global best cost, W_1, W_2 and W_3 are generated and the transfer function of the controller is obtained. This controller has been used as speed controller whose output will be the torque reference.

The objective function of the problem is defined with conventional PSO as

$$min\ f(W_1, W_2, W_3) = \sum_{n=1}^{T/dT} \left(\left|\omega_{r(n)} - \omega_{(n)}\right|\right) \quad (4.40)$$

Where W_1, W_2 and W_3 are the weights

T is the simulation time

dT is the step size

$\omega_{r(n)}$ – Reference speed at nth sample

$\omega_{(n)}$ – Estimated speed at nth sample

Steps involved in PSO algorithm

Step 1: Initialize the problem with following parameters

i. Number of particles

ii. Number of Evaluations

iii. C_1, C_2 - learning factors

iv. Search space limits

Step 2: Initialize random particle positions within the search space.

Step 3: Perform H infinity synthesis based on the weights formulated from the particle positions.

Step 4: Simulate the Model with the synthesized H infinity controller and find out the fitness value.

Step 5: Obtain the local best solution for each particle and global best solution for the entire problem.

Step 6: Perform the following steps in the main loop

i. Update the velocity of the particle using equation (2.10)

ii. Based on velocity of the particle obtained update the position of the particle using equation (2.11)

Step 7: Repeat the steps 3 to 6 till maximum iterations are reached.

Step 8: The global best solution for the entire problem provides the optimal weights for the H infinity controller.

The flowchart for obtaining optimized controller is shown in Fig. 4.5.

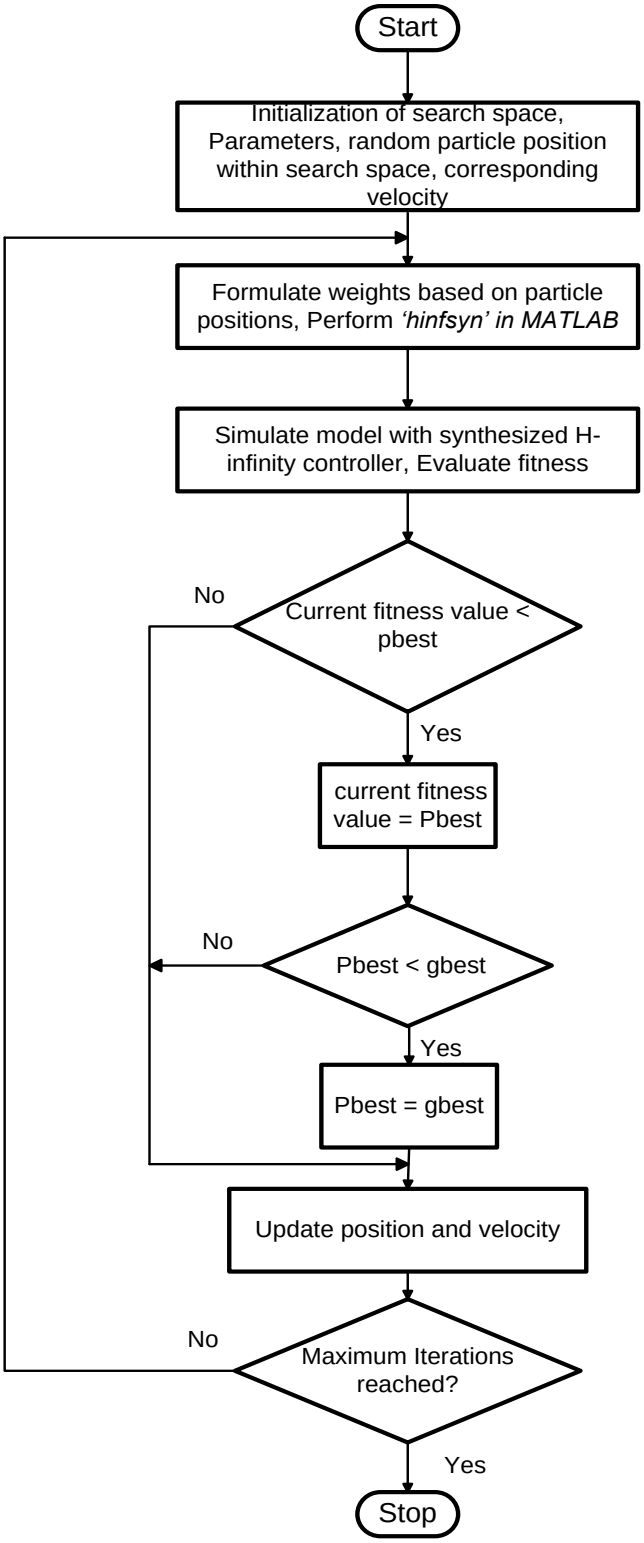

Fig. 4.5 Flow chart for obtaining optimized weights using PSO

4.5 Design of PI speed controller with PSO optimised gains

PI control is one of the common control techniques used in industry as it is easy to implement and does not involve much complex algorithms. By using PI control which is based on past and present error values, the steady state error can be reduced to zero, and at the same time the transient response can be improved. But it is suitable only when the system parameters are fully known and modeled. It offers low robust control when the system has uncertainties and modeling errors especially when the operating environment changes due to weather, temperature and so on. For comparison purpose, the speed controller is modeled with PI control as shown in Fig. 4.6 with its gains being optimized by PSO [12], [110] – [119] and the flow chart of which is shown in Fig. 4.7. The transfer function of PI controller can be obtained for an input *E(s)* as (4.41)

$$U(s) = \left(K_p + \frac{K_i}{s}\right) E(s) \tag{4.41}$$

Where K_p represents proportional gain and K_i represents integral gain.

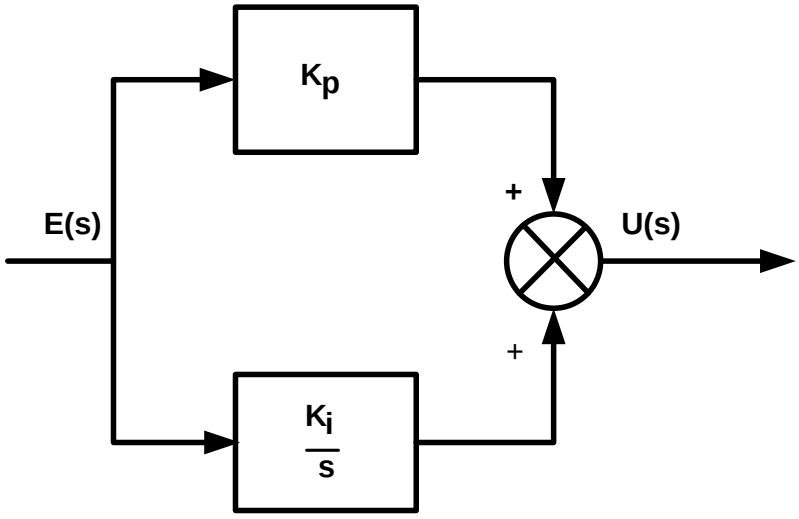

Fig. 4.6 Block diagram representation of PI controller

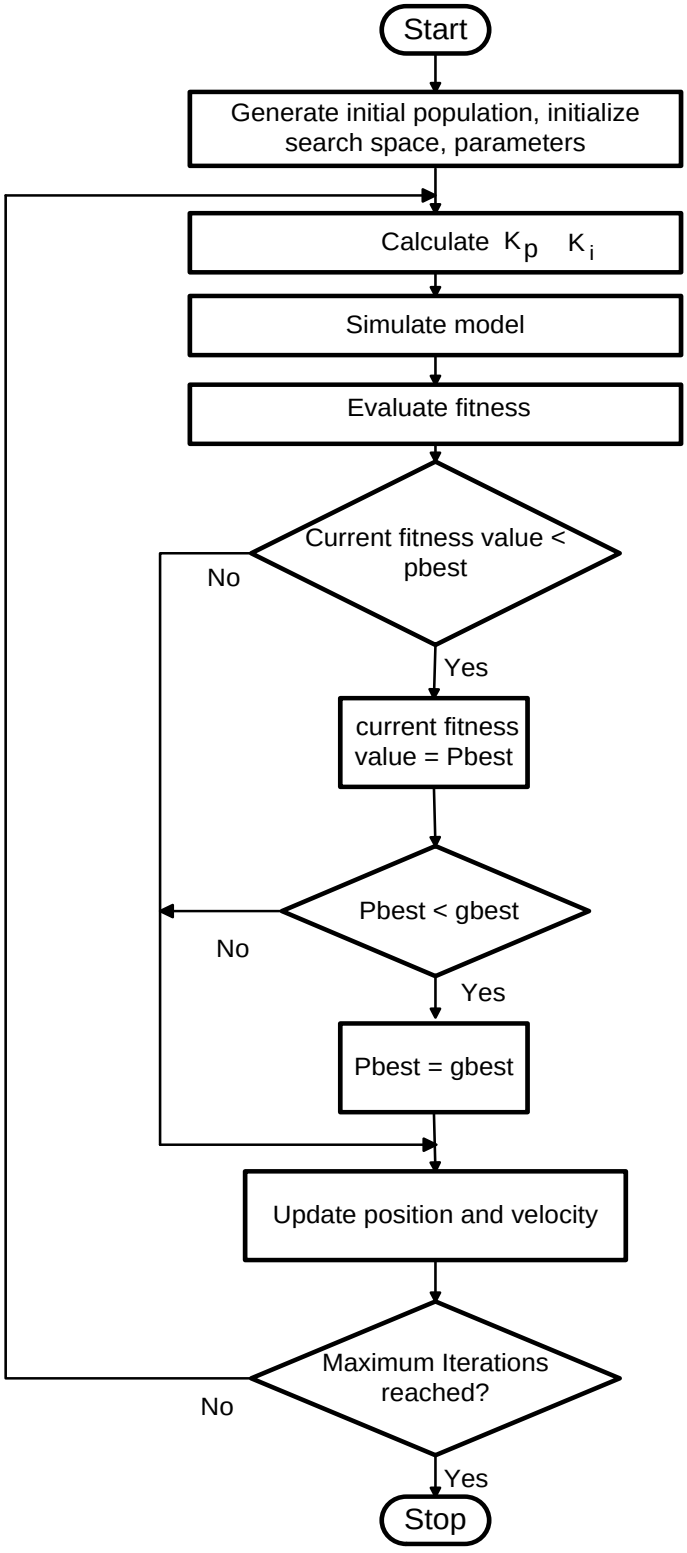

Fig. 4.7 Flow chart for PSO optimized gains of PI controller

Chapter Summary

The simulation model of BLDC motor has been designed with a step by step procedure. The rotor position sensing has been adapted by using a sensorless technique based on difference in line to line voltage difference. H infinity controller has been designed with its weights being optimized using PSO and has been implemented as speed controller for achieving robust speed control of BLDC motor. For the sake of comparison, a PI speed controller with its gains being optimized by PSO has been designed and implemented.

*****

Chapter 5

Simulation Study of PSO Optimised PI and H Infinity Speed Controllers

Contents

A detailed description of design of H infinity and PI speed controllers with tuning algorithm using PSO has been discussed in Chapter 4. Based on this, the simulation study is conducted for the performance comparison of the two controllers for a BLDC motor. The simulation results obtained in every stage such as current generation system, back EMF generation system and mechanical system are discussed in detail. The generation of commutation instants with sensorless technique which are the estimated hall sensor signals are also discussed. PWM pulse generation using triangle wave generator is discussed with simulated waveforms. Waveform of rotor position is also obtained. The speed, torque and speed error waveforms obtained with both speed controllers are compared.

5.1Simulation Results

The blocks developed in SIMULINK for robust speed control of BLDC motor are simulated in MATLAB 2016a version. The sampling time has been set for 2 microseconds. The specifications of BLDC motor considered for simulation study are shown in Table 5.1.

Table 5.1 Specifications of BLDC motor considered for simulation study

Specifications	Values
Power	3.8 KW
Peak Torque	30 Nm
Rated speed	3000 rpm
Stator phase resistance	0.2 Ω
Stator phase inductance	8.5mH
Voltage constant K_e	146.6
Torque constant K_t	1.4
Flux constant	0.175 V.s
Moment of Inertia (J)	0.089 $Kg.m^2$
Viscous friction coefficient (B)	0.005 Nms

Three phase current waveforms drawn by BLDC motor as shown in Fig. 5.1 clearly indicate the 120 degree conduction mode and it can be clearly observed that only two phases are conducting at an instant and third phase is not conducting as per the Table 4.1.

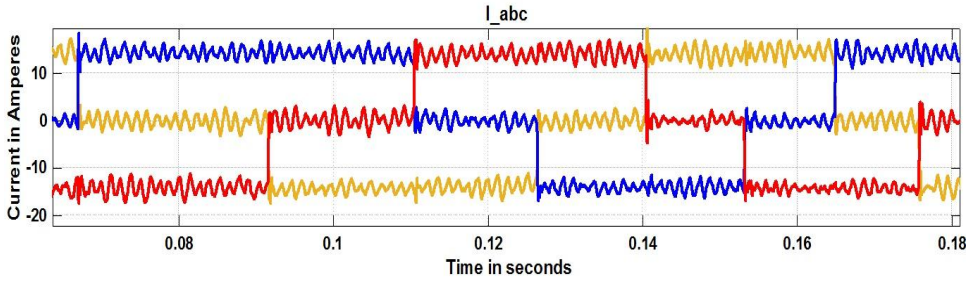

Fig. 5.1 Three phase currents of BLDC motor

The estimated trapezoidal BEMF waveforms of three phases are shown in Fig. 5.2. It can be observed that at every 60 degrees one of the BEMFs crosses zero which can be detected for estimating the commutation points.

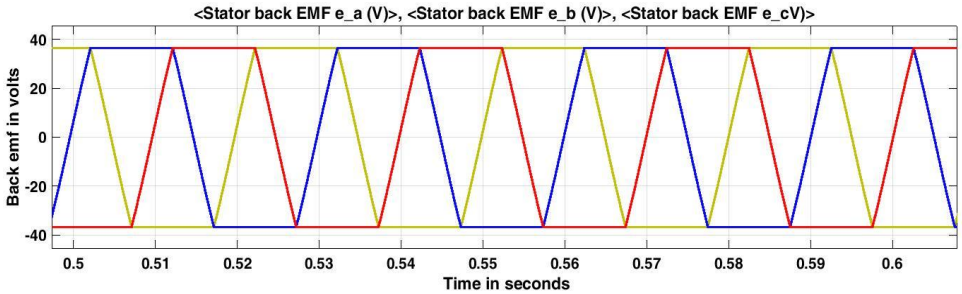

Fig. 5.2 Three phase trapezoidal back EMFs of BLDC motor

The inference of rotor position is used to ensure proper commutation of phases which is shown in Fig. 5.3. It can be observed that the estimated rotor angle changes from +180 to -180 degrees.

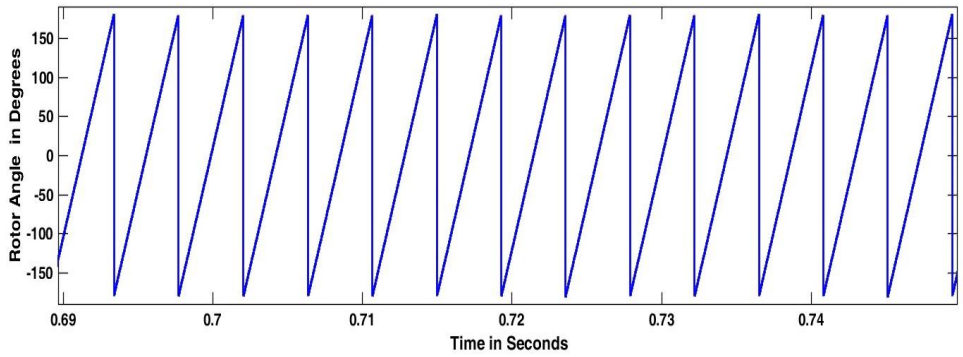

Fig. 5.3 Rotor position in terms of angles in degrees

The exact commutation point of phase current is 30 degrees lagging behind the zero cross over point of BEMF. This point has been estimated using line to line voltage difference [52] as shown in Fig. 5.4.

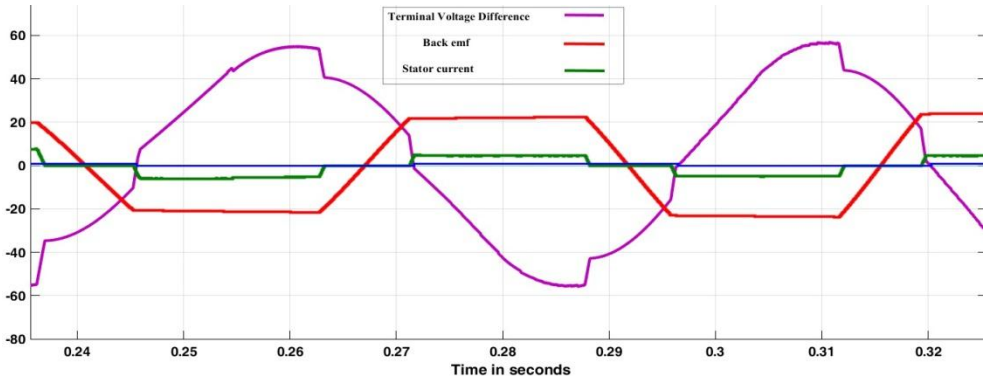

Fig. 5.4 Estimation of commutation points as the difference between line to line voltages

The three phase commutation signals have been shown in Fig. 5.5. Table 5.2 shows that the estimated pulse code is the same as physical hall sensor code for each electrical cycle for the motor to rotate in clockwise direction.

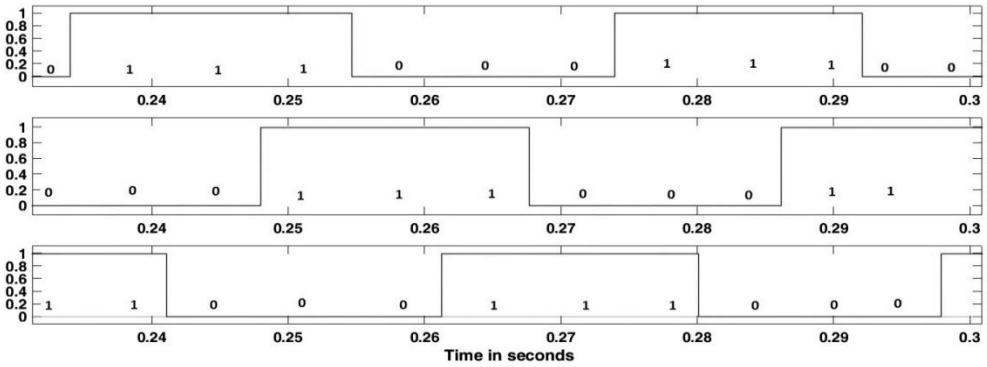

Fig. 5.5 Estimated commutation signals

Table 5.2 Physical and Estimated hall sensor code

Physical hall sensor code	Estimated hall sensor code
001	001
101	101
100	100
110	110
010	010
011	011

The simulation of the speed control of BLDC motor has been carried out with two speed controllers such as conventional PI controller with its gains optimized by PSO and H infinity controller with coefficients of its weights being optimized by PSO in order to carry out the comparative study.

The parameters of PSO for both gain and weight selection of PI and H infinity controllers respectively are shown in Table. 5.3.

Table 5.3 Parameters of PSO algorithm for both PI and H Infinity controllers

Parameters	PI	H infinity
C_1	0.12	1.5
C_2	1.2	2.5
Dimension of search space	2	6
Damp ratio	0.95	0.95
Inertia	$1.1058*10^{-9}$	$4.3723*10^{-7}$
No. of particles	20	20
Particle steps	20	12
Variable Low	[0.1 0.00001]	[0.05 1 0.1 0.1 0.000001 0.00001]
Variable High	[4 1]	[0.9 500 200 50 0.08 0.01]
Evaluations	421	279
Global Best Fitness	$3.3258*10^{4}$	$4.2969*10^{6}$

Based on PSO, the optimised gain values and weights of the controllers obtained are shown in Table 5.4.

Table 5.4 Gains and weights of controllers

Gains of PI controller		Weights of H infinity controller		
K_p	K_i	W_1	W_2	W_3
1.22	0.09	$\frac{0.2406s + 118.6}{0.105s + 50}$	0.008	0.01

The convergence plot of PSO for PI controller is shown in Fig. 5.6. The corresponding optimal transfer function of controller is obtained as equation (5.1)

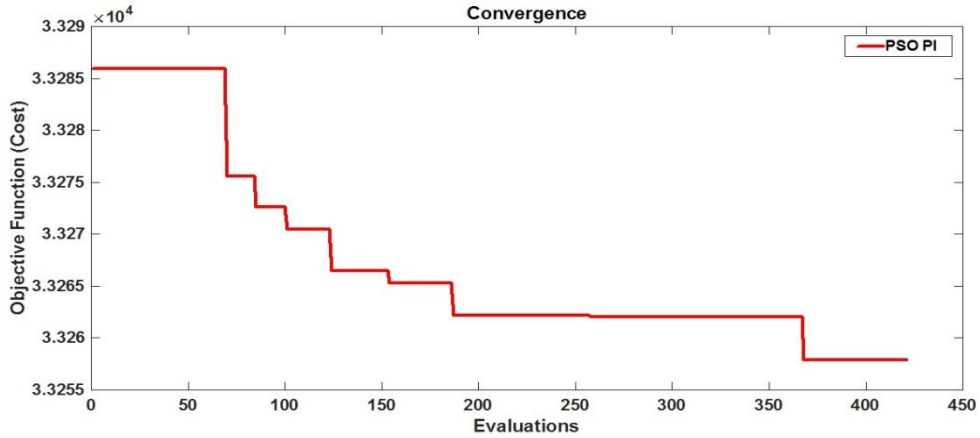

Fig. 5.6 Convergence plot for obtaining optimal PI controller

$$KT = \frac{1.22s+0.09}{s} \tag{5.1}$$

The convergence plot of PSO for obtaining weights of H infinity controller is shown in Fig. 5.7 and the optimal transfer function is obtained as equation (5.2) and the value of γ is obtained as 2.3285.

$$K = \frac{638.4s^2+1.527e04\ s+1.726e08}{s^3+394.6s^2+2.994e05\ s+8.413e07} \tag{5.2}$$

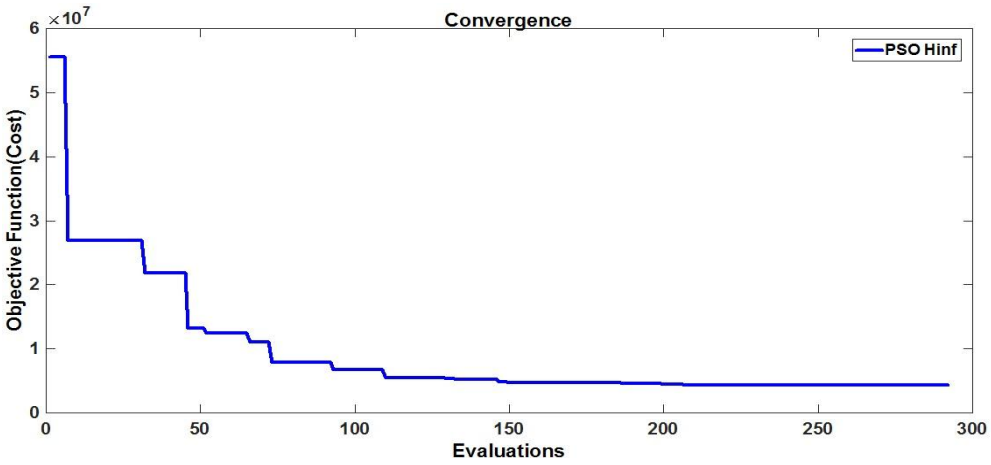

Fig. 5.7 Convergence plot with PSO for H infinity controller

Sensitivity and complementary sensitivity plots of the controller are shown in Fig. 5.8 (*a)* and (*b).* It can be seen that sensitivity function is small for low frequency region and complementary sensitivity function is low for high frequency region which is the trade-off required for good reference tracking, disturbance rejection, insensitivity to modelling errors and noise [3]. It can be observed that the controller can provide -0.22 dB sensitivity at low frequencies.

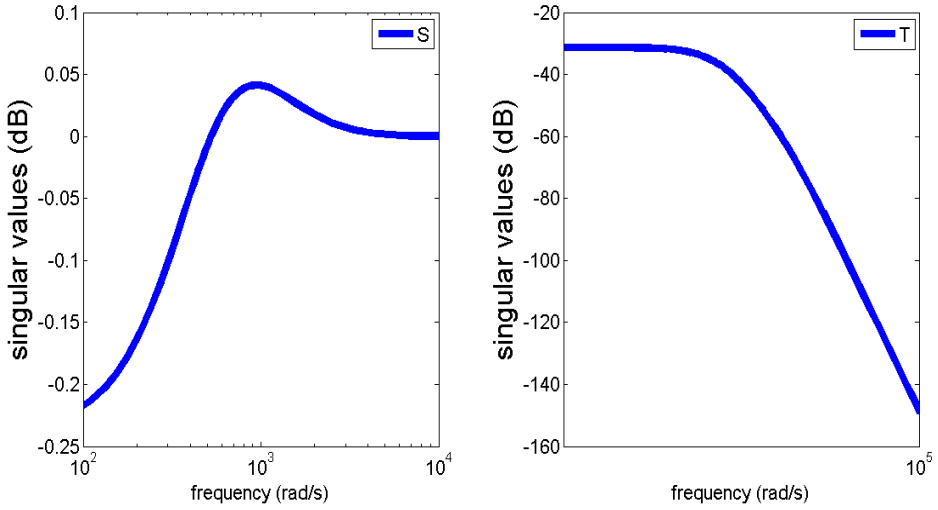

(a) (b)

Fig. 5.8 Robust response curves (a) Sensitivity plot (b) Complementary sensitivity plot

PWM is a technique in which a control signal has been sampled at fixed intervals and the amplitude of each sample has been encoded with a constant amplitude pulse with a duration proportional to sample amplitude. Hence the duty cycle which is the ratio of ON time to total time determines the percentage of conduction time of the switch. This determines the magnitude of output voltage. Here the triangle wave is compared with the output of controller and pulses are generated whenever the control signal is greater than triangular waveform as shown in Fig. 5.9.

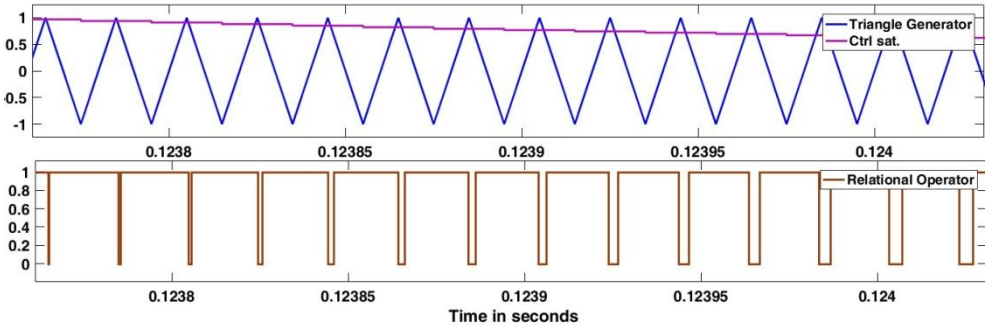

Fig. 5.9 Generation of PWM pulses

5.2 Performance study

A case study has been conducted with PI as well as H infinity speed controllers in order to analyse the effects of reference tracking and load disturbance and the results obtained with PI controller have been validated with the experimental results available in literature [185].

Reference speed is set as 1000 rpm and a torque of 12 Nm is applied to the motor at 0.7 sec by an external load. The speed waveforms of the motor with both PI and H infinity controllers are shown in Fig. 5.10. It can be observed that speed with *H* infinity controller shows an improvement in rise time by 0.6% and better stability than PI controller when load is applied at 0.7 sec.

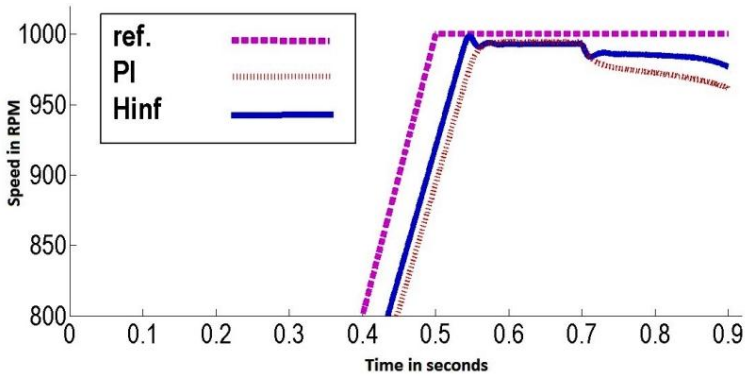

Fig. 5.10 Speed performance analysis of the controllers under load

The enlarged version of speed waveform is shown in Fig 5.12 (a) and (b). It can be observed from Fig. 5.11 (a) that with PI controller when the load is applied at 0.7 sec the speed settles down at 988 rpm whereas with H infinity controller, it settles down at 993 rpm.

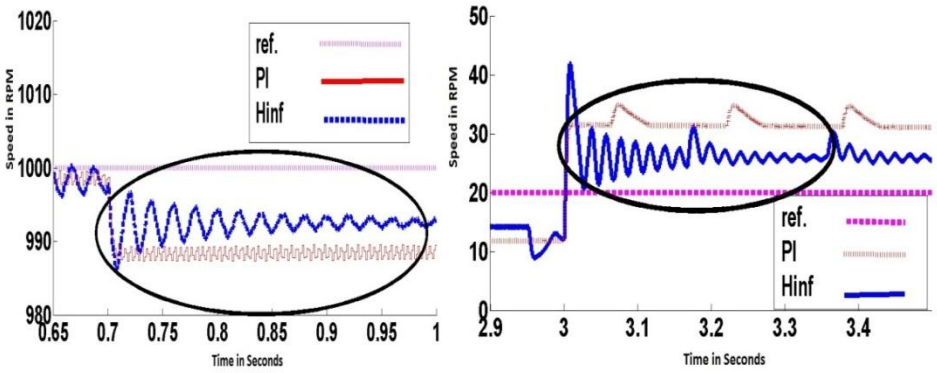

Fig. 5.11 Performance of speed when the load is applied (a) at 0.7 sec.(b) at 3 sec

Then the reference speed is reduced to 20 rpm at 1.5 sec. (braking mode) and a load torque of 12 Nm is applied in the reversed direction at 3 sec. After 3 sec. the speed settles down at 32 rpm and 26 rpm with PI and H infinity controllers respectively as shown in Fig. 5.11 (b). This shows that H infinity controller shows better tracking of speed commands thereby reduces steady state error. A comparison of performance parameters of the two controllers are summarised in Table 5.5.

The electromagnetic torque with PI and H infinity controllers is shown in Fig. 5.12. It is observed that at steady state electromagnetic torque oscillates between +6 Nm to -4 Nm with PI whereas it oscillates between ± 1 Nm with H infinity controller thereby there is a considerable reduction in torque ripples.

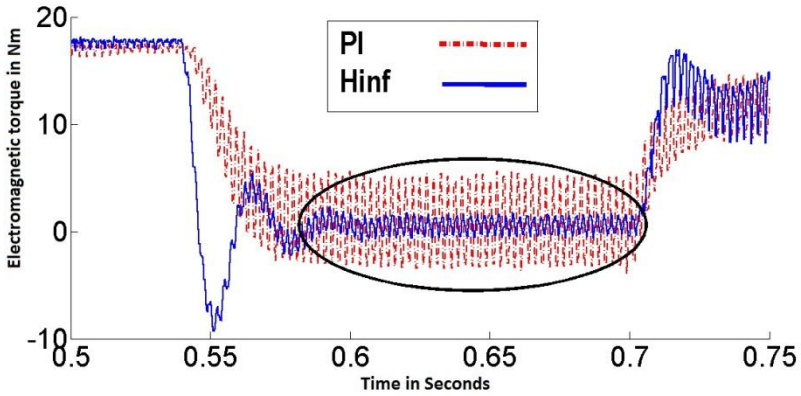

Fig. 5.12 Comparison of Electromagnetic Torque

A comparison of speed error with both controllers is shown in Fig. 5.13 and it can be observed that a decrease in speed error of 25 rpm has been observed with H infinity compared to PI controller.

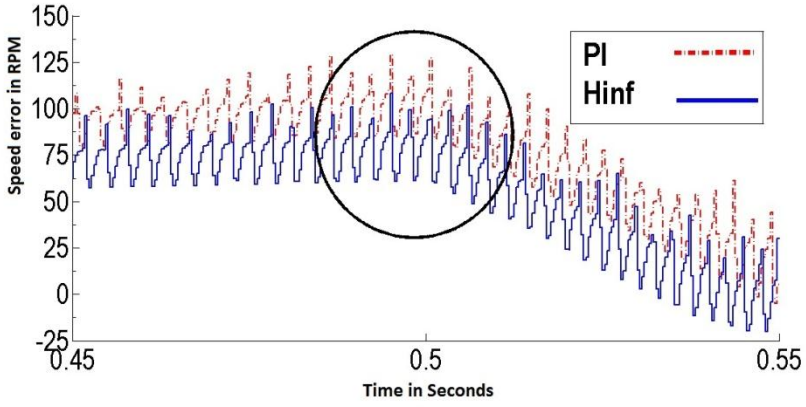

Fig. 5.13 Comparison of Speed errors

Table 5.5 Comparison of Performance parameters with both controllers

Controllers	Rise time (sec)	Maximum Speed error (rpm)	Steady state error %
PI	0.57	125	1.5
H infinity	0.54	100	1

The bode plot of H infinity controller is shown in Fig. 5.15. It can be inferred that the gain margin is infinity and phase margin is 104 degrees which makes the controller inherently stable. The gain of the system drops below -3dB at the cut of frequency of 300 rad/s.

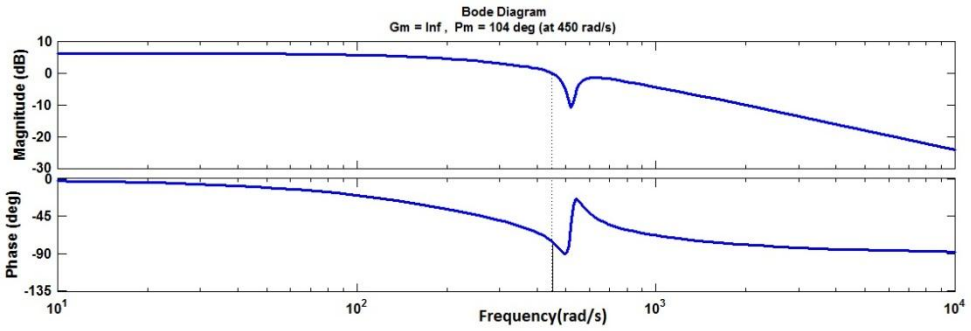

Fig. 5.14 Bode plot of H infinity controller

Chapter Summary

The BLDC motor model has been simulated with sensorless algorithm with its speed being controlled by an H infinity controller with its weights optimized by PSO. A comparative study of its simulation results with PI controller with its gains optimized by PSO has been carried out. The performance parameters have been compared and tabulated.

*****

Chapter 6

Hardware Realization of the Proposed Controller Strategy

Contents

As the experimental validation of simulation results is very important in order to establish the feasibility and significance of the proposed work, a prototype has been built in hardware. In this work, the 'C' code for the hardware realization has been developed in MATLAB/SIMULINK environment, using Code Composer Studio (CCS) which is an Integrated Development Environment (IDE) as well as Control SUITE which includes drivers, examples and other necessary software support. This generated code is deployed into hardware through an USB interface. Speed estimation and average current generation methods adopted are simulated for verifying the authenticity of hardware results and the simulation results are also discussed.

6.1Components used

The functional block diagram depicting the development of hardware setup is shown in Fig. 6.1. The main components used include power supply, microcontroller development board, three phase inverter with its control circuitry and the motor to be controlled. The detailed description of the above said components is discussed in the following sections.

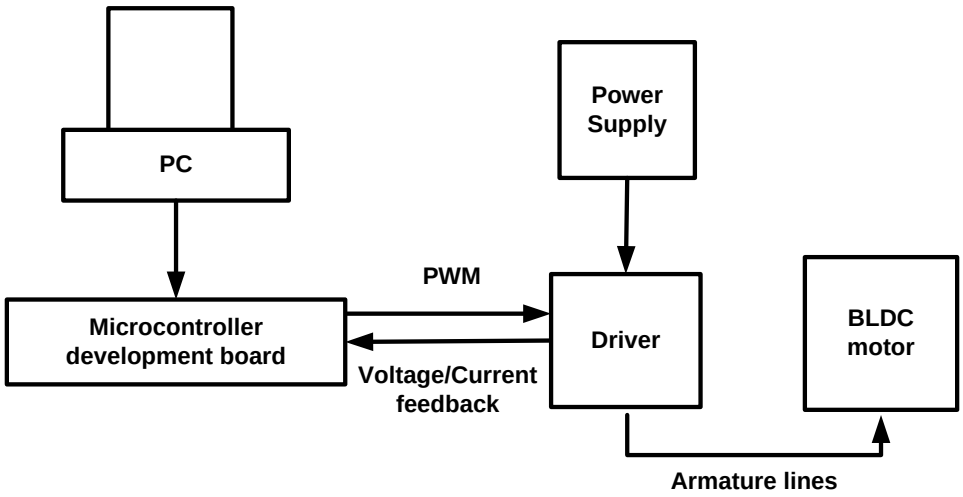

Fig. 6.1 Block diagram depicting development of hardware setup

6.1.1 Power supply

A single output 120W, 24V, 5A switching power supply with model No. S-120-24 has been used and its specifications are shown in Table 6.1.

Table 6.1 Specifications of power supply

Model No.	S-120-24
Output power	120 W
Input voltage	220 V
Output voltage	24V
Output frequency	47~63 Hz
Output current	5A
Protections	Short circuit/ Overload/ Overvolt/Overtemp

6.1.2 Microcontroller development board

The microcontroller development board used for hardware implementation is C2000™ Delfino™ LaunchPad™ LAUNCHXL-F28377S. It is a development board for the Texas Instruments Delfino F2837xS devices which is shown in Fig. 6.2. This stands good for motor control applications, power conversion applications, signal processing etc. The LAUNCHXL-F28377S includes a pre-programmed TMS320F28377S device. This kit

includes all hardware and software requirements that are essential to develop applications based on TMS320F28377S microprocessor. In order to reduce software development time, controlSUITE software which is a set of software tools has been employed in this work. CCS Version 6 has been downloaded in order to write the code, download onto the LAUNCHXL-F28377S board and to debug. An USB interface which provides a UART serial communication between F28377S device and PC which makes it user friendly has been utilized [186]. The pin diagram of LAUNCHXL-F28377S is included in Appendix I. The Delfino™ TMS320F2837xS is a powerful 32-bit floating-point microcontroller unit (MCU) with a signal processing frequency of 200 MHz designed for advanced closed-loop control applications such as industrial drives, servo motor control, solar inverters, converters, transportation and power line communications. The functional block diagram of the same is included in Appendix II [187].

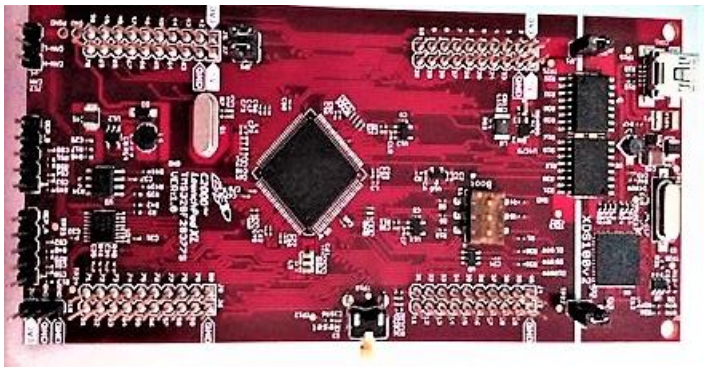

Fig. 6.2 Snapshot of LAUNCHXL-F28377S

Four independent 16-bit Analog to Digital Converters (ADC) provide precise and efficient management of multiple analog signals, which ultimately boosts system output. Other analog peripherals include Digital to Analog Converter (DAC), temperature sensor and comparator subsystem (CMPSS). The control peripherals include Enhanced PWM channels (ePWM), Enhanced Capture (eCAP) Modules, Enhanced Quadrature Encoder Pulse (eQEP) Modules and Sigma-Delta Filter Module (SDFM). The ePWM peripheral is a

key element in controlling many of the power electronic systems found in both commercial and industrial equipment. It is able to generate complex pulse width waveforms with minimal CPU overhead.

6.1.3 Driver

The motor drive used in this research work is BOOSTXL DRV 8301. It is the Booster pack based on DRV 8301 with three phase pre driver and CSD 18533Q5A N- channel power MOSFETs. It provides a complete drive stage for motor applications. It can be combined with LAUNCHXL kits to provide a three phase motor drive control. It has been designed with three phase voltage sense outputs and three phase low-side shunt current sense outputs. Its inbuilt *Instaspin* FOC sensorless control solution [188] has not been adopted. Instead hall signals have been estimated using three phase voltages sensed through three phase voltage sense pins. The pin diagram of DRV 8301 is included in Appendix III. The driver circuit BOOSTXL DRV8301 has been interfaced with LAUNCHXL F28377S board to achieve proper speed control of the BLDC motor.

6.1.4 BLDC motor

The BLDC motor used for building the prototype is a 42BL61 Brushless motor with the specifications given in Table. 6.2.

Table 6.2 Specifications of BLDC motor used for prototype

Parameters	**Specification**
Number of poles	8
Number of phases	3
Rated voltage	24V
Rated speed	4000 RPM
Rated Torque	0.125 Nm
Torque constant	0.036 Nm/A
Line to line resistance	0.72Ω
Line to line inductance	1.2 mH
Moment of inertia	0.0048Kg-cm^2
Max. Peak current	10.6 A
Length	61 mm
Weight	0.45 Kg

6.2 Hardware implementation

The implementation has been carried out through the following steps. The block diagram representation of the hardware implementation is shown in Fig. 6.3.

1. Implementation of sensorless algorithm
2. Generation of PWM
3. Motor Starting strategy
4. Speed estimation
5. Speed controller strategy using H infinity control with PSO optimized weight generation
6. Current controller
7. Hardware in Loop Verification

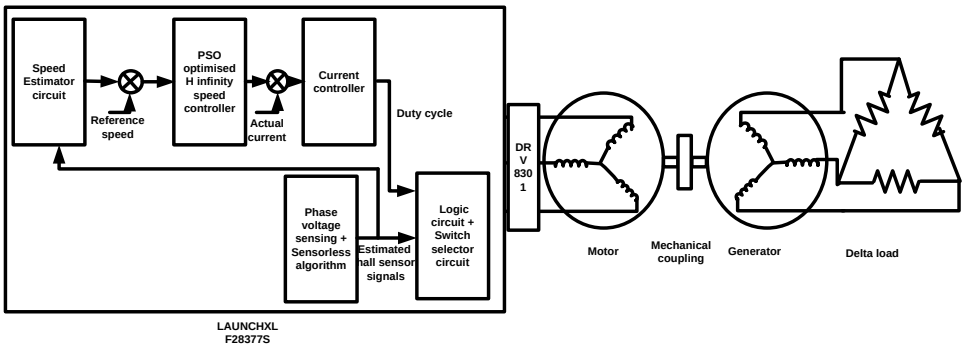

Fig. 6.3 Block diagram representation of hardware implementation

6.2.1 Implementation of sensorless algorithm

Phase voltages which have been sensed through VA-FB, VB-FB and VC-FB of BOOSTXL DRV 8301 have been connected to channels ADCIN0, ADCIN2 and ADCIN5 of module A respectively in LAUNCHXL F28377S.

The ADC triggering and conversion sequencing is accomplished through configurable start-of-conversions (SOCs). Each SOC is a

configuration set defining the single conversion of a single channel. In that set, three parameters that are to be configured are the trigger source that starts the conversion, the channel to convert, and the acquisition (sample) window duration. Upon receiving the trigger configured for a SOC, the wrapper will ensure that the specified channel is captured using the specified acquisition window duration [189]. Enhanced PWM feature is used to generate PWM pulses with switching frequency 10KHz. Fig. 6.4 shows the screenshot of ADC block parameters in which ADC has been synchronized with ePWM2 and the event trigger setting of ePWM and ADC have been synchronized with SOCA.

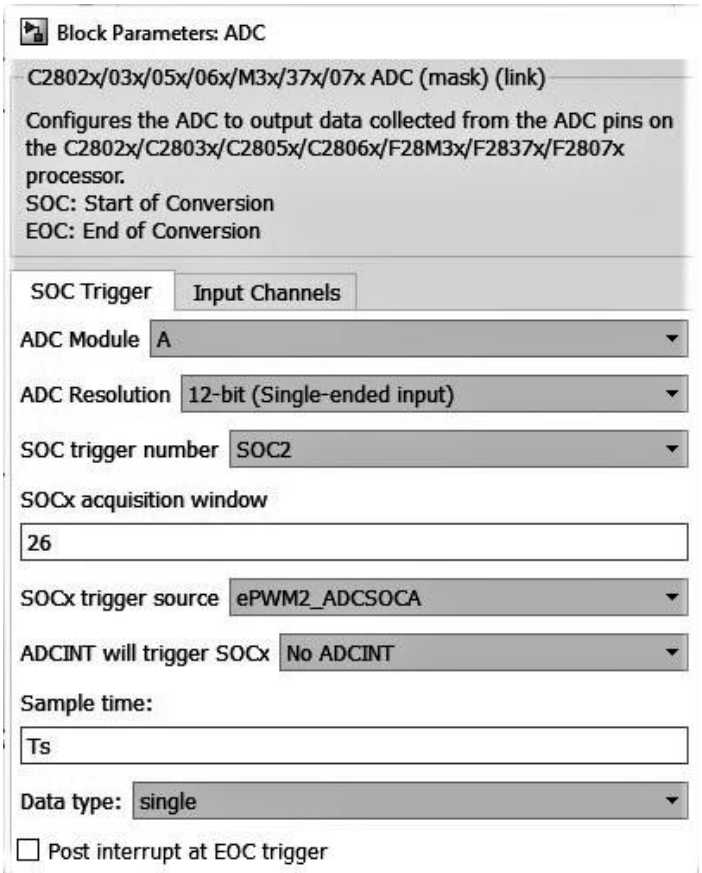

Fig. 6.4 Block parameters of ADC

Based on the phase voltage values captured, the sensorless algorithm has been incorporated as discussed in section 4.1.2 of chapter 4. For

verification purpose, the commutation instants obtained from physical hall sensors and emulated hall sensor signals are obtained using logic analyzer as shown in Fig. 6.5. The first three channels from 0 – 2 depicts the physical hall sensor signals and last three channels from 3 – 5 shows emulated hall sensor signals obtained through GPIO digital outputs. It can be observed that the sequence is same in both methods.

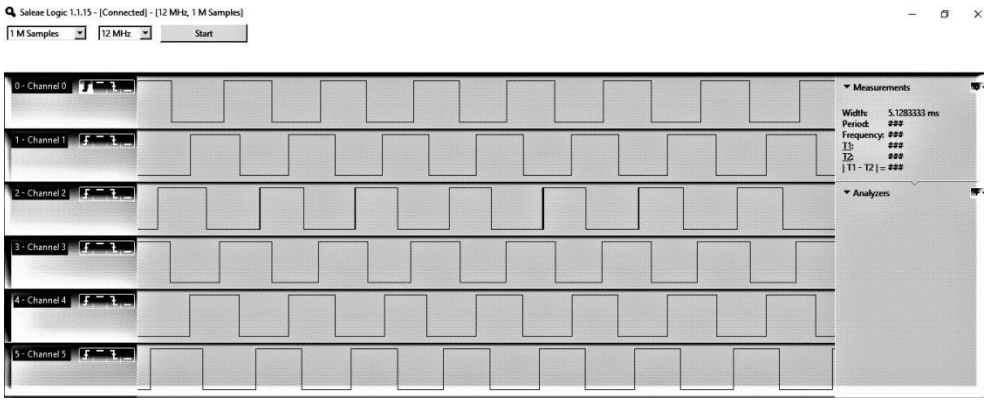

Fig. 6.5 Screenshot of physical hall sensor and emulated hall sensor signals

6.2.2 Motor Starting strategy

As the sensorless algorithm depends on zero crossing of back EMF, initially motor requires a starting strategy for the back EMF to build up. Once the motor rotates, back EMF builds up and the rotor position can be detected, so that appropriate switching signals can be given for further rotation and the motor catches up with the sensorless algorithm. For achieving this, the initial hall sensor signals which are the replica of switching signals emulated by sensorless method are given for 2 seconds. Table 6.3 shows the emulated hall sensor signals, their corresponding commutation signals.

Table 6.3 Commutation signals corresponding to emulated hall sensor signals

Emulated hall sensor signals			Corresponding commutation signals		
h_a	**h_b**	**h_c**	**Phase a**	**Phase b**	**Phase c**
0	1	1	-1	0	1
0	1	0	-1	1	0
1	1	0	0	1	-1
1	0	0	1	0	-1
1	0	1	1	-1	0
0	0	1	0	-1	1

The code for starting the motor which represent the initial hall sensor signals Sa1, Sb1, Sc1 shown below are given for 2 seconds..

Sa1 : [0 0 1 1 1 0]

Sb1: [1 1 1 0 0 0]

Sc1: [1 0 0 0 1 1]

After 2 seconds, once the motor starts to build up back EMF, the emulated hall sensor signals Sa, Sb, Sc from sensorless algorithm picks up and the motor continues rotating.

6.2.3 Generation of PWM

The two switches in an inverter leg cannot be switched on simultaneously at a particular instant as this will lead to a short circuit which should be avoided. A logic circuit is designed for the appropriate switching of inverter switches. Based on the logic circuit and emulated hall sensor signals, the inverter switches are selected. Based on the regulated output obtained from current controller, PWM signals are generated using ePWM blocks of TMS320F28377S. A and B channels of three PWM modules such as ePWM2, ePWM6, and ePWM10 are used for generating six PWM pulses for six switches.

For the proper synchronization of ADC and ePWM, the event trigger has been enabled at ADC start of conversion for module A and a screenshot of the block parameters of ePWM showing event trigger is shown in Fig. 6.6.

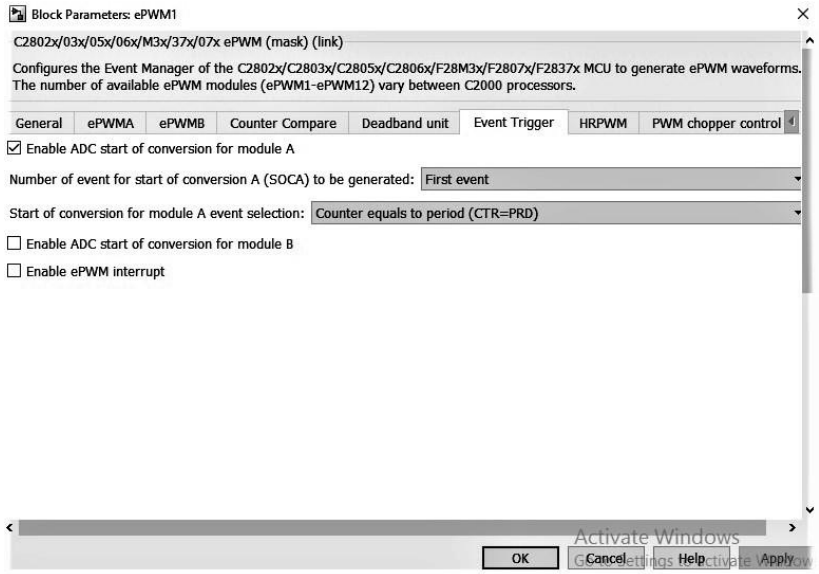

Fig. 6.6 Block parameters of ePWM showing event trigger

The PWM pulse output obtained through channels 0 -5 of logic analyzer is shown in Fig. 6.7. Among these, channels 0, 2 and 4 represent PWM pulses for the upper switches S_1, S_3 and S_5 respectively. Similarly channels 1, 3 and 5 represent the PWM pulses for the lower switches S_2, S_4 and S_6 respectively.

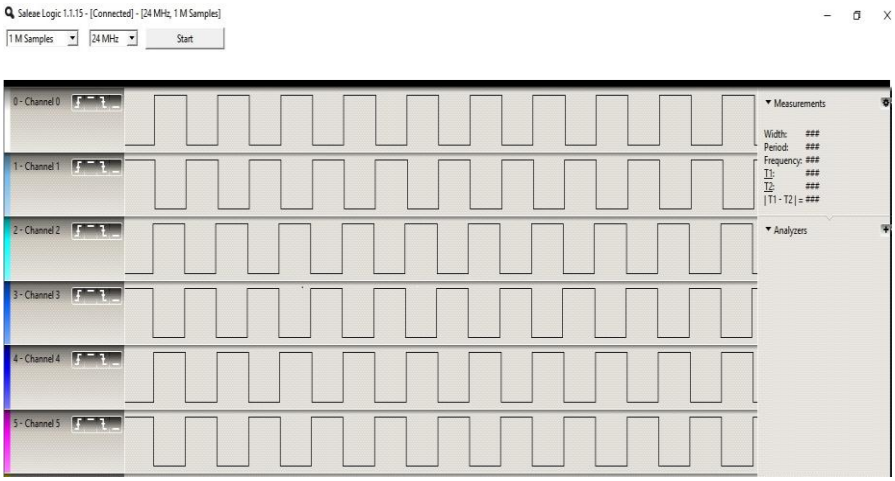

Fig. 6.7 Screenshot of six PWM pulses

6.2.4 Speed estimation

Usually the eCAP feature in TI C2000 is used to capture the hall sensor signal to estimate the time period, frequency and hence the speed of rotor. The prototype developed using hardware support package for C2000 TMS320F28377S in MATLAB 2016a version does not contain eCAP feature in its library. Since the hall sensors are replaced with sensorless technique, here the *ecap* feature has been mimicked using a counter at every rising edge of one of the emulated hall sensor signal.

For verification purpose, the emulated hall sensor signal is replaced with a pulse generator of time period 10 milliseconds. The waveforms shown in Fig. 6. 8 show that the counter is reset at every rising edge of the pulse and the sample is held at that time. From this, the time period (T) can be obtained. Frequency is given by the reciprocal of time period and with a scaling factor speed can be obtained.

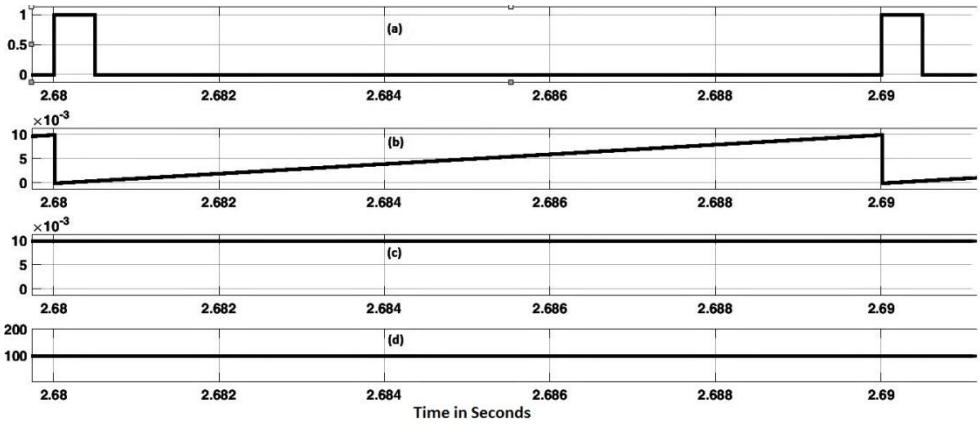

Fig. 6.8 Simulation results of speed estimator circuit (a) Pulses (b) Counter between two rising edges (c) Time period (d) Frequency

6.2.5 Speed controller strategy using H infinity control with PSO optimized weight generation

The estimated speed thus obtained is compared with the reference value and the error is passed on to the H infinity speed controller whose

weights are optimized using PSO algorithm. The convergence plot of PSO is shown in Fig. 6.9. The total number of evaluations is 822.

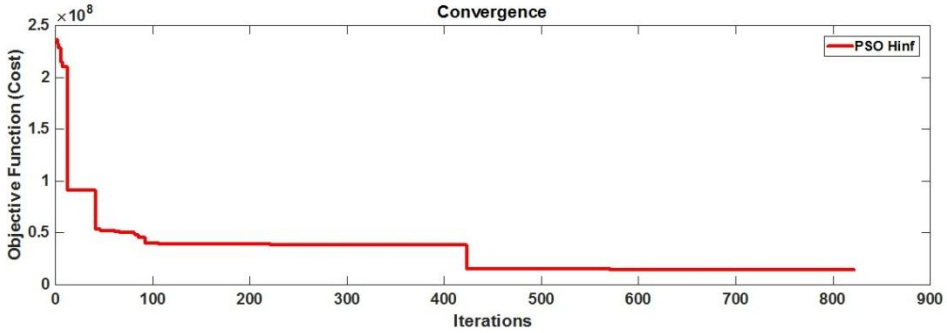

Fig. 6.9 Convergence plot of PSO

The controller transfer function is given by Eq (6.1).

$$KT = \frac{3206s^2+4.499e04s+4.45e08}{s^3+2133s^2+2.097e06\,s+1.112e08} \tag{6.1}$$

The optimized weight W_1 is given by Eq (6.2) and W_2 and W_3 are 0.16 and 0.02 respectively.

$$W_1 = \frac{0.0796s+39.8}{0.1s+27.36} \tag{6.2}$$

From the bode plot of the controller which is shown in Fig. 6.10 it can be inferred that the gain margin is 32.8dB and the phase margin is between -139 to 132.

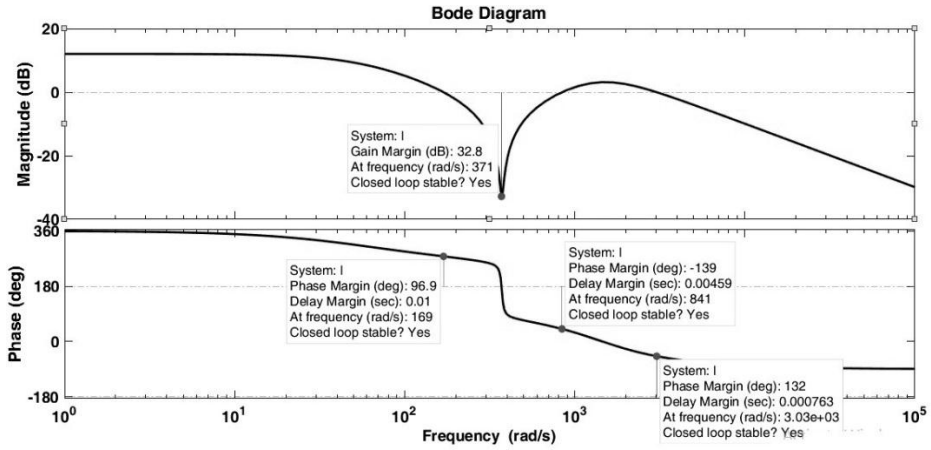

Fig. 6.10 Bode plot of controller

The sensitivity and complementary sensitivity plots of the controller are shown in Fig. 6.11(a) & 6.11(b) respectively. It can be observed that the controller can provide -80 dB sensitivity at low frequencies. The sensitivity and complementary plots follow the trade off in which sensitivity function S is low for lower frequencies thereby achieves better reference tracking as well as disturbance rejection and complementary sensitivity function T is lower for high frequencies which leads to insensitivity to noise and errors in modeling.

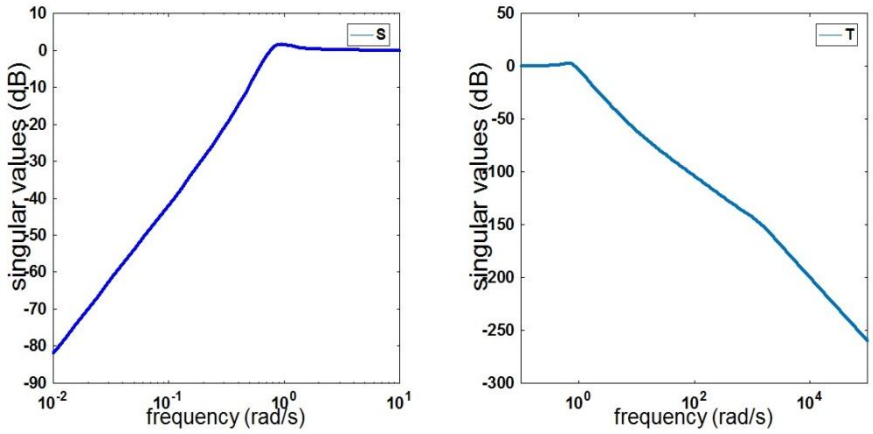

(a) (b)

Fig. 6. 11 (a). Sensitivity plot (b). Complementary sensitivity plot

6.2.6 Current controller

DRV 8301 BOOSTXL has low side current shunt sense in each leg and the currents in each leg of inverter are sensed through channels 1, 3 and 4 of ADC module A. These current values obtained through ADCs are then added to get the average current value. Fig. 6.12 shows the simulation result of three phase currents and their average current. This average current value is compared with the current reference value obtained from outer speed loop and the error is then passed onto the current controller which is PI controller. Table 6.4 shows the proportional and integral values of PI controller. PWM signals are generated from the controller's output to switch on and off the inverter switches.

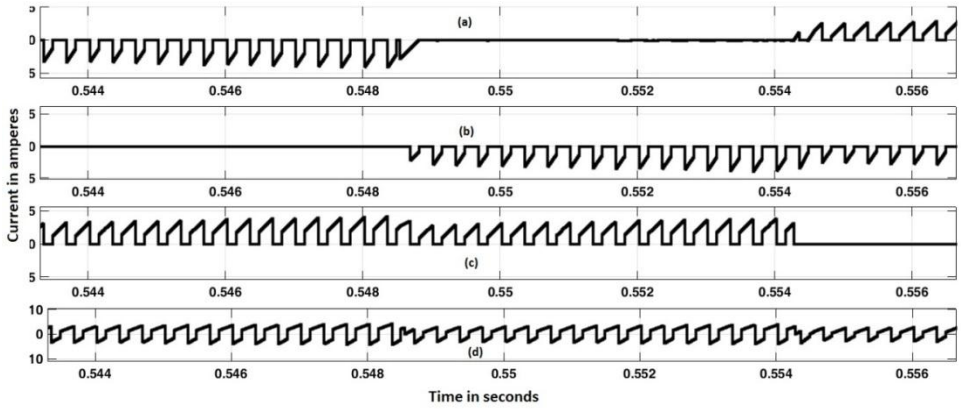

Fig. 6.12 Simulation results showing three phase currents and the average current (a) Phase current ia (b) Phase current ib (c) Phase current ic (d) Average current

Table 6.4 Constants of PI controller

Constant	Value
Proportional (Kp)	0.023
Integral (K_i)	0.012

6.2.7 Hardware in Loop Verification

The code that has been developed in SIMULINK with Embedded coder has been deployed to hardware and made to run. In order to obtain and verify the speed and current outputs, instead of Digital Storage Oscilloscope (DSO), Hardware in Loop verification is used in this work. This enables the data to be transmitted through Serial Communication Interface (SCI) Transmit and Receive registers. The values and their corresponding waveforms are viewed and verified through Hardware in Loop (HIL) verification via SCI as shown in Fig. 6.13.

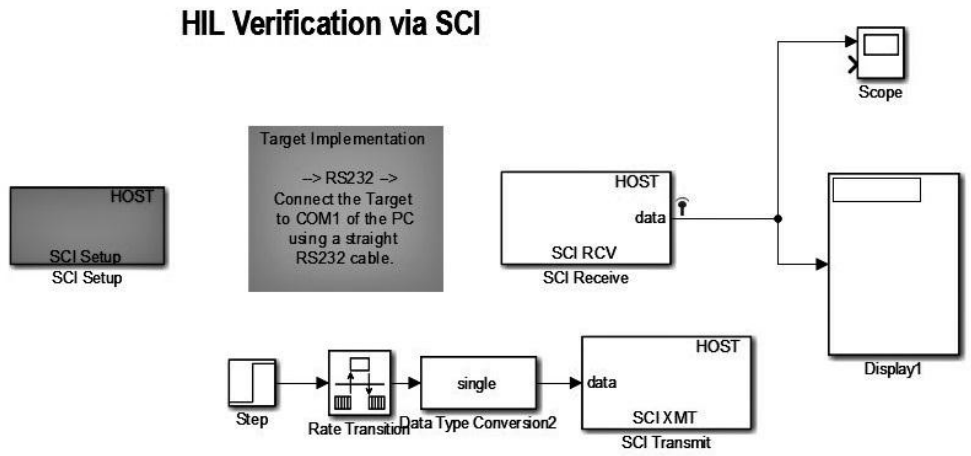

Fig. 6.13 Hardware in Loop Verification through SCI

6.3 Experimental Setup

Using the components discussed under section 6.1, a prototype has been setup for experimental validation under no load as well as under loaded conditions. The waveforms of speed and current obtained with both PI as well as H infinity controllers are analyzed for reference tracking and disturbance rejection under sudden load variations and compared.

6.3.1 Validation of motor performance under no load

The hardware setup for experimental validation of the proposed controller for motor under no load is shown in Fig. 6. 14. The experiment has been conducted in order to study the performance of controllers for change in reference speed with the motor under no load. The reference speed has been initially set as 2500 rpm and at 30 seconds it has been increased to 3000 rpm. The experiment is conducted with PSO optimized PI speed controller as well as H infinity speed controller in the speed loop and the results are compared.

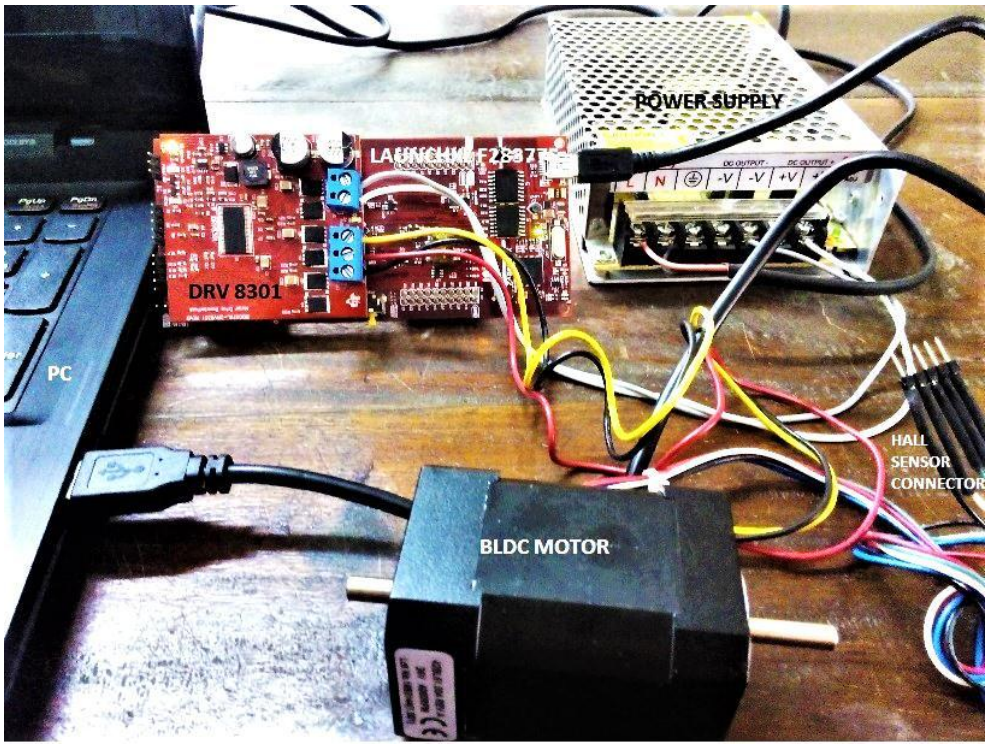

Fig. 6.14 Experimental setup with motor under no load condition

The rotor speed of the motor with both controllers are shown in Fig. 6.15 from which it can be inferred that both controllers track the reference speed but the PSO optimized H infinity controller with less overshoot.

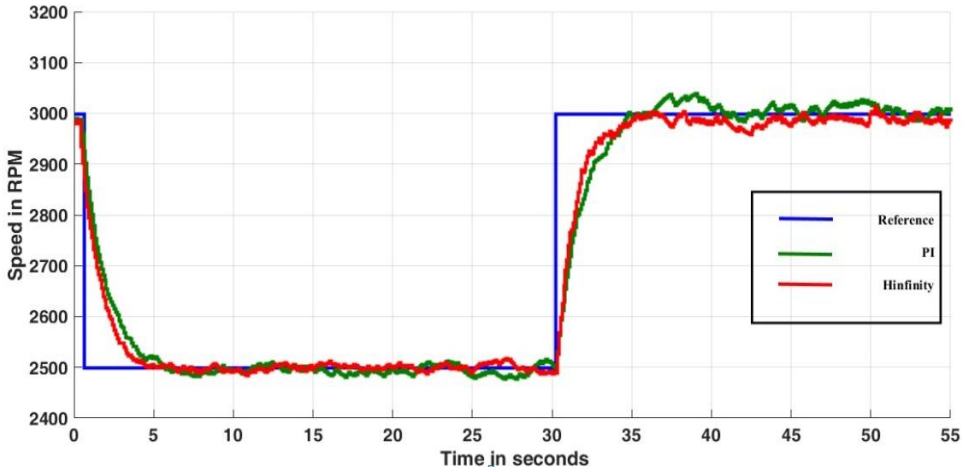

Fig. 6.15 Reference tracking of PI and H infinity controllers

Table 6.5 and Table 6.6 show the performance parameters of both PI and PSO optimised H infinity controller when the reference speed is changed from 3000 rpm to initial set speed of 2500 rpm and when it is again changed from 2500 rpm to 3000 rpm respectively.

Table 6.5 Comparison of parameters of both controllers when the reference speed is changed to initial set speed of 2500 rpm

Controller	Rise time (s)	Peak Time (s)	% Overshoot
PI	4.9	6.2	-0.32
H infinity	4.5	6.5	-0.12

Table 6.6 Comparison of parameters of both controllers when the reference speed is changed to final set speed of 3000 rpm

Controller	Rise time (s)	Peak Time (s)	% Overshoot
PI	4.8	7.5	1.26
H infinity	4.6	6.4	0.1

The current waveforms with both controllers are shown in Fig. 6.16 for a comparative study. It can be observed that the ripples in the current waveform of proposed controller is less than the PI controller which implies the reduction of torque ripples.

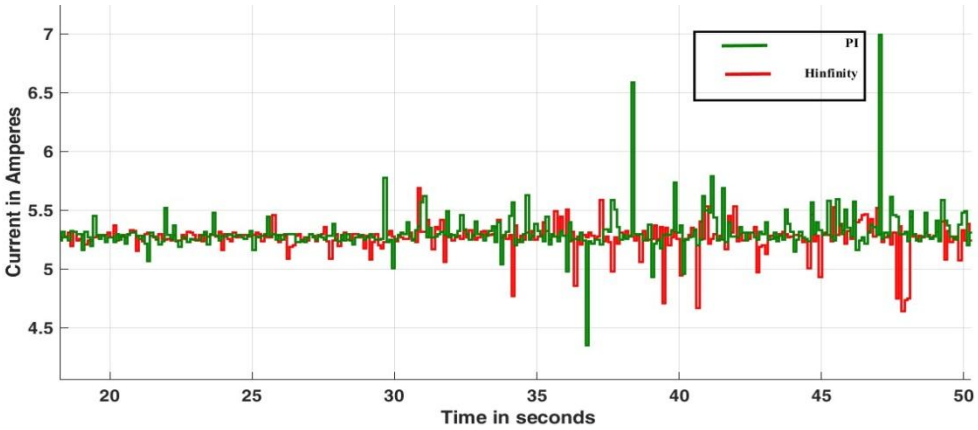

Fig. 6.16 Current waveforms of PI and H infinity controllers

6.3.2 Experimental setup on load

The performance of BLDC motor has been analyzed by coupling the motor with a generator supplying delta connected resistance network. The experimental set up with 42BL61 BLDC motor connected to another 42BL61 BLDC motor which acts as a generator is shown in Fig. 6.17. The generator has been electrically loaded using a balanced delta connected resistors of 47 ohms 10W in each arm. The study has been carried out during starting and also by applying the load during the period 30 - 40 seconds and by removing the load suddenly during the period 50 - 60 seconds.

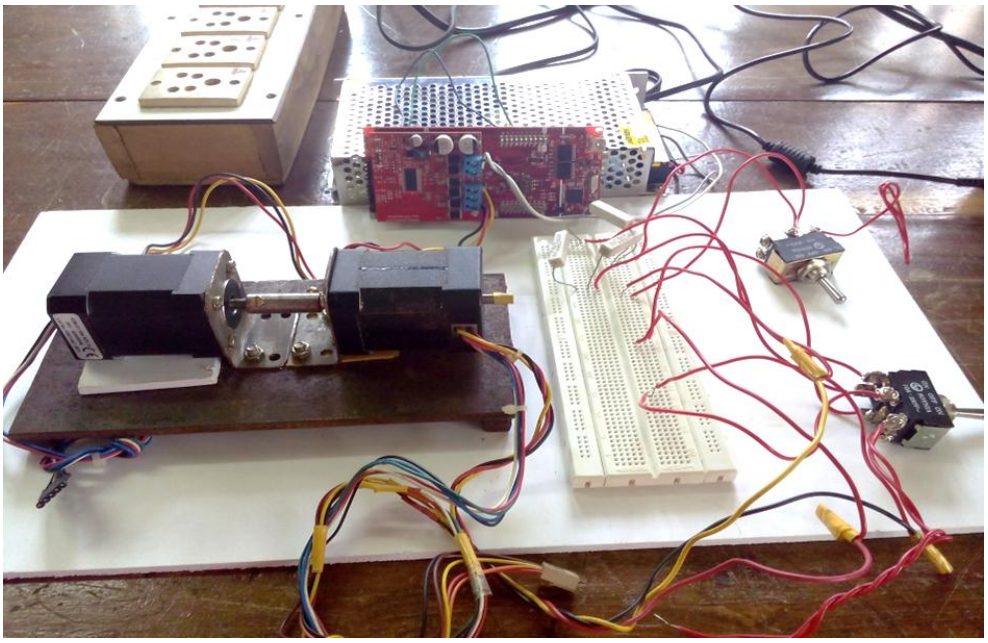

Fig. 6.17 Experimental setup for study of motor performance on load

The speed tracking of BLDC motor on load with PI controller as well as proposed strategy is shown in Fig. 6.18 and Fig. 6.19 respectively. It can be observed that the proposed strategy exhibits better reference tracking compared with PI controller. It has been found that percentage overshoot, settling time and steady state error for the proposed strategy is less compared to PI controller during starting.

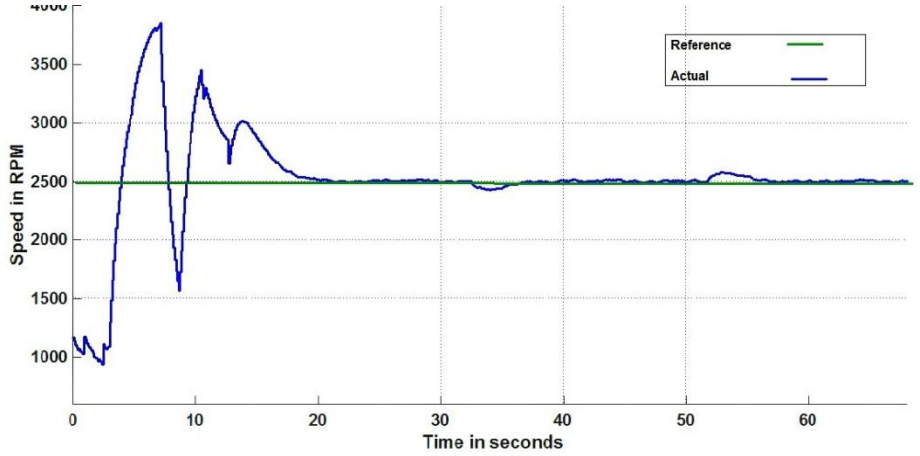

Fig. 6.18 Performance of BLDC motor on load with PI controller

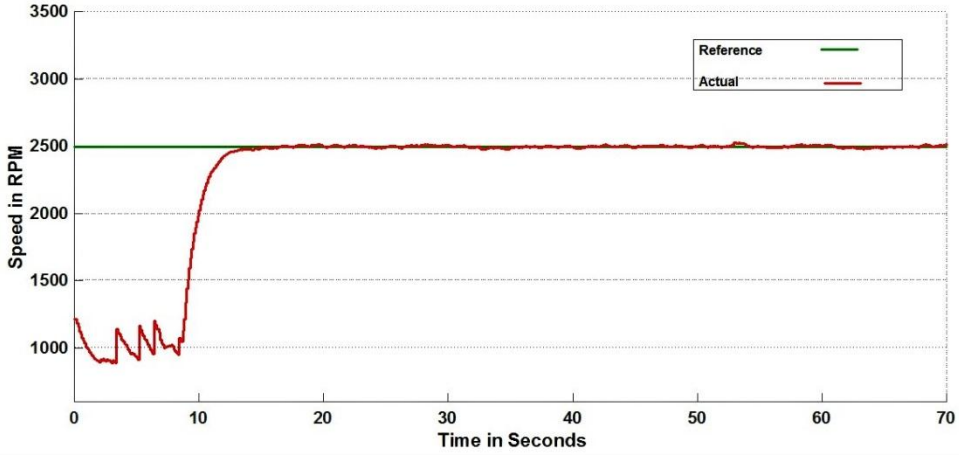

Fig. 6.19 Performance of BLDC motor on load with H infinity controller

The enlarged view of speed tracking with the application and removal of electrical load is shown in Fig. 6.20. It has been observed that the performance of H infinity controller displays more robust behavior during application and removal load. The results have been tabulated in Table. 6.7 and Table. 6.8.

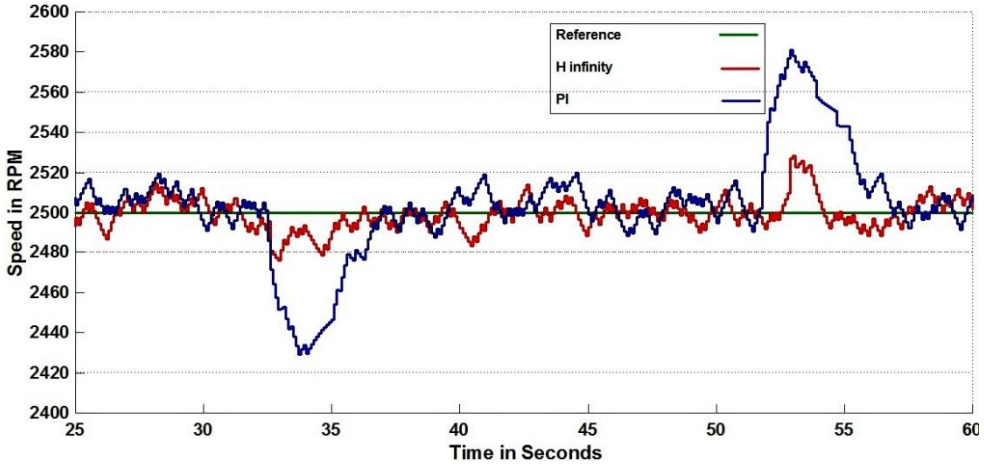

Fig. 6.20 Enlarged portion of speed waveforms during load application and load removal

Table 6.7 Performance parameters with PI controller

Characteristic	Time Interval (s)	Rise time (s)	Peak Time (s)	% Overshoot	Settling Time (s)	Steady state error
Starting	0-20	1.4	4.7	53.8	19.7	0.76%
Application of load	30-40	-	1.2	-2.8	4.6	0.8%
Load removal	50-60	-	1.2	3.24	4.6	0.36%

Table 6.8 Performance parameters with PSO optimized H infinity controller

Characteristic	Time Interval (s)	Rise time (s)	Peak Time (s)	% Overshoot	Settling Time (s)	Steady state error
Starting	0-20	8.2	8.3	0.24	8.7	0.6%
Application of load	30-40	-	1.5	-0.96	4.0	0.12%
Load removal	50-60	-	0.5	1.12	1.7	0.12%

When the load is applied during 30-40 seconds, a significant reduction of 1.84% of percentage overshoot, 0.6 seconds of settling time and 0.68% of steady state error has been observed with proposed strategy compared with PI controller. Similarly when the load is removed suddenly during 50-60 seconds, a reduction of 2.12% of percentage overshoot, 2.9 seconds of settling time and 0.24% of steady state error has been observed. The reduction in percentage overshoot, settling time and steady state error with PSO optimized H infinity controller results in better reference tracking

in the presence of load disturbances.

The enlarged view of current waveforms with the application and removal of electrical load is shown in Fig. 6.21. It has been observed that the magnitude of maximum current ripples with H infinity controller is 0.886 whereas it is 1.079 with PI controller when the motor is under loaded condition. This implies a reduction of current ripples and hence a reduction in torque ripples with the proposed strategy compared with PI controller.

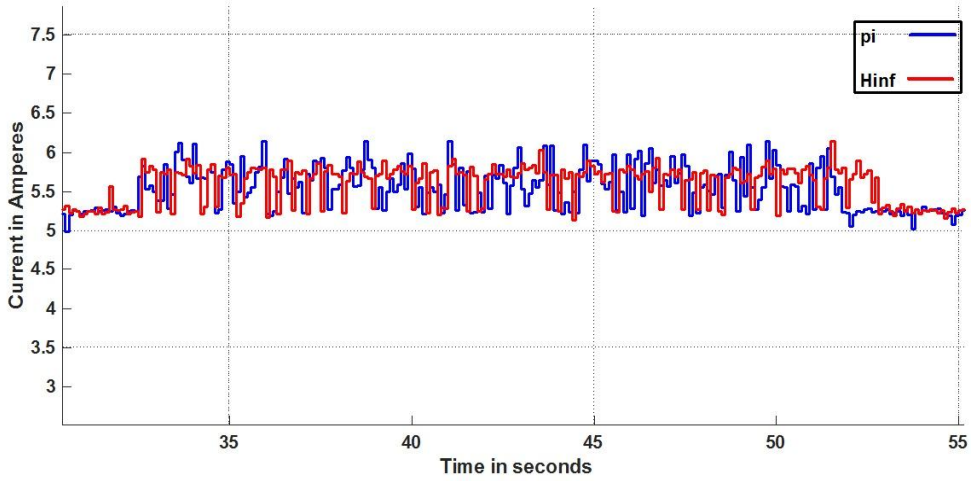

Fig. 6.21 Enlarged portion of current waveforms during load application and load removal

Thus a robust performance of BLDC motor has been achieved with the proposed strategy and it has been verified.

Chapter Summary

A prototype of H infinity speed controller with weights optimized by PSO technique for sensorless BLDC motor has been proposed, designed and implemented with TI C2000 Delfino LaunchPad LaunchXL-F28377S and BoostXL DRV 8301. Corresponding hardware support package has been utilized for the development of code. The sensorless technique has been adopted by calculating terminal voltage difference and thereby hall sensor signals are emulated. It has been observed that tracking reference with the

proposed strategy improves the overall performance of motor with less torque ripples and hence less vibration as well as smooth transition than conventional PI controller under no load condition. A detailed study of the parameters such as percentage overshoot, settling time and steady state error of the proposed strategy by the sudden application and removal of an electrical load has been done and the results have been compared with that of PI controller. It has been observed that there is a substantial reduction of these parameters with the proposed strategy when compared with PI controller. Moreover the current ripples are found to be reduced with the proposed strategy. This implies that the proposed strategy has been more robust with faster rejection of disturbances and better reference tracking thereby improves its performance on load.

*****

Chapter 7

Case Studies

Contents

Case studies have been conducted by simulation to prove the feasibility of proposed H infinity speed controller strategy in BLDC motors used as propulsion motors for submarines and AUVs. A submarine with standard operational profile and the four quadrant operation of the motor drive used in AUV have been studied and simulation results are discussed.

7.1 Submarines

A simplified electric propulsion power system [190] consists of a power generation unit in which the prime mover can be a diesel engine or a gas turbine coupled with a synchronous generator, a step down transformer, a power converter consisting of AC - DC rectifier along with an inverter and an electric motor coupled with propeller as depicted in Fig. 7.1. For the submarine considered for case study, the prime mover is a gas turbine and a synchronous generator is used to generate the rated voltage. This voltage is being stepped down using a delta-delta transformer. The operational profile of a submarine uses medium cruising speed. The remaining power obtained can be used for other loads including hotel loads as well as for pumps which is an added advantage. The rectifier and inverter decouple the power generation system with motor drive.

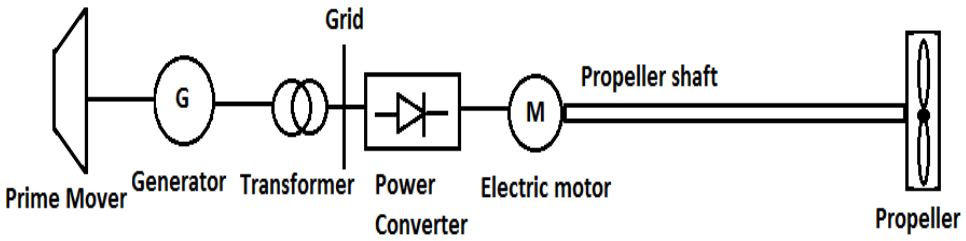

Fig. 7.1 Simplified block diagram of power flow in electric propulsion

A BLDC motor is adopted as propulsion motor in the submarine considered since the literature suggests the implementation of this motor in submarines for its advantages such as noise reduction and low electromagnetic interference [159], [191]. The motor considered has specifications shown in Table 7.1. With these motor specifications, the transfer function of motor G(s) can be derived as (7.1).

$$G(s) = \frac{285.53}{s^2+847.83s+25} \tag{7.1}$$

Table 7.1 Specifications of BLDC motor used in submarine

Parameters	Specifications
Phase Resistance	1.95Ω
Phase Inductance	2.3mH
Rotor Inertia	0.1340 Kgm^2
Voltage constant	0.088V.s/rad
Torque constant	0.088Nm/A

PSO parameters derived for tuning gains of PI controller and H infinity controllers for the speed control of the motor considered are shown in Table 7.2.

Table 7.2 Parameters of PSO algorithm for both PI and H Infinity controllers

Parameters	PI	H infinity
C1	0.12	1.5
C2	1.2	2.5
Dimension	2	6
Damp ratio	0.95	0.95
Inertia	$1.1058*10^{-9}$	0.005
No. of birds	20	20
Bird steps	20	5
Variable Low	[0.1 0.00001]	[0.05 1 0.1 0.1 0.000001 0.00001]
Variable High	[4 1]	[1.8 500 20 50 0.16 0.02]
Evaluations	421	101
Global Best Fitness	$2.0364*10^{4}$	$5.089*10^{6}$

The optimal values of PI controller gains and weights of H infinity controller obtained through PSO are shown in Table 7.3.

Table 7.3 Gains and weights of controllers

Gains of PI controller		Weights of H infinity controller		
K_p	K_i	W_1	W_2	W_3
1.24	0.125	$\frac{1.7975s + 444.8}{81.08s + 0.1}$	0.1162	0.02

The convergence plots of PSO for PI as well as for H infinity controller are shown in Fig. 7.2 and Fig. 7.3 respectively.

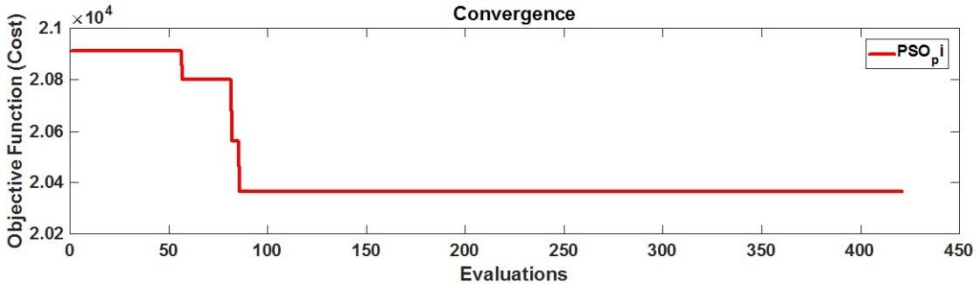

Fig. 7.2 Convergence plot of PSO for PI controller

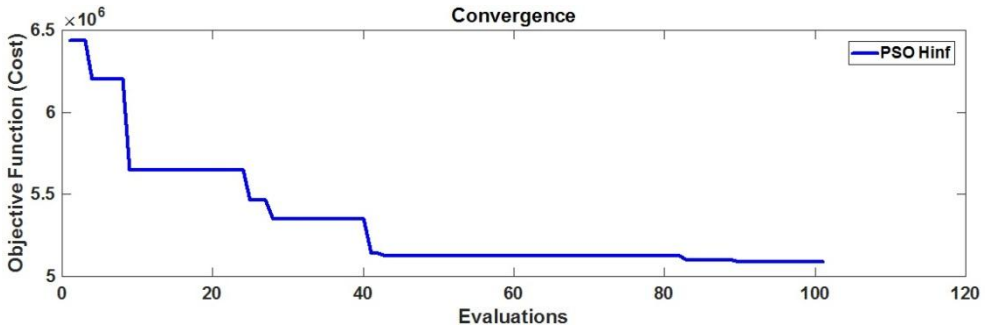

Fig. 7.3 Convergence plot of PSO for H infinity controller

The optimal transfer function of controller obtained with coefficients of its weights being optimized by PSO is given in (7.2) and the value of γ is obtained as 1.85.

$$K = \frac{8.056e04\ s^2+6.83e07\ s+2.014e06}{s^3+5038\ s^2+3.58e06\ s+5371} \tag{7.2}$$

7.1.1 Simulation results

A model of electric power system incorporating the power generation has been simulated in MATLAB/ SIMULINK/ SIMSCAPE platform with a gas turbine as the prime mover for a synchronous generator [190]. A delta-delta transformer is used to step down the voltage to 500V. This ac voltage is then rectified with a diode rectifier whose output is fed to the sensorless BLDC motor through an inverter. The primary and secondary phase voltages of delta-delta transformer are shown in Fig. 7.4. It can be observed that rms values of primary and secondary phase voltages are obtained from measurements as 8051V and 291V respectively for the corresponding rated line voltages of 13.8 kV and 500V.

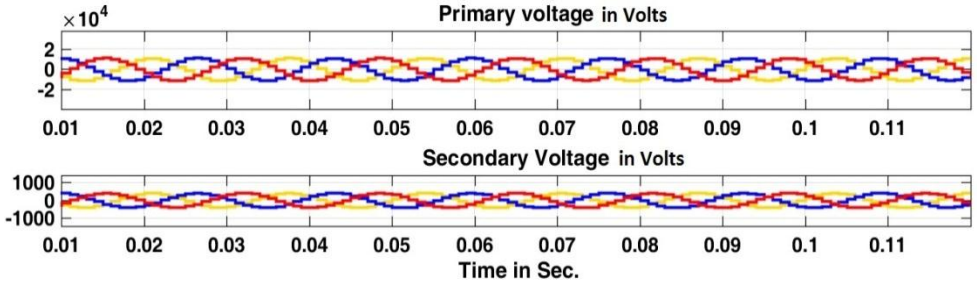

Fig. 7.4 Primary and secondary voltages of transformer

The corresponding dc output of rectifier is shown in Fig. 7.5. It is obtained as 685V which can be verified from (7.3)

$$V_{dc} = \frac{3\sqrt{6}}{\pi} V_{ph} \tag{7.3}$$

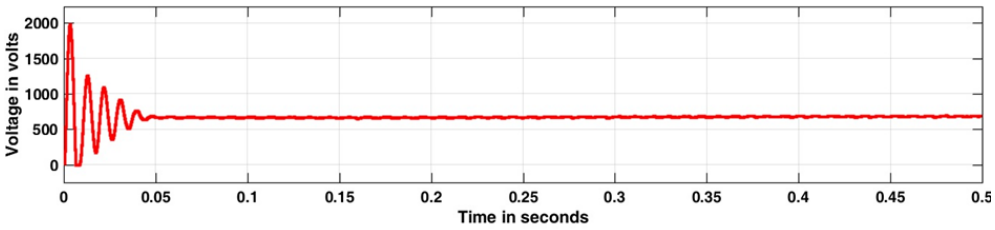

Fig. 7.5 DC voltage output of rectifier

A simulation study has been conducted with operational profile of submarine VII C available in British admiralty report [192] which is shown in Table 7.4. A performance comparison study of proposed H infinity controller and PI controller has been carried out and results have been discussed.

Table 7.4 Operational profile of submarine VIIC

KNOTS	1.5	3	4.1	5.23	6.1	7.4
Speed in RPM	60	112	160	200	233	280
	Dead slow	Slow	Half speed	3/5 speed	¾ speed	Full

The rotor speed is set to follow the standard operational profile which is shown in Fig. 7.6. At 0.3 sec, a load torque of 11Nm is applied and at 1.5sec a reversed torque of 11Nm is applied. The rotor speed with H infinity controller is found to be tracking the reference speed with less speed error than with PI controller in the presence of load disturbance.

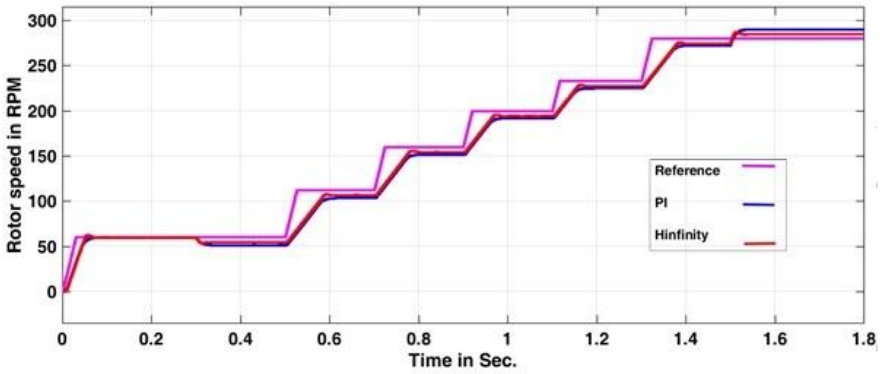

Fig. 7.6 Rotor speed with a standard operational profile

From the enlarged version of the speed characteristics shown in Fig. 7.7 (a) and (b) it can be concluded that H infinity controller shows better command tracking and reduction in steady state error compared to PI controller.

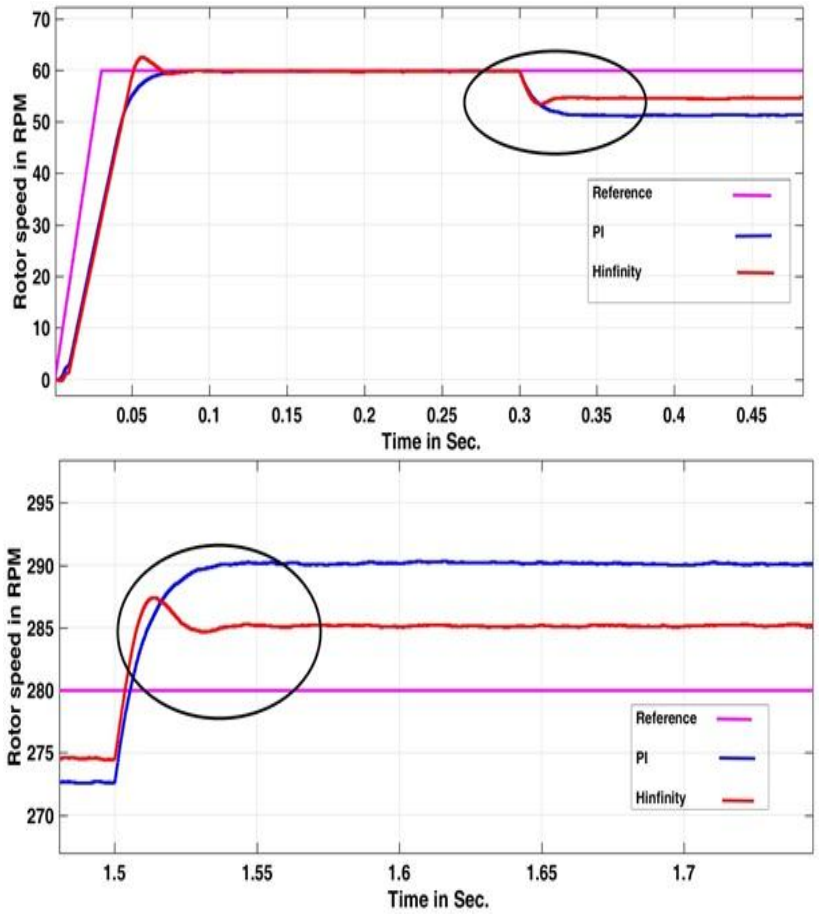

Fig. 7.7 (a). Rotor speed at 0.3 sec (b) Rotor speed at 1.5 sec

The waveforms of electromagnetic torque obtained using both controllers when a load torque of 11Nm is applied at 0.3 seconds are shown in Fig. 7.8. It can be inferred that the torque ripples with H infinity control has been found to be less resulting in reduced vibration and noise signature which are the prerequisites in submarines.

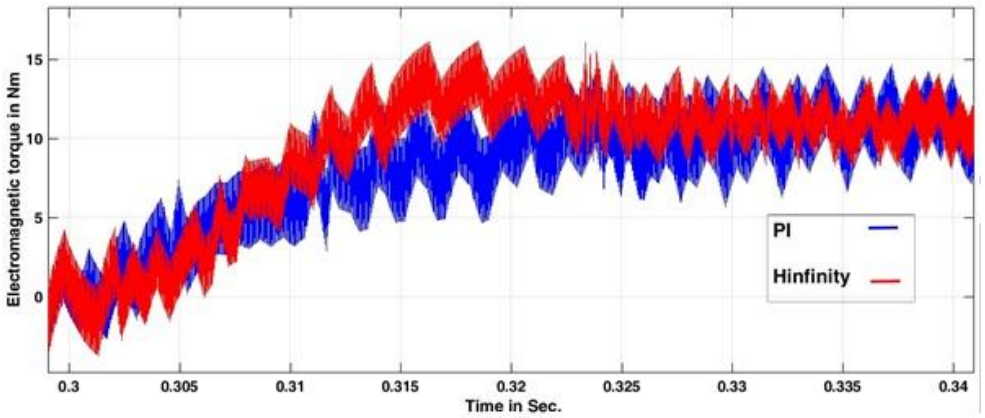

Fig. 7.8 Electromagnetic torque

7.2 Autonomous Underwater Vehicles

Autonomous Underwater Vehicle as the name indicates is a self-controlled robot for performing a predefined task under sea or ocean. It is an independent swimming robot which has its power pack, guidance, control, navigation, sensors and thrusters intact on board. AUV finds its applications in various fields such as conservation of marine biodiversity, provision of exact information regarding coral reefs, concentration of fish population, quality of water like its oxygen concentration, pH concentration and so on. These tasks are performed with high reliability and precision with the help of advanced sensors than the older methods with human intervention. Also it is used in military applications such as detection of underwater mining, torpedo propulsion and so on where precision and accuracy is of primary concern.

A computer based mission control system has been designed and implemented in MARIUS AUV for the simple communication with the end

user. Fig. 7.9 shows the general block diagram with main blocks for vehicle control system [172]. In this, vehicle guidance and control block provides the reference speed to be achieved based on the reference trajectory inputs from mission control system and navigation system to the actuator control system. This is necessary for the proper trajectory tracking in the presence of uncertainties such as variation in vehicle parameters and also due to external disturbances such as varying sea currents due to weather disturbances. As the name of AUV indicates it should be autonomous in every aspect. There are two controllers involved in proper propulsion of AUVs. The first one is motor controller and the second one is vehicle controller. In this context, the work presented here mainly focuses on the motor controller significant in controlling the speed of thrusters which are coupled with propellers. Thus this work is of utmost important for maintaining the required velocity of the vehicle.

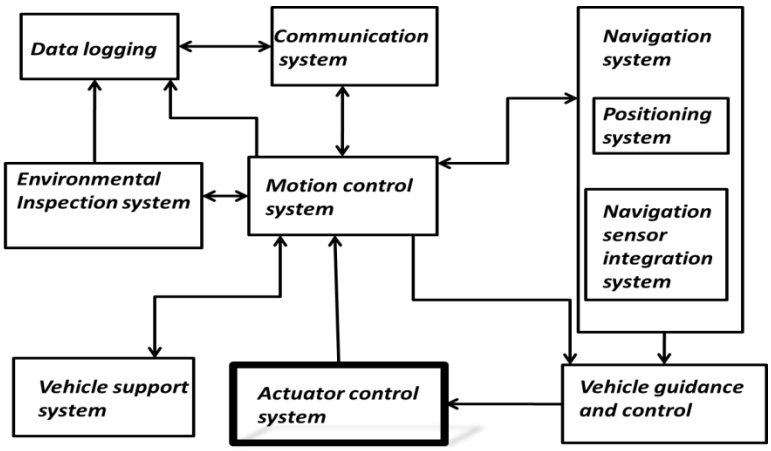

Fig. 7.9 Vehicle control system

The component diagram is shown in Fig. 7.10. The major components of electric thrusters include electric motors, motor controllers, gear box, shaft, propeller, and electric connector.

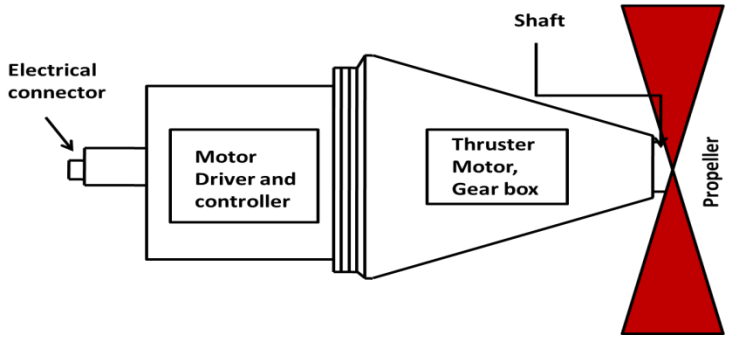

Fig. 7.10 Component diagram of thruster motor

7.2.1 Four quadrant operation

An electric motor can be operated in two modes – motoring and braking or regenerating. In motoring mode, it converts electrical energy to mechanical energy that supports its motion. In braking mode it acts as a generator and converts mechanical energy to electrical energy that opposes its motion. It has four quadrants of operation as shown in Fig. 7.11. In the first quadrant, both speed and torque are positive thereby forward motoring takes place. In the second quadrant, speed is positive but torque is negative indicates the forward braking region. Similarly in the third quadrant, both speed and torque are negative which indicates the reverse motoring region and in the fourth quadrant, speed is negative but torque is positive which indicates the reverse braking region. As a case study, reference speed of BLDC motor is set at 1000 rpm. The four quadrant operation of the motor has been analyzed with both PI and H infinity controllers and the simulation results have been studied.

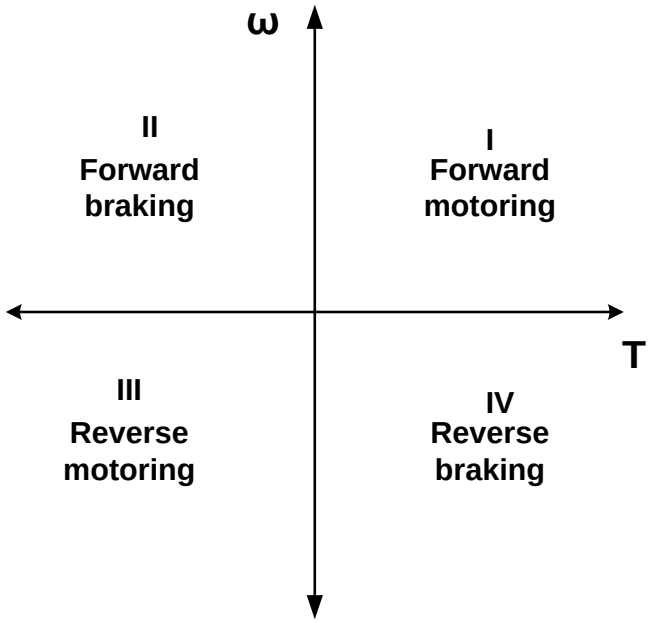

Fig. 7.11 Four quadrant operation of an electric drive

The specifications of BLDC motor based on which the simulations have been carried out are shown in Table 7.5.

Table 7.5 Specifications of BLDC motor used in AUV

Rated Voltage	48 V DC
Rated Current	17.95 A
Rated Power	660W
Rated Torque	2.1 Nm
Rated Speed	3000 rpm
Line to line Resistance	0.07Ω
Line to line inductance	0.1mH
Rotor inertia	0.00024Kgm^2
Torque constant	0.117Nm/A

The transfer function of the motor has been derived as (7.4). Table 7.6 shows parameters involved in generation of optimal controllers using PSO.

$$G(s) = \frac{0.117}{2.8e{-}08s^2 + 2.265e{-}05s + 0.1205} \quad (7.4)$$

Table 7.6 Parameters of PSO algorithm for both PI and H Infinity controllers

Parameters	PI	H infinity
C1	0.12	1.5
C2	1.2	2.5
Dimension	2	6
Damp ratio	0.95	0.95
Inertia	$1.1058*10^{-9}$	$3.3267*10^{-10}$
No. of birds	20	20
Bird steps	20	20
Variable Low	[0.1 0.00001]	[0.05 1 0.1 0.1 0.001 0.0001]
Variable High	[1 1]	[1.8 500 200 50 0.16 0.02]
Evaluations	421	422
Global Best Fitness	$4.0852*10^{5}$	$3.8215*10^{7}$

The PSO optimized gains of PI controller and weights of H infinity controller are shown in Table 7.7.

Table 7.7 Gains and weights of controllers

Gains of PI controller		Weights of H infinity controller		
K_p	K_i	W_1	W_2	W_3
0.9977	0.8561	$\frac{0.0796s + 500}{0.1s + 27.3579}$	0.14	0.015

Fig. 7.12 and Fig. 7.13 represent the convergence plots of PSO for both PI and H infinity controllers.

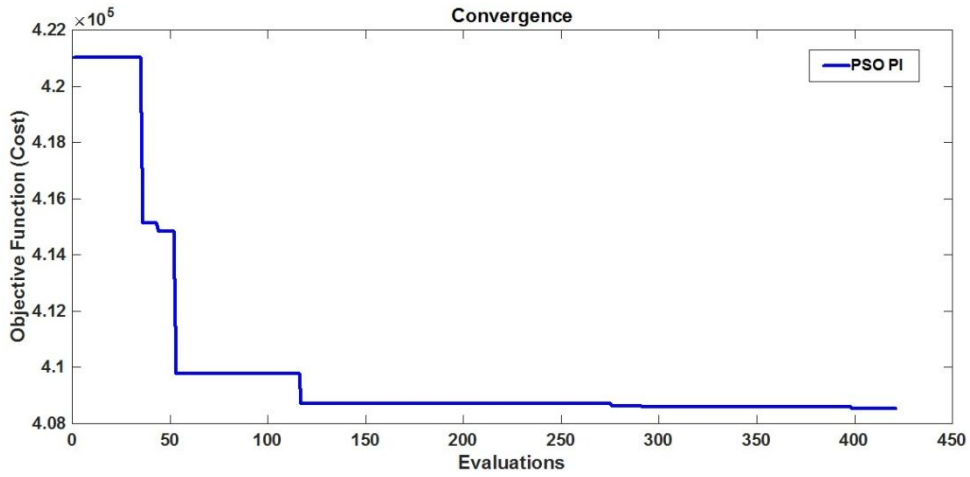

Fig. 7.12 Convergence plot of PSO for PI controller

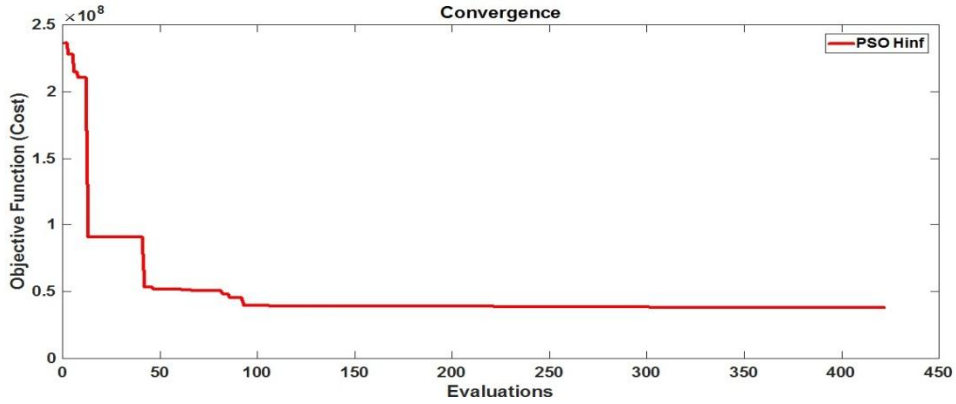

Fig. 7.13 Convergence plot of PSO with H infinity controller

The transfer function of the controller is obtained as (7.5)

$$KT = \frac{186.5s^2+4462s+5.044e07}{s^3+371.6s^2+2.867e05s+8.747e07} \quad (7.5)$$

7.2.2 Simulation results

A simple trapezoidal trajectory is enough to increase the velocity of the vehicle from zero to desired value and then to reduce it back to zero. It should be kept in mind that while generating trajectory, the acceleration and velocity should be limited based on vehicle's capabilities [193]. As part of

analysis in the four quadrants the reference speed and load torque are set [194] as shown in Table. 7.8. As a detailed study the performance of motor is analysed in each quadrant.

Table 7.8 Reference speed and load torque values

Quadrant	Mode	Time in seconds	Speed (ω)	Torque in Nm	Power
I	Forward Motoring	0.5	1000	1	Positive
IV	Reverse Braking	0.7	-1000	1	Negative
III	Reverse Motoring	1.0	-1000	-1	Positive
II	Forward Braking	1.2	1000	-1	Negative

Accordingly the simulation has been carried out with both speed controllers in order to compare their performance with the motor drive under four quadrant operation. The speed waveforms of the motor in the first and fourth quadrants as well as in the third and second quadrants with both controllers are shown in Fig. 7.14 and Fig. 7.15 respectively.

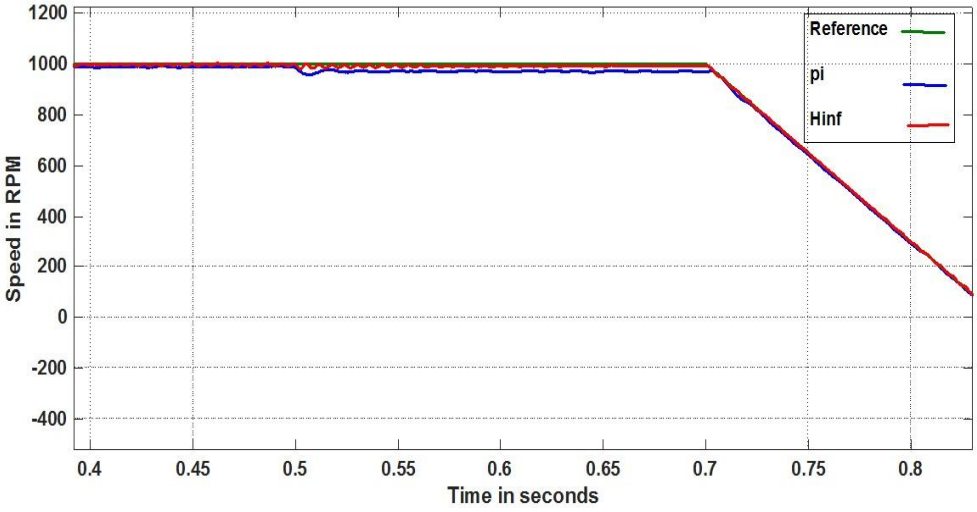

Fig. 7.14 Speed waveform of the motor operating in first and fourth quadrants

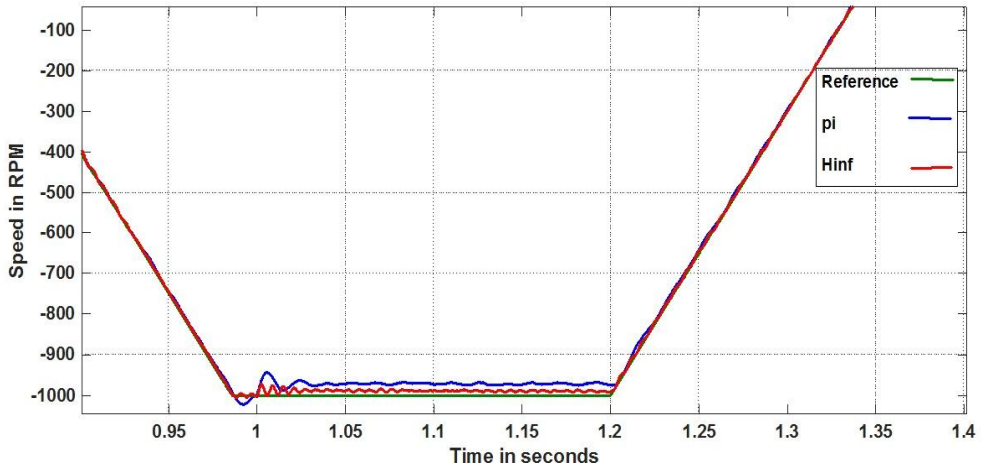

Fig. 7.15 Speed waveform of the motor operating in third and second quadrants

It can be inferred that in the forward and reverse motoring region (I & III quadrants), the proposed strategy tracks the reference speed with an overshoot of 2% less than PI controller. Similarly when there is a change in reference speed at 0.7 seconds during reverse braking region (IV quadrant) and at 1.2 seconds during forward braking region (II quadrant), the tendency of proposed strategy to track the reference speed is more significant than PI controller. These features make the proposed strategy more robust than PI controller in the presence of disturbances such as load reversals and reference speed change.

Moreover Fig. 7.16 depicts the electromagnetic torque ripples in first (I), second (II), third (III) and fourth (IV) quadrant operations. It can be inferred that during regenerating modes as shown in second and fourth quadrants, the torque ripples are higher with PI controller compared with proposed H infinity control strategy. It is observed that in the forward braking region (II quadrant), the torque oscillates between 5.464 Nm to -6.217 Nm with PI controller whereas the oscillations are between 1.692 Nm and -1.28 Nm with H infinity controller. Similarly, in the reverse braking region (IV quadrant), the torque oscillates between 5.356 Nm and -5.298 Nm with PI controller whereas it oscillates between 2.014 Nm and -1.474 Nm with the proposed strategy.

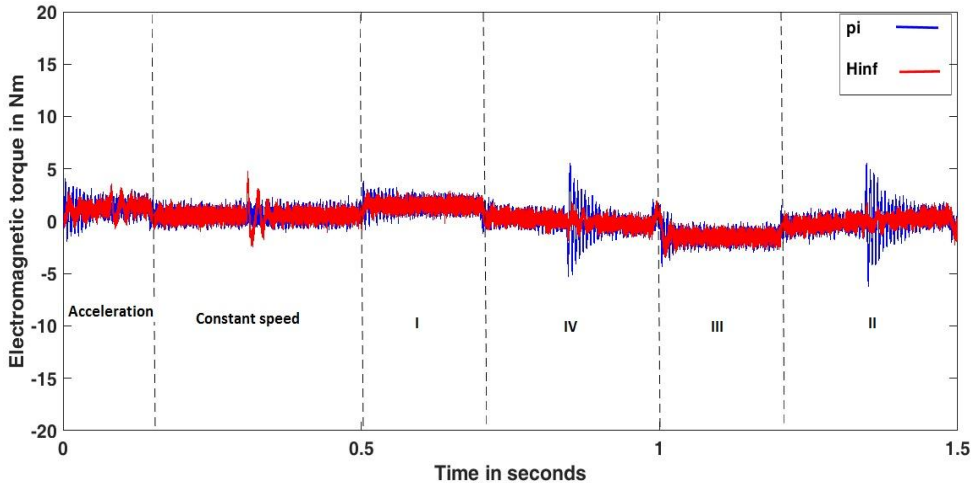

Fig. 7.16 Comparison of Electromagnetic torque of both controllers with the motor in four quadrant operation

Chapter Summary

A case study through simulation has been conducted using PSO optimized H infinity controller as speed controller of BLDC motors used as propulsion motors in submarines. A comparative study of the proposed strategy has been supplemented with PSO optimized PI controller and the simulation results show that the proposed strategy improves the steady state error, reduces noise and vibration as well as exhibits better speed command tracking. This leads to improved maneuverability, reduced noise signatures which are the requisites for submarines. Similarly this strategy has been simulated for electrical thrusters in AUV and a four quadrant operation has been studied with both controllers. The simulation results confirm the good reference tracking and rejection of load disturbances with the proposed strategy when compared with PI controller. During braking operation of the motor drive, the proposed controller strategy exhibits reduced torque ripples compared to PI controller. This helps in achieving a smooth operation of AUV.

*****

Chapter 8

Conclusion

The robust control of BLDC motors is a vast developing area as it finds its applications in military, aerospace, marine electric propulsion and so on. Insensitivity to disturbances, uncertainties and modeling errors is expected from the motors used in these applications. A detailed research review has been conducted in order to identify the research gap that exists in this field and the implementation of H infinity speed controller with its coefficients of weights optimized by PSO to make the BLDC motor performance robust against load disturbances and reference changes is proposed.

The sensorless technique using line to line voltage difference has been adapted for the rotor position detection of BLDC motor control since this saves cost, space, external wiring and phase correction circuitry. The speed control of BLDC motor has been designed with a H infinity controller with its coefficients of weights optimized by PSO for achieving robust performance. For comparison purpose a PI speed controller has been designed with its gains optimized by PSO.

The speed control of BLDC motor with the adapted sensorless technique has been modeled in MATLAB / SIMULINK environment and a case study in simulation has been conducted. It has been observed that the controller can provide -0.22 dB sensitivity at low frequencies. The simulation results were compared with that of a PI controller. An improvement of 0.6% of rise time, 0.5% reduction in steady state error has been observed.

The simulation studies conducted have been validated with the implementation of the model in hardware using C2000™ Delfino™ LaunchPad™ LAUNCHXL-F28377S as the development board and Booster pack based on DRV 8301 as the motor driver. The code has been generated in MATLAB environment using CCS Version 6 and control SUITE.

Experimental study has been conducted with the motor on no load and loaded conditions and a comparative study has been carried out with both controllers. The speed and current / torque variations were observed for change in reference speed and sudden load variations. It has been observed that the controller can provide -80 dB sensitivity at low frequencies. It has also been observed that there is an improvement of 0.2 seconds in rise time, 1.1 seconds in peak time as well as 1.25% in overshoot during reference tracking. The current ripples with the proposed controller strategy are found to be less which implies the reduction of torque ripples. Similarly there is an improvement of 0.3 seconds in peak time, 1.84% in overshoot, 0.6 seconds in settling time and 0.68% in steady state error has been observed during the sudden application of load. During the sudden removal of load, the proposed H infinity controller shows an improvement of 0.6 seconds in peak time, 1.12% in overshoot, 2.9 seconds in settling time and 0.24% in steady state error.

BLDC motor has been used in marine electric propulsion system as propulsion motor and as thruster motor coupled with propellers in AUVs due to their high torque, high efficiency, low EMI, and less noise. Case studies were conducted with the proposed controller strategy in BLDC motors used in submarines with a standard operational profile and the four quadrant operation of the motor in AUVs.

A comparative study of the proposed controller and PI controller has been conducted through simulation with operational profile of submarine

VIIC available in British admiralty report. It has been observed that whenever there is change in reference speed and during the load disturbances, the proposed control strategy exhibits a robust behavior with reduction in rise time and steady state error. The reduction of torque ripples reduces noise and vibration which is the prerequisite for escape from enemy detection in submarines.

The four quadrant operation of the BLDC motor used as thruster motor coupled with propellers has been studied due to their applications in sea surface area exploration, sea border surveillance and their role in underwater study. A comparative study of both controllers has been done and the results have been discussed. During forward braking region, the torque ripples with the proposed controller strategy are found to be reduced by 8.709 Nm. Similarly in the reverse braking region, a reduction of 7.161 Nm in torque ripples has been observed with the proposed controller strategy compared with PI controller. This demonstrates the robust behaviour of the proposed H infinity speed controller with its coefficients of weights optimized by PSO compared with PI speed controller with its gains optimized by PSO.

Significant contribution

- Implementation of H infinity speed controller for the robust control of sensorless BLDC motor drive.
- Adaptation of PSO technique for optimal tuning of coefficients of weights in an H infinity controller.
- Hardware realization using Texas Instruments C2000 Delfino Launchpad LAUNCHXL F28377S microcontrollers with its hardware development package along with motor drive booster pack BOOSTXL DRV8301 for achieving BLDC motor control with sensorless technique for validation of simulation results.

- Simulation of case studies for submarines with realistic operational profile has been conducted. A four quadrant operation of the motor used in AUV with proposed controller has been done in order to study its performance in the motoring and regenerating modes.
- Improvement in speed tracking, reduction of torque ripples and response time as well as improvement in stability of the motor under disturbances have been achieved by implementing H infinity controller as speed controller

Limitations

The synthesized H infinity controller is unique for each system. This led to the optimization procedure to be repeated for each motor specification. Moreover it does not respond well to non-linear constraints such as saturation. The success of this control lies in the proper choice of weighting function.

PSO has been incorporated as an offline optimization. The values of system parameters are defined before the actual implementation. This results in the negligence of variation in parameters that may happen in real case. Moreover PSO also has the disadvantage of premature convergence.

The basic conventional PSO algorithm has been implemented in this work without any constraints and there is only one objective of minimization of the error.

Future scope

PI controller has been used in the inner current loop in this work. H infinity controller can be incorporated as current controller also and the complete system can be controlled with H infinity theory.

Online optimization strictly depends upon optimization time since data collection, sampling and processing of real time data consumes time. Since the parameters required in the case of PSO is less, its optimization time is also less and hence it can be used for online optimization. The constraints pertaining to error can also be applied.

A comparative study can also be conducted with the weighting functions optimized by other optimization techniques such as Genetic Algorithm, ant colony algorithm or hybrid optimization techniques such as Particle swarm Optimization Cuckoo search (PSO-CS), PSO-GA and Genetic Ant Colony Optimization (GACO).

Hardware realization of an AUV with its propulsion motor control using the proposed strategy can be accomplished. The four quadrant operation of the motor can be studied in hardware for achieving the realistic improvement in its performance.

*****

References

[1] Kemin Zhou and John. C. Doyle, *Essentials of robust control*, Pearson publisher, 1999.

[2] A.A. Stoorvogel, *The H∞ control problem: a state space approach*, 2000.

[3] John E. Bibel and D. Stephen Malyevac, "Guidelines for the selection of weighting functions for H-infinity control", 1992.

[4] Alexander Lanzon, Xavier Bombois and Brian DO Anderson, "On weight adjustments in *H∞* control design", In Proceedings of the 2003 European Control Conference, Cambridge, UK, 2003.

[5] Rania Hassan, Babak Cohanim and Olivier de Weck, "A comparison of particle swarm optimization and the genetic algorithm", 46th AIAA/ASME/ASCE/AHS/ASC Structures, Structural Dynamics and Materials Conference, 2005.

[6] H. I. A.li, S. B. Mohd Noor, M. H. Marhaban and S. M. Bashi, "Design of H-inf Controller with Tuning of Weights Using Particle Swarm Optimization Method", *IAENG International Journal of Computer Science*, Vol. 38, No. 2, 2002.

[7] Costa M. H. and Silva, V. V. R, "Selecting the control configuration for a nonlinear system by on-line controllers' parameters optimization", Proceedings of the 18th World Congress The International Federation of Automatic Control Milano (Italy) 2011.

[8] Jose F. M. Amaral, Ricardo Tanscheit and Marco A. C. Pacheco, "Tuning PID Controllers through Genetic Algorithms", *Article*, 2001.

[9] Andri Mirzal, Shinichiro Yoshii and Masashi Furukawa, "PID Parameters Optimization by Using Genetic Algorithm", *ISTE Journal Of Science And Technology Policy*, 2006.

[10] Arturo Y. Jaen-Cuellar, Rene de J. Romero-Troncoso, Luis Morales-Velazquez and Roque A. Osornio-Rios, "PID-Controller Tuning Optimization with Genetic Algorithms in Servo Systems", *International Journal of Advanced Robotic Systems,* 2013.

[11] A. Jayachitra and R. Vinodha, "Genetic Algorithm Based PID Controller Tuning Approach for Continuous Stirred Tank Reactor", *Research Article, Hindawi Publishing Corporation Advances in Artificial Intelligence,* 2004.

[12] Zwe-Lee Gaing, "A Particle Swarm Optimization Approach for Optimum Design of PID Controller in AVR System", *IEEE Transactions on Energy Conversion*, Vol. 19, No. 2, 2004.

[13] William P Symington, Alan Belle, Hung D Nguyen and Jonathan R Binns, "Emerging technologies in marine electric propulsion", *Journal of Engineering for the Maritime Environment,* Vol. 230, No. 1, pp. 187–198, 2016.

[14] A. Tashakori, M. Ektesabi, and N. Hosseinzadeh, "Modeling of BLDC Motor with Ideal Back- EMF for Automotive Applications", Proceedings of the World Congress on Engineering, Vol II, 2011.

[15] R.Manikandan, R.Arulmozhiyal and M.Sangeetha, "Sensorless Speed Control of FSTPI Fed Brushless DC Motor Drive Using Terminal Voltage Sensing Method", *International Journal of Soft Computing and Engineering (IJSCE)*, Vol.4, Iss. 1, 2014.

[16] R. Krishnan, *Electric Motor Drives: Modeling, Analysis and Control*, Prentice Hall, 2001.

[17] Bilal Akin and Manish Bhardwaj, "Sensorless Trapezoidal Control of BLDC Motors", Application Report, Texas Instruments, 2015.

[18] Robert Playter, " Control system design using H∞ optimization", Thesis, MIT, 1988.

[19] Leo Rollins, "Robust Control Theory", Carnegie Mellon University, 1999.

[20] Karl Johan Astrom, *Control System Design*, 2002.

[21] A. Megretski, *Multivariable Control Systems*, 2004.

[22] Gary Balas, Richard Chiang, Andy Packard and Michael Safonov, Robust Control Toolbox™ 3, Reference, The *MathWorks*, Inc. 2010.

[23] J.C. Doyle, K. Glover, P.P. Khargonekar and B.A. Francis, "State-space solutions to standard H_2 and H infinity control problems", *IEEE Transactions on Automatic Control*, Vol. 34, Iss. 8, pp. 831 – 847, 1989.

[24] Keith Glover and J.C. Doyle, "State-space formulae for all stabilizing controllers that satisfy an *H*∞-norm bound and relations to risk sensitivity", Systems & Control Letters 11, pp. 167-172, 1988.

[25] Matthew Settles, "An Introduction to Particle Swarm Optimization", 2005.

[26] Kennedy, J. and Eberhart R, "Particle swarm optimization", Proceedings IEEE International Conference on Neural Network, pp. 1942-1948, 1995.

[27] Yuhui Shi, "Particle swarm optimization: developments, applications and resources", Proceedings of the Congress on evolutionary computation, Vol. 1, pp. 81-86, 2001.

[28] Pragasen Pillay, Ramu Krishnan, "Modeling, Simulation, and Analysis of Permanent-Magnet Motor Drives, Part II: The Brushless DC Motor Drive" *IEEE Transactions on Industry Applications*, Vol. 25, No. 2, pp 274-279, 1989.

[29] Burger F, Besse P.A, Popovic R.S, " New Single Chip Hall Sensor for Three Phases Brushless Motor Control", *Sensors and Actuators, A-Physical*, Vol.81, pp. 320-323, 2000.

[30] Devendra. P, Madhavi TVVS, K Alice Mary, Ch. Saibabu, "Microcontroller Based Control Of Three Phase BLDC Motor", Journal of Engineering Research and Studies, Research Article, Vol. 2, Issue 4, pp. 68-71, 2011.

[31] Singh C.P, Kulkarni S.S, Rana S.C, Kapil Deo, "State-Space Based Simulink Modeling of BLDC Motor and its Speed Control using Fuzzy PID Controller", International Journal of Advances in Engineering Science and Technology, Vol. 2 No. 3, pp. 359-369, 2013.

[32] Pindoriya. R. M, Rajendran. S, Chauhan. P. J, "Speed Control of BLDC Motor using Sinusoidal PWM Technique", International Journal of Advance Engineering and Research Development, pp 1-6, 2014.

[33] Mohd Tariq, Nidhi Varshney, "Digital simulation and analysis of six modes of operation of BLDC motor drives using hysteresis band PWM switching scheme", International Journal of Energy and Power Engineering, Vol. 3, No. 2, pp. 57-64, 2014.

[34] Lei Hao and Hamid A. Toliyat, "BLDC Motor Full-Speed Operation Using Hybrid Sliding Mode Observer", Eighteenth Annual IEEE Applied Power Electronics Conference and Exposition, pp. 286-293, 2003.

[35] Dasheng Lee, "Wireless and Powerless Sensing Node System Developed for Monitoring Motors", Sensors, Vol. 8, pp. 5005-5022, 2008.

[36] Vinatha U, Pola S, Vittal K.P, "Recent Developments in Control Schemes of BLDC Motors", IEEE International Conference on Industrial Technology, pp. 477-482, 2006.

[37] Kim T, Lee H.W, Ehsani M, "Position Sensorless Brushless DC Motor/Generator Drives: Review and Future Trends", IET Electrical Power Applications, Vol. 1, pp. 557-564, 2007.

[38] Jose Carlos Gamazo-Real, Ernesto Vazquez-Sanchez and Jaime Gomez-Gil, "Position and Speed Control of Brushless DC Motors Using Sensorless Techniques and Application Trends", Review, Sensors, Vol. 10, pp. 6901-6947, 2010.

[39] Geethu Zacharia, Annai Raina, "A Survey on Back EMF Sensing Methods for Sensorless Brushless DC Motor Drives", International Journal of Emerging Trends in Engineering Research, Vol. 2, No. 2, pp. 15-19, February 2014.

[40] Ivan Lovas, "BLDC Sensorless Algorithm Tuning", Application Note; AN4597, Freescale Semiconductor, pp. 1-9, 2012.

[41] Tae-Hyung Kim, and Mehrdad Ehsani, "Sensorless Control of the BLDC Motors from Near-Zero to High Speeds", IEEE Transactions On Power Electronics, Vol. 19, No. 6, pp. 1635 – 1645, 2004.

[42] Cheng-Hu Chen and Ming-Yang Cheng, "A New Cost Effective Sensorless Commutation Method for Brushless DC Motors Without Phase Shift Circuit and Neutral Voltage", IEEE Transactions on Power Electronics, Vol. 22, No. 2, pp. 644-653, 2007.

[43] Wang H.B, Liu H.P, "A novel sensorless control method for brushless DC motor", IET Electric Power Applications, Vol. 3, Iss. 3, pp. 240-246, 2009.

[44] Salih Baris Ozturk, and Hamid A. Toliyat, "Direct Torque and Indirect Flux Control of Brushless DC Motor", IEEE/ASME Transactions On Mechatronics, Vol. 16, No. 2, pp.351-359, 2011.

[45] Jianwen Shao and Dennis Nolan, "Further Improvement of Direct Back EMF Detection for Sensorless Brushless DC (BLDC) Motor Drives", Twentieth Annual IEEE Applied Power Electronics Conference and Exposition, Vol. 2. pp. 933-937, 2005.

[46] Jianwen Shao, Dennis Nolan, and Thomas Hopkins, "Improved Direct Back EMF Detection for Sensorless Brushless DC (BLDC) Motor Drives", Eighteenth Annual IEEE Applied Power Electronics Conference and Exposition, Vol. 1, pp. 300-305, 2003.

[47] Zicheng Li , Shanmei Cheng, Yi Qin, Kai Cai, "A Novel Line-to-line Back EMF Calculation for Sensorless Brushless DC Motor Drives", International Conference on Electrical Machines and Systems, pp. 1406-1411, 2008.

[48] Ming Lu, Yaohua Li, " New Design for Sensorless BLDC Motor Using Half-Bridge Driver Circuit", International conference on E product, E service, E entertainment, pp. 1-4, 2010.

[49] Yuanyuan Wu, Zhiquan Deng, Xiaolin Wang, Xing Ling, and Xin Cao, "Position Sensorless Control Based on Coordinate Transformation for Brushless DC Motor Drives", IEEE Transactions On Power Electronics, Vol. 25, No. 9, pp. 2365-2371, 2010.

[50] Tzuen-Lih Chern, Ping-Lung Pan, Yu-Lun Chern and Der-Min Tsay, "Sensorless Speed Control of BLDC Motor Using Six Step Square Wave and Rotor Position Detection", IEEE conference on Industrial Electronics and Applications, pp.1358-1362, 2010.

[51] Carlo Concari, Fabrizio Troni, "Sensorless Control of BLDC Motors at Low Speed Based on Differential BEMF Measurement", IEEE Energy Conversion Congress and Exposition, pp.1772-1777, 2010.

[52] Damodharan. P and Krishna Vasudevan, "Sensorless Brushless DC Motor Drive Based on the Zero-Crossing Detection of Back Electromotive Force (EMF) from the Line Voltage Difference", IEEE Transactions On Energy Conversion, Vol. 25, No. 3, pp. 661 – 668, 2010.

[53] Taeyeon Kim, Chungil Kim, Joon Lyou, "A New Sensorless Drive Scheme for a BLDC Motor Based on the Terminal Voltage Difference", Annual Conference on IEEE Industrial Electronics Society, pp. 1710 – 1715, 2011.

[54] Joshuwa. S, Sathishkumar. E, Ramsankar. S, "Advanced Rotor Position Detection Technique For Sensorless BLDC Motor Control", International Journal of Soft Computing and Engineering, Vol. 2, Iss. 1, pp. 311-315, 2012.

[55] Abdelali Boughaba, Mabrouk Chaabane, Said Benaggoune, "Robust Sensorless Control of BLDC Motor using Second Derivative Function of the Sum of Terminal Voltages", Serbian Journal Of Electrical Engineering, Vol. 10, No. 2, pp. 275-291, 2013.

[56] Ogasawara S, Akagi H, "An Approach to Position Sensorless Drive for Brushless DC Motors", IEEE Transactions on Industrial Applications, Vol. 27, pp. 928-933, 1991.

[57] Shen J. X, and Iwasaki. S, " Sensorless Control of Ultrahigh-Speed PM Brushless Motor Using PLL and Third Harmonic Back EMF", IEEE Transactions On Industrial Electronics, Vol. 53, No. 2, pp. 421-428, 2006.

[58] Markos Tawadros, Jamal Rizk, Mahmood Nagrial, "Estimation of commutation instances using back emf mapping for sensorless control of brushless permanent magnet motors", IET Electric Power Applications, Vol. 7, Iss. 4, pp. 270–277, 2013.

[59] Ashish P.R, Vincent G, " Sensorless Control Of Bldc Motor Using Third Harmonic Back Emf", International Journal of Industrial Electronics and Electrical Engineering, Vol. 2, Iss. 1, pp. 35-38, 2014.

[60] Lu Wenqi, Hu Yuwen, Huang Wenxin, Chu Jianbo, Yang Jianfei, "A Hybrid Approach of Sensorless Rotor Position Self-sensing for Brushless Dc Motor", Journal of Mechanical Engineering, pp.1334-1337, 2008.

[61] Oyedepo J. A and Folaponmile. A, "Application Of Adaptive Sliding Mode Position Controller With PI Tuning To Permanent Magnet Brushless DC Motor Drive System", Jorind (9) 1, Pp.71-78, 2011.

[62] Deenadayalan. A, Saravana Ilango. G , "Modified Sliding Mode Observer for Position and Speed Estimations in Brushless DC Motor", Annual IEEE India Conference (INDICON), pp. 1-4, 2011.

[63] Dhaouadi R, Mohan N, Norum L, "Design and Implementation of an Extended Kalman Filter for the State Estimation of a Permanent Magnet Synchronous Motor", IEEE Transactions on Power Electronics, Vol. 6, pp. 491-497, 1991.

[64] Bozo Terzic, and Martin Jadric, "Design and Implementation of the Extended Kalman Filter for the Speed and Rotor Position Estimation of Brushless DC Motor", IEEE Transactions On Industrial Electronics, Vol. 48, No. 6, pp. 1065-1073, 2001.

[65] Joyce Jacob, Surya Susan Alex, Asha Elizabeth Daniel, "Speed Control of Brushless DC Motor Implementing Extended Kalman Filter", International Journal of Engineering and Innovative Technology, Vol. 3, Iss. 1, pp. 305-309, 2013.

[66] Dadkhah. R, Givi. H, Mehdipour. A, "Parameter Estimation of the Induction Motor Using Extended Kalman Filter for Wide Range Speed Control", International Power Electronics Drive Systems and Technologies Conference, pp. 137-142, 2015.

[67] Mohamed Rasheed, Peter F. A. MacConnell, A. Fraser Stronach, and Paul Acarnley, "Sensorless Indirect-Rotor-Field-Orientation Speed Control of a Permanent-Magnet Synchronous Motor With Stator-Resistance Estimation", IEEE Transactions On Industrial Electronics, Vol. 54, No. 3, pp. 1664-1675, 2007.

[68] Kojabadi, H.M, "Active Power and MRAS Based Rotor Resistance Identification of an IM Drive" Simulation Modelling Practice and Theory, Vol. 17, pp. 376–389, 2009.

[69] G.Sunil, B.Rajasekhar, "Simulation of MRAC based speed control of brushless DC motor with low-resolution hall-effect sensors", International Journal of Innovative Research In Electrical, Electronics, Instrumentation And Control Engineering, Vol. 2, Iss. 12, pp. 2293-2297, 2014.

[70] Tae-Sung Kim, Byoung-Gun Park, Dong-Myung Lee, Ji-Su Ryu, and Dong-Seok Hyun, "A New Approach to Sensorless Control Method for Brushless DC Motors", International Journal of Control, Automation, and Systems, vol. 6, no. 4, pp. 477-487, 2008.

[71] Pan Lei, Wang Bei-Bei and Sun He-Xu, "A Novel Control Method for BLDCM Based on Phase Back-EMF Observation", Research Journal of Applied Sciences, Engineering and Technology, Vol. 6, Iss. 13, pp. 2474-2482, 2013.

[72] Cassio Luciano Baratieri, and Humberto Pinheiro, "Sensorless Vector Control for PM Brushless Motors with Nonsinusoidal Back-EMF", IEEE International Conference on Electrical Machines, pp. 915-921, 2014.

[73] Samuel Wang, Chin-Hsuan Lu, and An-Chen Lee, "Disturbance Observer Structure Applied to Sensorless Brushless DC Motors Drive", International Journal of Computer Theory and Engineering, Vol. 7, No. 2, pp. 92-96, 2015.

[74] Wook-Jin Lee, and Seung-Ki Sul, "A New Starting Method of BLDC Motors Without Position Sensor", IEEE Transactions On Industry Applications, Vol. 42, No. 6, pp.1532-1538, 2006.

[75] Neethi S.Pillai, Salitha.K & Chikku Abraham, "Analysis And Simulation Studies For The Estimation Of Rotor Position In Sensorless BLDC", International Journal of Electrical and Electronics Engineering, Vol. 2, Iss. 1, pp. 86-90, 2012.

[76] Wang Dafang, Qi Ji, Zhu Cheng, Liao Jiangmin,1 and Yuan Yechen, "Strategy of Starting Sensorless BLDCM with Inductance Method and EMF Integration", Research article, Hindawi Publishing Corporation Mathematical Problems in Engineering, Vol. 2, pp. 1-8, 2013.

[77] Wudhichai Assawinchaichote and Nattapat Chayaopas, "Linear Matrix Inequality Approach to Robust H∞ Fuzzy Speed Control Design for Brushless DC Motor System", *Applied Mathematics & Information Sciences*, Vol. 10, No. 3, pp. 987-995, 2016.

[78] H M Soliman, E H E Bayoumi, M Soliman, "Linear-matrix-inequality-based sliding mode control for brushless d.c. motor drives", Proceedings of the Institution of Mechanical Engineers, *Part I: Journal of Systems and Control Engineering*, Vol. 223, Iss. 8, pp.1035-1043, 2009.

[79] Kamil Orman, Kaan Can, Abdullah Başcı, Adnan Derdiyok, "Real-Time Speed Control of BLDC Motor Based On Fractional Sliding Mode Controller", *International Journal of Applied Mathematics, Electronics and Computers,* Vol. 4 (Special Issue), pp.314–318, 2016.

[80] I.N. Lee, K.H. Kim, J.H. Lee, D.H. Lee and K.H. You, "Robust Linear Quadratic Sliding-Mode Control for BLDC Motor Positioning System", *Applied Mechanics and Materials,* Vols. 278-280, pp. 1615-1619, 2013.

[81] J.S. Ko, J.H. Lee, S.K. Chung and M.J. Youn, "A robust digital position control of brushless DC motor with dead beat load torque observer", *IEEE Transactions on Industrial Electronics,* Vol. 40, Iss. 5, pp. 512 – 520, 1993.

[82] Chung-Wen Hung and Jia-Yush Yen, "A Robust Variable Sampling Time BLDC Motor Control Design Based upon μ-Synthesis", The Scientific World Journal, pp. 1-7, 2013.

[83] N. Hemati, J. S. Thorp and Ming-Chuan Leu, "Robust Nonlinear Control of Brushless DC Motors for Direct-Drive Robotic Applications", *Mechanical and Aerospace Engineering*, Missouri University of Science and Technology, 1990.

[84] P. Bharat Kumar, P. Sujatha and K. S. R. Anjaneyulu, "Design and Analysis of Different Control Strategies for BLDC Motor", *International Journal of Innovative Research in Science, Engineering and Technology*, Vol. 2, Iss. 9, pp. 4298-4308, 2013.

[85] Vishnu C.S and Riya Mary Francis, "Speed Control of BLDC Motor by Using Tuned Linear Quadratic Regulator", *International Journal of Scientific Engineering and Research (IJSER)*, Vol. 3 Iss. 8, 2015.

[86] Kiyoshi Ohishi, Kouhei Ohnishi, Katunori Taniguchi and Masaaki Hotta, "Robust Control Of Brushless Dc Servo Motor Using Dual Passive Adaptive Control Loop", Robotics and IECON '87 Conferences, Vol. 854, pp. 265-271, 1987.

[87] Thirusakthimurugan. P, "Studies on the Controller Design and Identification for the PMBLDC Motor", Thesis, 2008.

[88] MozaffariNiapour S.A.KH, Tabarraie. M, Feyzi M. R, " A new robust speed sensorless control strategy for high-performance brushless DC motor drives with reduced torque ripple", *Control Engineering Practice, Elsevier*, Vol. 24, pp. 42-54, 2014.

[89] Basam Venkat, "Evolutionary Approach Based Design of BLDC Motor Controller with H∞ Objectives", *Conference on Computer Aided Methods for Modelling, Simulation and Optimization*, 2010.

[90] Masamoto Takano, Kenichi Kurotani, Kenzo Taked, "Application of H infinity Control to Motor Speed Control System", *International Conference on Industrial Electronics, Control and Instrumentation*, Vol. 1, pp. 839-842, 1991.

[91] Lucas Brezina and Tomas Brezina, "H-Infinity Controller Design For A DC Motor Model With Uncertain Parameters", *Engineering MECHANICS*, Vol. 18, No. 5/6, pp. 271–279, 2011.

[92] Chuanwei Zhang, Zhifeng Bai, Binggang Cao, And Jiarang Lin, " Simulation And Experiment Of Driving Control System For Electric Vehicle", *International Journal of Information And Systems Sciences*, Vol. 1, No. 3-4, pp. 283-292, 2005.

[93] Ashu Ahuja & Bhawna Tandon, "Robust Pid And Polynomial Controllers Tuning For DC Motor Speed Control Using PSO And GA: A Comparative Study*", International Journal of Electrical And Electronics Engineering Research*, Vol. 3, Iss. 1, 2013.

[94] Liu Bingyou, "Research on H infinity Robust Tracking Controller for Permanent Magnet Synchronous Motor Servo System", International Conference on Information Engineering and Computer Science, pp. 1-5, 2009.

[95] Lu Hongliang, **"**Robust H∞ control for **t**he vertical lifting system driven by Permanent Magnet Linear Synchronous Motor (PMLSM)**"**, *International Conference on E-Product E-Service and E-Entertainment*, pp.1-4**,** 2010.

[96] Shamsul Aizam Zulkifli, Md Zarafi Ahmad, "H infinity Speed Control for Permanent Magnet Synchronous Motor", International Conference on Electronic Devices, Systems & Applications, pp. 290-293, 2011.

[97] Huaiquan ZANG, Zhe QIN, Yan DAI, "Robust H-infinity Space Vector Model of Permanent Magnet Synchronous Motor Based on Genetic Algorithm", *Journal of Computational Information Systems*, pp. 5897- 5905, 2014.

[98] Rajendran. A, Padma. S, "H-infinity robust control technique for controlling the speed of switched reluctance motor", Research Article, *Frontiers of Electrical and Electronics Engineering, Springer*, Vol. 7, No. 3, pp. 337–346, 2012.

[99] Rajendran. A, Padma. S, "Optimization Algorithm Based H∞ Control Method For Controlling Switched Reluctance Motor (SRM)", *Journal of Theoretical and Applied Information Technology*, Vol. 62, No. 3, pp. 618-626, 2014.

[100] Safanah M. Raafat, Rini Akmeliawati, Ismael Abdulljabaar, "Robust H∞ Controller for High Precision Positioning System, Design, Analysis, and Implementation", *Intelligent Control and Automation, Scientific Research,* Vol. 3, pp. 262-273**,** 2012.

[101] Guangzhong Cao, Suxiang Fan, Gang Xu, "The Characteristics Analysis of Magnetic Bearing Based on H-infinity Controller", 5^{th} World Congress on Intelligent Control and Automation, pp. 752-756, 2004.

[102] Jiankun Hu, Christian Bohn, H.R. Wu, " Systematic H Infinity weighting function selection and its application to the real-time control of a vertical take off aircraft", *Control Engineering Practice*, Vol. 8, pp. 241-252, 2000.

[103] Guang-Ren Duan, Zhan-Yuan Wu, Chris Bingham, and David Howe, " Robust Magnetic Bearing Control Using Stabilizing Dynamical Compensators", *IEEE Transactions On Industry Applications,* Vol. 36, No. 6, November/December 2000.

[104] Sarath S Nair, M V vaidyan, M joy, "Generalized Design and Disturbance Analysis of Robust H infinity Control of Active Magnetic Bearings", *IEEE/ASME International Conference on Advanced Intelligent Mechatronics*, pp. 1124-1129, 2009.

[105] Sarath S Nair, "Automatic Weight Selection Algorithm for Designing H Infinity controller for Active Magnetic Bearing", *International Journal of Engineering Science and Technology*, Vol. 3 No. 1, pp. 122-138, 2011.

[106] Chapter 8 Design issues, http://users.abo.fi/htoivone/courses/robust/rob8.pdf

[107] Randeep Kaur and Jyoti Ohri, "PSO Based Weight Selection and Fixed Structure Robust Loop Shaping Control for Pneumatic Servo System with 2DOF Controller", World Academy of Science, Engineering and Technology, *International Journal of Electrical and Computer Engineering*, Vol. 8, No. 8, 2014.

[108] Peter Lundstrom, Sigurd Skogestad and Zi Qin Wang, "Weight selction of H infinity and mu control methods- Insights and examples from process control", Symposium on Robust control system design using H infinity and related methods, 1991.

[109] Anna-Karin Christiansson and Bengt Lennartson, "Weight Selection for $H\infty$ Control Using Genetic Algorlthms", 14th Triennial World Congress, 1999.

[110] A. Visioli, "Tuning of PID controllers with Fuzzy logic", *Proc. Inst. Elect. Eng. Contr. Theory Applicat.*, Vol. 148, No. 1, pp. 1-8, 2001.

[111] T. L. Seng, M. B. Khalid, and R. Yusof, "Tuning of a neuro-fuzzy controller by genetic algorithm", *IEEE Syst., Man, Cybern. B*, Vol. 29, pp. 226-236, 1999.

[112] R. A. Krohling and J. P. Rey, "Design of optimal disturbance rejection PID controllers using gentic algorithm", *IEEE Trans. Evol. Comput.*, Vol. 5, pp. 78-82, 2001.

[113] Tae-Hyoung Kim, Ichiro Maruta and Toshiharu Sugie, "Particle Swarm Optimization based Robust PID Controller Tuning Scheme," Proceedings of the 46th IEEE Conference on Decision and Control, 2007.

[114] K. J. Astrom and T. Hagglund, "The future of PID control", *Control Engineering Practice*, Vol. 9, No. 11, pp. 1163-1175, 2001.

[115] S. Hara, T. Iwasaki, and D. Shiokata, "Robust PID control using generalized KYP synthesis," *IEEE Control Systems Magazine*, Vol. 26, Iss. 1, pp. 80-91, 2006.

[116] N. J. Killingsworth and M. Krstic, " PID tuning using extremum seeking: online, model- free performance optimization," *IEEE Control Systems Magazine*, Vol. 26, Iss. 1, pp. 70-79, 2006.

[117] K. Sedlaczek and P.Eberhard, "Using augmented Lagrangian particle swarm optimization for constrained problems in engineering," *Structural and Multidisciplinary Optimization*, Vo. 32, Iss. 4, pp. 277-286, 2006.

[118] M F Aranza, J Kustija, B Trisno and D L Hakim, "Tunning PID controller using particle swarm optimization algorithm on automatic voltage regulator system", International Conference on Innovation in Engineering and Vocational Education, 2016.

[119] S. J. Bassi, M. K. Mishra, and E. E. Omizegba, "Automatic Tuning Of Proportional–Integral–Derivative (PID) Controller Using Particle Swarm Optimization (PSO) Algorithm", *International Journal of Artificial Intelligence & Applications (IJAIA)*, Vol.2, No.4, 2011.

[120] Ibrahem S. Fatah, "PSO-Based Tunning Of PID Controller for Speed Control of DC Motor," *Diyala Journal of Engineering Sciences*, Vol. 07, No. 03, pp. 65- 79, 2014.

[121] M. V. Ramesh, Gorantla. S. Rao, J. Amarnath, S. Kamakshaiah, B. Jawaharlal, "Speed Torque Characteristics of Brushless DC motor in Either Direction on Load using ARM controller", IEEE PES Innovative Smart Grid Technologies – India 2011.

[122] Implementation of a Sensorless Speed Controlled Brushless DC drive using TMS320F240 Literature Number: BPRA072, Texas Instruments Europe, November 1997.

[123] Pierre Voultoury, "Sensorless Speed Controlled Brushless DC Drive using the TMS320C242 DSP Controller", Application Report, Texas Instruments, 1998.

[124] Suneeta, R Srinivasan, Ram Sagar, "FPGA Based Control Method for Three Phase BLDC Motor", *International Journal of Electrical and Computer Engineering*, Vol. 6, Iss. 4, pp. 1434-1440, 2016.

[125] Sathish kumar Shanmugam and Meenakumari Ramachandran "Design and Implementation of Embedded Processor Based Brushless Motor Drive using Lead Acid Battery as Source with Lithium Ion Capacitor", *TELKOMNIKA Indonesian Journal of Electrical Engineering*, Vol. 14, Iss. 3, pp. 455-469, 2015.

[126] G. Madhusudhana Rao, and B.V. Sanker Ram, "Speed Control of BLDC Motor with Common Current," International Journal of Recent Trends in Engineering, Vol 2, No. 6, 2009.

[127] G. Ranjithkumar and K.N.V. Prasad, " Minimization of Torque Ripple Content for BLDC Motor by Current Controller using MLI", *Procedia Engineering, Elsevier*, Vol. 38, pp. 3113-3121, 2012.

[128] Dixon JW and Leal IA, "Current Control Strategy for Brushless DC Motors Based on Common DC Signal", *IEEE Transactions on Power Electronics*, Vol. 17, No. 2, pp. 232–240, 2002.

[129] Tony Mathew, and Caroline Ann Sam, "Modeling and Closed Loop Control of BLDC Motor Using A Single Current Sensor", *International Journal of Advanced Research in Electrical, Electronics and Instrumentation Engineering*, Vol. 2, Iss. 6, 2013.

[130] Francesco Parasiliti, Roberto Petrella, and Marco Tursini, "A Novel Solution for Phase Current Sensing in PWM-VSI Based AC Drives", Proc. of the European Conference on Power Electronics and Applications (EPE), 2001.

[131] Chang-hee Won, Joong-Ho Song, and Ick Choy, "Commutation Torque Ripple Reduction in Brushless DC Motor Drives Using a Single DC Current Sensor", *IEEE Transactions on Power Electronics*, Vol. 19, Iss. 2, 2004.

[132] Implementation of current regulator for BLDC motor control with ST7FMC, Application note, STMicroelectronics, 2006.

[133] Jason Bridgmon and Carolus Andrews, Current Sensing for Inline Motor-Control Applications, Application Report, 2016.

[134] Scott Hill, Low-Drift, Precision, In-Line Motor Current Measurements With Enhanced PWM Rejection, TI Tech Notes, 2016.

[135] S. P. Gawande and M. R. Ramteke, "Current Controlled PWM for Multilevel Voltage-Source Inverters with Variable and Constant Switching Frequency Regulation Techniques: A Review", Journal of Power Electronics, Vol. 14, No. 2, pp. 302-314, 2014.

[136] Reza Davoodnezhad, Hysteresis Current Regulation of Voltage Source Inverters with Constant Switching Frequency, Thesis, 2008.

[137] Z. Song, C. Xia and T. Liu, " Predictive current control of three phase grid connected converters with constant frequency for wind energy systems," *IEEE Trans. Ind. Appl.,* Vol. 60, No. 6, pp. 2451-1464, 2012.

[138] R.Wu, S.B.Dewan, and G.R.Slemon, "Analysis of a PWM ac to dc voltage source converter under the predicted current control with a fixed switching frequency," *IEEE Trans. Ind. Appl.*,Vol. 27, No. 4,pp.756-764, 1991.

[139] L.Zhang and F.Hardan, "Vector controlled VSI-fed AC drive using a predictive space-vector current regulation scheme," in *Proc. IECON*., pp.61-66, 1994.

[140] R.Vargas, P.Cortes, U.Ammann, J.Rodriguez, and J.Pontt, "Predictive control of a three-phase neutral-point-clamped inverter,"*IEEE Trans. Ind. Electron.*, Vol. 54, No.5, pp.2697-2705, 2007.

[141] M.A.Dzienialowski, and M.P.Kazmierkowski, "Self-tuned fuzzy PI current controller for PWM-VSI,"in *Proc. EPE*, pp.1308-1313, 1995.

[142] M.A.Dzieniakowski and P.Z.Grabowski, "Fuzzy logic controller with state recognition for three phase PWM-VSI," in *Proc.ISIE*, pp.438-443, 1996.

[143] S. Mikkili and A. K. Panda, "Types-1 and -2 fuzzy logic controllers-based shunt active-filter Id-Iqcontrol strategy with different fuzzy membership functions for power quality improvement using RTDS hardware," *IET Power Electron.*, Vol. 6, No. 4, pp. 818-833, Apr. 2013.

[144] A.M.S. Yunus, A.-A.-S., and M.A.S.Masoum, "Improving dynamic performance of wind energy conversion systems using fuzzy-based hysteresis current-controlled superconducting magnetic energy storage," *IET Power Electron.*, Vol. 5, No. 8, pp. 1305-1314, Sep. 2012.

[145] M. Moghadasian and M. Amiri, "Sensorless speed control of IM using adaptive neural-fuzzy inference system," in *Proc. AIM*, pp. 1028-1033, 2011.

[146] F.Harashima, Y.Demizu, S.Kondo, and H.Hashimoto, "Application of neural networks to power converter control," in *Proc. IAS*, pp. 1087-1091, 1989.

[147] M. R. Buhl and R.D.Lorenz, "Design and implementation of neural networks for digital current regulation of inverter drive,"in*Proc. IAS*, pp.415-421,1991.

[148] B.Burton, R.G.Harley, G.Diana, and J.R.Rodgerson, "Implementation of a neural network to adaptively identify and control VSI fed induction motor stator currents," in *Proc. IAS*, pp.1733-1740, 1994.

[149] B.Burton, F.Kamran, R.G.Harley, T.G.Habetler, M.A.Brooke, and R.Poddar, "Identification and control of induction motor stator currents using fast on-line random training of a neural network," *IEEE Trans. Ind. Appl.*,Vol. 33, No. 3,pp.697-704, May/Jun. 1997.

[150] B. Singh and V.Rajagopal, "Neural-network-based integrated electronic load controller for isolated asynchronous generators in small hydro generation," *IEEE Trans. Ind. Electron*., Vol. 58, No. 9, pp. 4264-4274, Sep. 2011.

[151] H. Shayeghi, A. Akbarimajd, A. Mohammadian,G. Shokri, "Speed and Current Controllers Design of BLDC Motor Using SNR Optimization Technique", International Research Journal of Applied and Basic Sciences, Vol. 4, No. 1, pp. 99-106, 2013.

[152] Swathi Kumari. A, Y. Laxminarayana, and Dr. S.Tarakalyani, "Modeling and Simulation of Bldc Motor for Aiding and Opposing Loads", *IOSR Journal of Electrical and Electronics Engineering (IOSR-JEEE),* Vol. 7, Iss. 4, pp. 59-67, 2013.

[153] Adel A. El-samahy, and Mohamed A. Shamseldin, "Brushless DC motor tracking control using self-tuning fuzzy PID control and model reference adaptive control", *Ain Shams Engineering Journal* 2016.

[154] Jagat Jyoti Rath, "Effective Speed Control in 3-Phase BLDC Motor by Reaching Law based Sliding Mode Technique", *International Journal of Computer Applications,* Vol. 43, No.16, pp. 0975 – 8887, 2012.

[155] M.V.Ramesh, Gorantla.S.Rao, J.Amarnath, S.Kamakshaiah, and B.Jawaharlal, "Speed Torque Characteristics of Brushless DC motor in Either Direction on Load using ARM controller", IEEE PES Innovative Smart Grid Technologies – India, 2011.

[156] Akash Varshney, Deeksha Gupta, and Bharti Dwivedi, "Speed response of brushless DC motor using fuzzy PID controller under varying load condition", *Journal of Electrical Systems and Information Technology,* 2017.

[157] Espen Skjong, Egil Rødskar, Marta Molinas, Tor Arne Johansen and Joseph Cunningham, "The Marine Vessel's Electrical Power System: From its Birth to Present Day", IEEE Proceedings, Vol. 103, Iss. 12, 2015.

[158] C G Hodge, and D J Mattick, "The Electric Warship Then, Now And Later", INEC 2008.

[159] Alf Kåre Ådnanes, Maritime Electrical Installations And Diesel Electric Propulsion, ABB, 2003.

[160] Hari Prastowo, Francisco Pinto and Semin, "Advanced Ship Propulsion Technology: A Review", *Asian Journal of Applied Sciences*, Vol. 04, Iss. 03, 2016.

[161] William P Symington, Alan Belle, Hung D Nguyen and Jonathan R Binns, "Emerging technologies in marine electric propulsion", *Journal of Engineering for the Maritime Environment,* Vol. 230, Iss. 1, pp. 187–198, 2016.

[162] Nova Scotia Boatbuilders Association, Review of All-Electric and Hybrid-Electric Propulsion Technology for Small Vessels, 2015.

[163] Ballard, Michael A, Impacts of electric propulsion systems on submarine design, Thesis, 1989.

[164] Mehdi Shirania, Abbass Aghajania, Saeed Shabania and Jalil Jamalib, "A review on recent applications of brushless DC electric machines and their potential in energy saving", *Energy Equipment and Systems*, Vol. 3, No. 1, pp. 57-71, 2015.

[165] John Buckingham, "Submarine Power and Propulsion - Application of Technology to Deliver Customer Benefit", Submarine power and propulsion technology developments, 2008.

[166] Arash H. Isfahani, and Farid Ahmadi, "Mechanical Coupled BLDC Motors for Energy Saving in Submarine Application", Przegląd Elektrotechniczny (Electrical Review), pp. 316-320, 2011.

[167] Massimo Barcaro, Nicola Bianchi and Silverio Bolognani "Hybrid electric propulsion system using submersed SPM machine", 18th International Conference on Electrical Machines, 2008.

[168] Youlong Wang, Wen Xuhui, Shan Xue, Tao Fan, and Zeng Lili, "Analysis and design of high power factor interior permanent magnet motor with concentrated windings for undersea vehicle propulsion", IEEE Vehicle Power and Propulsion Conference, 2008.

[169] M. Jafarboland and J. Faiz, "Modelling and designing controller of two different mechanical coupled motors for enhancement of underwater vehicles performance", IET Electric Power Applications, Vol. 4, Iss. 7, 2010.

[170] Branimir Ružojčić, Damir Žarko, and Drago Ban, "Interior Permanent-Magnet Motor for Ship Propulsion, Design and Testing", 13th European Conference on Power Electronics and Applications, 2009.

[171] Wenfang Liu, Qiaodi Zhou, Qinghua Sheng and Qingpeng Kong, "Brushless DC motor control system based on submarine hybrid transmission technology", Oceans - San Diego, 2013.

[172] P. Oliveira, A. Pascoal, V. Silva, and C. Silvestre," Mission Control of the MARIUS AUV: System Design, Implementation, and Sea Trials", *International Journal of Systems Science,* Vol. 29, No. 10, pp. 1065-1080, 1998.

[173] Elgar Desa, R. Madhan and P. Maurya.," Potential of autonomous underwater vehicles as new generation ocean data platforms", Current Science, Vol. 90, No. 9, pp. 1202–1209, 2006.

[174] Yang Qing, and Gao De-xin, "Optimal Disturbance Rejection Control of Under actuated Autonomous Underwater in Vertical Plane", *TELKOMNIKA Indonesian Journal of Electrical Engineering,* Vol. 13, No. 1, pp. 91 – 100, 2015.

[175] Amrul Faruq, Shahrum Shah Bin Abdullah, and M. Fauzi Nor Shah, "Optimization of an Intelligent Controller for an Unmanned Underwater Vehicle", TELKOMNIKA Indonesian Journal of Electrical Engineering, Vol. 9, No. 2, pp. 245-256, 2011.

[176] James A. Schultz, "Autonomous Underwater Vehicle (AUV) Propulsion System Analysis and Optimization", Thesis, 2009.

[177] S.S. Ohol, Subodh Bhosale, Lalit Palve, and Hrushikesh Joshi, "Design and development of the hydro quad rotor" *International Journal of Mechanical and Production Engineering,* Vol. 2, Iss. 2, pp. 2320–2092, 2014.

[178] Tae-Yeong Kim, Byoung-Kuk Lee, and Chung-Yuen Won, "Modeling and Simulation of Multiphase BLDC Motor Drive Systems for Autonomous Underwater Vehicles", IEEE International Electric Machines & Drives Conference, pp.1366–71, 2007.

[179] Sang-Hoon Song, Yong-Ho Yoon, Byoung-Kuk Lee and Chung-Yuen Won, "Autonomous Underwater Vehicles with Modeling and Analysis of 7-Phase BLDC Motor Drives", *Journal of Electrical Engineering & Technology*, Vol. 9, No. 3, pp. 932-941, 2014.

[180] Srujana Eega, Matthew Joordens, " Design of a low cost Thruster for an Autonomous Underwater Vehicle Design of a low cost Thruster for an Autonomous Underwater Vehicle", 2016.

[181] D. Ishak, N.A.A Manap, M.S. Ahmad and M.R. Arshad, "Electrically Actuated Thrusters for Autonomous Underwater Vehicle", 11th International workshop on Advanced Motion Control, , pp. 619–624, 2010.

[182] Chang-liang Xia, Permanent Magnet Brushless DC Motor Drives and Controls, John Wiley & Sons Singapore Pte. Ltd, 2012.

[183] Huibert Kwakernaak, "Robust Control and H_∞ Optimization", *Automatica,* Vol. 29, No. 2, pp. 255-273, 1993.

[184] J Treurnicht, H_∞ Control, 2007.

[185] Lei P. Bei-Bei W, and He-Xu S, "A Novel Control Method for BLDCM Based on Phase Back-EMF Observation", *Research Journal of Applied Sciences, Engineering and Technology,* Vol. 6,Iss. 13, pp. 2474-2482, 2013.

[186] LAUNCHXL-F28377S Overview, User's Guide, Texas Instruments, Literature Number: SPRUI25, 2015.

[187] TMS320F2837xS Delfino™ Microcontrollers, Texas Instruments, SPRS881C –August 2014–Revised May 2016.

[188] BOOSTXL-DRV8301 Hardware User's Guide, Texas Instruments, SLVU974–October 2013.

[189] TMS320F2837xS Delfino Microcontrollers, Technical Reference Manual, Literature Number: SPRUHX5E, August 2014–Revised September 2017.

[190] Qiuli Yu and Dr. Noel N. Schulz, "Design, Modeling, and Simulation of Power Generation and Electric Propulsion System for IPS for All-Electric Ships", Mississippi State University, 2006.

[191] SINAVY Permasyn – small, reliable, and difficult to trace, Marine & shipbuilding, Siemens, 2013.

[192] http://www.subsim.com/radioroom/showthread.php?t=135629

[193] Louis Andrew Gonzalez, "Design, Modeling and Control of an Autonomous Underwater Vehicle", Thesis 2004.

[194] Sung Yeul Park, "Design and Implementation of Four-quadrant Operation in Single-Switch Based Switched Reluctance Motor Drive System", Thesis, 2004.

*****

Pin diagram of Launchpad LAUNCHXL-F28377S

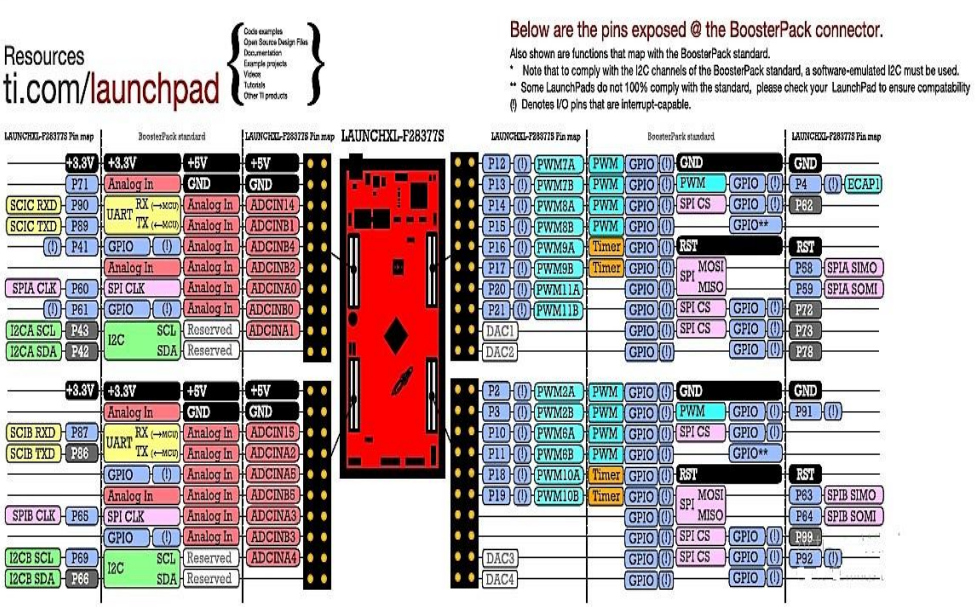

Appendix II

Functional block diagram of TMS320F28377S

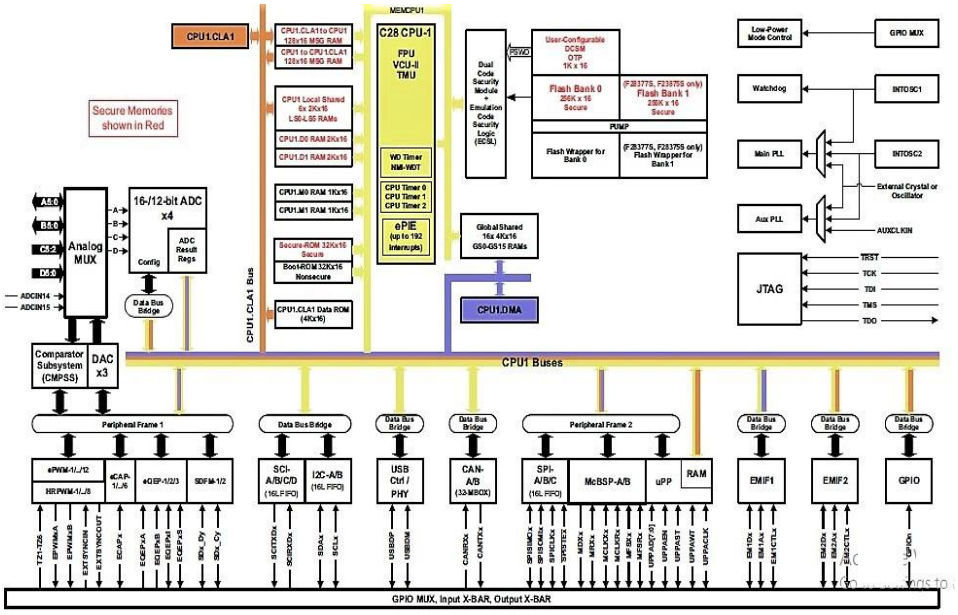

Appendix III

Pin diagram of BOOSTXL DRV 8301

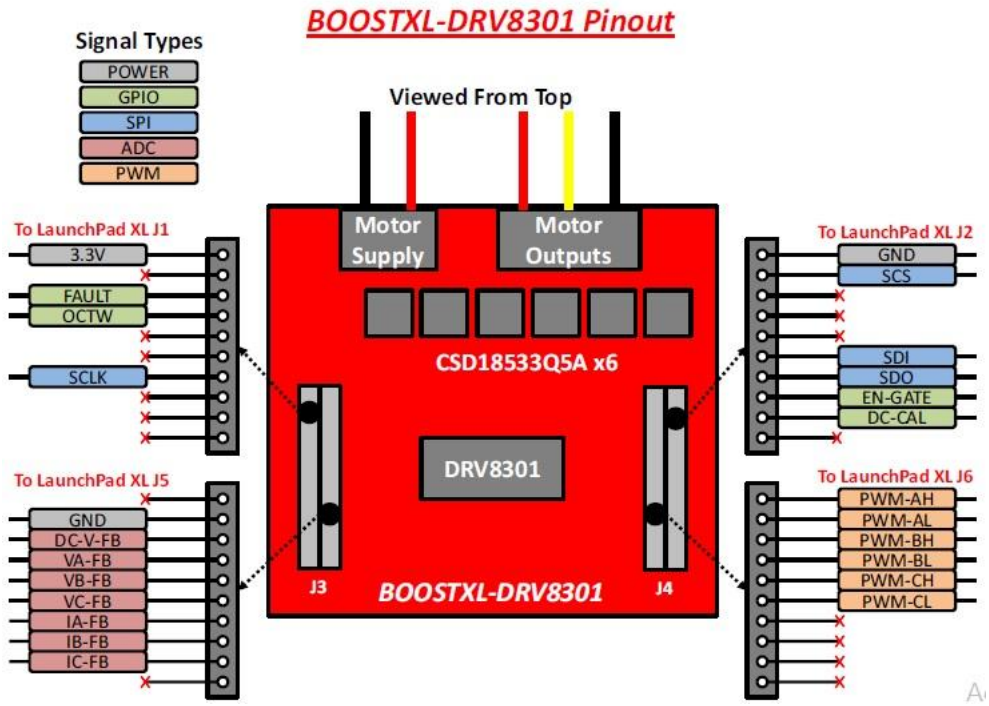

*****

List of Papers

[1] K. Vinida and Mariamma Chacko, "Performance of Sensorless BLDC motor on load using particle swarm optimized weights for an H infinity controller in speed control" Communicated to Ain Shams Engineering Journal, Elsevier.

[2] K. Vinida and Mariamma Chacko, " An optimized speed Controller for electrical thrusters in an Autonomous Underwater Vehicle", *International Journal of Power Electronics and Drive System*, (ISSN: 2088-8694), Vol. 9, No. 3, September 2018, pp. 1166-1177 .

[3] K. Vinida and Mariamma Chacko, "Analysis of four quadrant operation of thruster motor in an AUV using an optimized H infinity speed controller", *International Journal of Applied Engineering Research*, (ISSN 0973-4562) Volume 13, Number 15 (2018) pp. 11990-11995.

[4] K. Vinida and Mariamma Chacko, "An optimized H infinity strategy for robust control of sensorless BLDC propulsion motor in submarines for improved manoeuvrability", *IEEE International conference on Power Electronics, Drives and Electrical Systems (PEDES 2016*), December 14-17, Thiruvananthapuram.

[5] K. Vinida and Mariamma Chacko, "A novel strategy using H infinity theory with optimum weight selection for the robust control of sensorless brushless DC motor", *2016 IEEE 7th International Symposium on Sensorless Control for Electrical Drives (SLED 2016)*, June 5-6, Nadi, Fiji.

[6] K Vinida, Mariamma Chacko, "Sensorless Control of Brushless DC motors and H∞ Control Theory Applications - A Literature Review*", IOSR Journal of Electrical and Electronics Engineering (IOSR-JEEE*), Volume 11, Issue 1 Ver. IV (Jan. – Feb. 2016), pp 19-25.

*****

INDEX